Technical University of Crete
School of Electric and Computer Engineering

Design and Implementation of Algorithms for Operation Control, Leakage Detection and Decision Making for the Management of a Water Distribution Network

Vasileios Boglou

Thesis Committee

Professor George Stavrakakis, Supervisor

Associate Professor Eftichios Koutroulis

Dr. Eleftheria Sergaki, Co-advisor

A Thesis submitted in partial fulfilment of the requirements for the degree of Diploma in Electrical and Computer Engineering

Chania, September 2018

This work is licensed under a Creative Commons “Attribution 4.0 International” license.

This thesis is dedicated to my parents Anastasios and Georgia for their support and encouragement

Abstract

A distributed water supply system is a system based on engineered hydraulic components which conveys water from the source to the consumers. A typical distributed water supply system consists of the water sources, a pipe network, storage facilities like reservoirs and water tanks, pumping stations and the consumption nodes. This Thesis is based on the project "An Intelligent system for sustainable management of water supply networks: application in the island of Crete", which was submitted for the purposes of the program GR02.03 - "Integrated marine and inland water management - Good environmental status in European marine and inland waters" and was funded by the European Economic Area grants 2009 - 2014 (EEA grants 2009 -2014). In this project, the distributed water supply system of the Organization for the Development of Crete S.A. (OAK.AE) was examined.

The first part of this Thesis deals with the operation and the flow control of the main pumping station of OAK.AE water network, named "Vlites". In an extended set of simulations, by using "SmartWaters" framework, four control algorithms are examined as they indirectly control the operation and the flow of "Vlites" pumping station, by tracking the level of the feeding tank, named "Korakies". In detail are examined: i) an algorithm based on pumping station's pumps scheduling control (ON/OFF) under constant speed operation and tank level control, ii) an algorithm based on pumping station's pumps scheduling control under variable speed operation and tank level control, iii) an algorithm based on a PI controller and tank level control iv) an algorithm based on a PID controller and tank level control. Algorithms (i) and (ii) were implemented by the team of the scientific project. Algorithms (iii) and (iv) are implemented in this Thesis framework.

The second part of this Thesis deals with the development of an algorithm for big water leakages localization (greater than 20-25 m^3/h), in OAK.AE distributed water network. Initially, an examination about the accurately simulation of water leakages in "SmartWaters" framework takes place, by simulating a leakage in a prototype network and verifying the accuracy of the leakages modeling. The algorithm is based on, a set of features, which are generated by pressure signals from an extended set of simulations in "SmartWaters framework", in order to extract features and examine which of them can be used for leakages detection. These features are: i) the discrete energy of the pressure signals ii) the entropy of the pressure signals and iii) the energy of detail coefficients of Daubechies 2 (db2), 3^{d} level discrete wavelets decomposition.

Keywords: Distributed water supply system, Tank level control, PI controller, PID controller, Leakages detection, Features extraction, EPANET, SmartWaters framework

Περίληψη

Ένα κατανεμημένο σύστημα διανομής νερού, αποτελείται από ποικίλα υδραυλικά στοιχεία. Το σύστημα περιλαμβάνει περιοχές από τις οποίες συλλέγεται νερό, από δίκτυο αγωγών, από εγκαταστάσεις αποθήκευσης (δεξαμενές και ρεζερβουάρ), αντλιοστάσια και κόμβους κατανάλωσης. Η παρούσα διπλωματική εργασία εκπονήθηκε στα πλαίσια εργασιών που έλαβαν χώρα κατά την υλοποίηση του προγράμματος ¨Σχεδιασμός ευφυούς συστήματος αειφόρου διαχείρισης υδατικών δικτύων: εφαρμογή στην Κρήτη¨, το οποίο υποβλήθηκε στα πλαίσια της ανοικτής πρόσκλησης ΓΡ02.03 - "Αύξηση της γνώσης σχετικά με την ολοκληρωμένη θαλάσσια και νησιωτική πολιτική ή την Προστασία και διαχείριση των παράκτιων Περιοχών", χρηματοδοτήθηκε από το Χρηματοδοτικό Μηχανισμό Ευρωπαϊκου Οικονομικού Χώρου περιόδου 2009 - 2014 (ΧΜ ΕΟΧ 2009 — 2014) και στο οποίο εξετάστηκε το κατανεμημένο σύστημα διανομής νερού του Οργανισμού Ανάπτυξης Κρήτης Α.Ε. (ΟΑΚ.ΑΕ).

Το πρώτο θέμα που εξετάζεται, αφορά τον έλεγχο της λειτουργίας και της ροής του κεντρικού αντλιοστασίου του δικτύου του ΟΑΚ.Α.Ε., το οποίο βρίσκεται στο Βλητέ. Σε ένα σύνολο από εκτεταμένες προσομοιώσεις, κάνοντας χρήση του "SmartWaters framework", το οποίο αναπτύχθηκε από την ομάδα του ερευνητικού έργου, εξετάζονται τέσσερις αλγόριθμοι, οι οποίοι ελέγχουν έμμεσα τη λειτουργία και τη ροή του αντλιοστασίου του Βλητέ, παρακολουθώντας τη στάθμη της δεξαμενής Κορακιών, η οποία τροφοδοτείται από αυτό το αντλιοστάσιο. Αναλυτικά εξετάζονται: i) ένας αλγόριθμος ελέγχου στάθμης δεξαμενής και προγραμματισμού λειτουργίας των αντλιών του Βλητέ με σταθερές στροφές λειτουργίας, ii) ένας αλγόριθμος ελέγχου στάθμης δεξαμενής και προγραμματισμού λειτουργίας των αντλιών του Βλητέ με μεταβλητές στροφές λειτουργίας, iii) ένας αλγόριθμος ελέγχου στάθμης δεξαμενής κάνοντας χρήση PI ελεγκτή και iv) ένας αλγόριθμος ελέγχου στάθμης δεξαμενής κάνοντας χρήση PID ελεγκτή. Οι αλγόριθμοι (i) και (ii), αναπτύχθηκαν στα πλαίσια του ερευνητικού έργου, από την ομάδα που συμμετείχε σε αυτό. Οι αλγόριθμοι (iii) και (iv), αναπτύσσονται στα πλαίσια της παρούσας διπλωματικής.

Το δεύτερο θέμα που εξετάζεται είναι η ανάπτυξη αλγόριθμου για τον εντοπισμό μεγάλων διαρροών (μεγαλύτερων από 20-25 m^3/h) στο σύστημα δικτύου του ΟΑΚ.ΑΕ. Αρχικά εξετάζεται η ακρίβεια του "SmartWaters framework", ως προς τη μοντελοποίηση των διαρροών, προσομοιώνοντας διαρροή σε δοκιμαστικό πρότυπο δίκτυο και συγκρίνοντας τα πειραματικά αποτελέσματα της προσομοίωσης με τα αντίστοιχα της μοντελοποίησης. Στη συνέχεια εξετάζονται χαρακτηριστικά σημάτων πίεσης με εκτεταμένες προσομοιώσεις στο "SmartWaters framework" με σκοπό να καθοριστεί ποια από αυτά τα χαρακτηριστικά μπορούν να χρησιμοποιηθούν για την ανίχνευση διαρροών. Τα υπό μελέτη χαρακτηριστικά είναι: i) η διακριτή ενέργεια των σημάτων πίεσης, ii) η εντροπία των σημάτων πίεσης και iii) η ενέργεια των detail συντελεστών του $3^{ου}$ επιπέδου του διακριτού μετασχηματισμού wavelet, χρησιμοποιώντας την οικογένεια Daubechies και συγκεκριμένα το 2ο βαθμό της συγκεκριμένης οικογένειας συναρτήσεων wavelet.

Λέξεις Κλειδιά: Κατανεμημένα συστήματα διανομής νερού, Έλεγχος στάθμης δεξαμενής, PI ελεγκτής, PID ελεγκτής, Ανίχνευση διαορροών, Εξαγωγή χαρακτηριστικών, EPANET, SmartWaters framework

Acknowledgements

I am using this opportunity to express my gratitude to everyone who helped me to finish my thesis. First of all, I would like to thank my supervisor and mentor, Professor George Stavrakakis, who supported me greatly, he was always willing to help me and trusted me, by assisting me to participate in the scientific project "An Intelligent system for sustainable management of water supply networks: application in the island of Crete". Moreover, I would like to give special thanks to Professor Anastasios Pouliezos who, as the scientific coordinator of the project, trusted me, gave me the opportunity to participate in it and helped me with the present thesis. Also I want to thank all the project members. I would also like to thank Associate Professor Eftichios Koutroulis, for his support and for the confidence he showed me during my studies. Furthermore, I would like to express my gratitude and give special thanks to my co,-advisor Dr. Eleftheria Sergaki, who helped and trusted me during my studies and she gave me the opportunity to come in contact with the wonderful world of control. Finally, I would like to thank my parents, my friends and especially my best friend and colleague, Nick Kyparissas, for their support and encouragement.

List of Tables

1 Basic pump terms 6
2 Main characteristics of Vlites pumps. 16
3 Tank level regions and corresponding active pumps on pumps scheduling control. 18
4 Matlab tuning procedure. Simulink simulation parameters. 22
5 Results of PI tuning process. Tuned PI controller gains. 23
6 Results of PID tuning process. Tuned PID controller gains. 25
7 Vlites pumping station pumps proposed operation, based on pumps flow capacity and tank level regulation. 27
8 SmartWaters simulation parameters. 31
9 Vlites energy consumption for all control methods. 33
10 Simulation parameters in order to test the correct simulation of leakages in SmartWaters program by using the prototype water network of Figure 31. . . . 42
11 Leakages modeling and simulation results of the prototype water network, in order to examine the accuracy of leakages simulations in SmartWaters framework. 42
12 Simulation parameters in order to examine and compare the behavior of the mentioned features in a set of normal and leaking pressure signals. 44
13 Experiments labels and leakages insertion times. 46
14 Energy of detail coefficients of Daubechies 2 3^{d} level wavelets decomposition thresholds for leak events classification. 52
15 Vlites pumping station pump groups and characteristics. 59

List of Figures

1 Inner components of a centrifugal pump [1]. 5
2 A set of pump curves from Tamesis Pumps [1]. 7
3 Series pump configuration example and resulting Head - Flow curve. Figure 3b downloaded from www.engineringtoolbox.com. 8
4 Parallel pump configuration example and resulting Head - Flow curve. Figure 4b downloaded from www.engineringtoolbox.com. 8
5 Under study distributed water network [1]. 1: Meskla village, 2: Myloniana tanks, 3: Daratso region, 4: Perivolia region, 5: Mournies region, 6: Nerokouro region, 7: Tsikalaria region, 8: Vlites pumping station, 9: Megala Chorafia region, 10: Korakies tanks, 11: Akrotiri region. Red color: main supply pipe, blue color: sub-networks pipes. 10
6 Block diagram of SmartWaters framework which was developed in [1]. 12
7 SmartWaters GUI. Network parameters window, as developed in [1]. 13
8 SmartWaters GUI. Network simulation window, as developed in [1]. 13
9 SmartWaters GUI. Example of flows results window, as developed in [1]. 14
10 SmartWaters GUI. Example of pressures results window, as developed in [1]. . . 14
11 Vlites pumping station structure. 15
12 Akrotiri irrigation supply sub-network, consists of 547 nodes and 495 pipes. . . . 16
13 Connection of Vlites pumping station with Akrotiri tank. Vlites MSL is 83 m and Korakies tank is 212 m. 17
14 Korakies irrigation tank and connected pipes. 17
15 Tank level control scheme 19
16 Tank level control closed loop system. w_{out} models the demand requirements of the network in Akrotiri region. The h_{out} is the level of the tank. 21
17 Simulink model disturbance time-series ($w_{out}(t)$) for the tuning processes of the PI and PID controllers, which models the demand requirements in Akrotiri region, as shown in Figure 16. 23
18 Matlab simulink simulation testing results for tuned PI controller. 24
19 Matlab simulink simulation testing results for tuned PID controller. 26
20 Pole - zero map (s-plane) of tank level closed loop system, when the PI controller is applied. Poles are symbolized as x and zeros as o. 28
21 Pole - zero map (s-plane) of tank level closed loop system, when the PID controller is applied. Poles are symbolized as x and zeros as o. 28
22 Standard daily demand multipliers, based on real data [1]. 31
23 Demand multipliers for each day of simulation. 32
24 Pumps scheduling control (ON/OFF) under constant speed operation based on boolean logic simulation results for third and sixth day. 34
25 Pumps scheduling control under variable speed operation based on boolean logic simulation results for third and sixth day. 35

26 PI pumps control method based on tank level control simulation results for third and sixth day. . . . 36
27 PID pumps control method based on tank level control simulation results for third and sixth day. . . . 37
28 Block logic diagram of one dimension level Wavelets decomposition using Mallat algorithm. Downsample keeps the even indexed elements. . . . 39
29 One dimensional discrete Multi level Wavelets decomposition using Mallat algorithm. . . . 40
30 Daubechies 2 wavelets family (db2) low pass and high pass decomposition filters. Horizontal axis: discrete time (n). Vertical axis: Amplitude. . . . 41
31 Prototype water supply network model used for SmartWaters's framework leakages testing. . . . 41
32 Testing network model simulation result, in order to test SmartWaters framework, when a leakage is applied. . . . 43
33 Daily demand pattern for the experimental simulation in order to examine and compare the behavior of the mentioned features in a set of normal and leaking pressure signals. . . . 45
34 Coefficients, which multiply the daily demand pattern of the experimental simulation in order to examine and compare the behavior of the mentioned features in a set of normal and leaking pressure signals. . . . 45
35 Under study node pressure signals. . . . 47
36 Hourly energy of under study node pressure signals. . . . 49
37 Hourly entropy of under study node pressure signals. . . . 50
38 Hourly energy of detail coefficients of Daubechies 2 3d level wavelets decomposition of under study node pressure signals. . . . 51
39 Proposed leakage detection algorithm block diagram. . . . 53
40 Vlites pumping station network. . . . 59
41 Pump's Head - Flow and efficiency curves for pumps of Group 2 60
42 Pump's Head - Flow and efficiency curves for pumps of Group 2 61
43 Pump's Head - Flow and efficiency curves for pumps of Group 3 62
44 Pumps scheduling control (ON/OFF) under constant speed operation based on boolean logic results. Korakies tank level response for days 1 to 6. . . . 63
45 Pumps scheduling control (ON/OFF) under constant speed operation based on boolean logic results. Korakies tank level response for days 7 to 12. . . . 64
46 Pumps scheduling control (ON/OFF) under constant speed operation based on boolean logic results. Vlites pumping station outflow for days 1 to 6. . . . 65
47 Pumps scheduling control (ON/OFF) under constant speed operation based on boolean logic results. Vlites pumping station outflow for days 7 to 12. . . . 66
48 Pumps scheduling control under variable speed operation based on boolean logic simulation results. Korakies tank level response for days 1 to 6. . . . 67

49 Pumps scheduling control under variable speed operation based on boolean logic simulation results. Korakies tank level response for days 7 to 12. 68
50 Pumps scheduling control under variable speed operation based on boolean logic simulation results. Vlites pumping station outflow for days 1 to 6. 69
51 Pumps scheduling control under variable speed operation based on boolean logic simulation results. Vlites pumping station outflow for days 7 to 12. 70
52 PI pumps control method based on tank level control simulation results. Korakies tank level response for days 1 to 6. 71
53 PI pumps control method based on tank level control simulation results. Korakies tank level response for days 7 to 12. 72
54 PI pumps control method based on tank level control simulation results. Vlites pumping station outflow for days 1 to 6. 73
55 PI pumps control method based on tank level control simulation results. Vlites pumping station outflow for days 7 to 12. 74
56 PID pumps control method based on tank level control simulation results. Korakies tank level response for days 1 to 6. 75
57 PID pumps control method based on tank level control simulation results. Korakies tank level response for days 7 to 12. 76
58 PID pumps control method based on tank level control simulation results. Vlites pumping station outflow for days 1 to 6. 77
59 PID pumps control method based on tank level control simulation results. Vlites pumping station outflow for days 7 to 12. 78

Contents

1 Introduction **1**

1.1 General . . . 1

1.2 SmartWaters Scientific project [1] . . . 1

1.3 Thesis goals . . . 2

1.4 Thesis structure . . . 2

2 Distributed water supply systems **4**

2.1 Introduction . . . 4

2.2 Water supply Systems modeling and simulation . . . 4

2.3 Leakages in water supply systems . . . 4

2.4 Pumps . . . 5

2.4.1 Pump fundamentals . . . 5

2.4.2 Pump affinity laws . . . 6

2.4.3 Pump curves . . . 7

2.4.4 Series pump operation . . . 8

2.4.5 Parallel pump operation . . . 8

2.4.6 Causes of water hammer . . . 9

2.4.7 Pumps speed control . . . 9

3 Description of the under study distributed water network, Epanet and SmartWaters Matlab GUI **10**

3.1 Under study water network description . . . 10

3.2 SmartWaters Matlab GUI and Epanet . . . 11

4 Vlites pumping station proposed control algorithms **15**

4.1 Under study main pumping station description . . . 15

4.2 Proposed pumps scheduling control (ON/OFF) under constant speed operation based on boolean logic . . . 18

4.3 Proposed pumps scheduling control under variable speed operation based on boolean logic . . . 18

4.4 Proposed PI(D) pumps control method based on tank level control . . . 19

4.4.1 Tank level system . . . 19

4.4.2 Mathematical model . . . 20

4.4.3 PI controller tuning for Korakies tank level control . . . 21

4.4.4 PID controller examination . . . 24

4.4.5 Pumping station flow matching . . . 26

4.4.6 Stability, controllability and observability of the tank level control closed loop system after PI and PID controllers tuning . . . 27

4.5 Test of the proposed control algorithms by using SmartWaters framework for the OAK.AE simulated model . . . 30

4.5.1 SmartWaters simulation scenario . . . 30
4.5.2 Water demand scenario . . . 31
4.6 Testing simulation results and discussion . . . 32

5 Proposed leakages detection algorithm 38
5.1 Introduction . . . 38
5.2 Examined features from node pressure signals . . . 38
5.2.1 Energy . . . 38
5.2.2 Entropy . . . 38
5.2.3 Discrete Wavelets decomposition (DWD) . . . 39
5.3 Modeling and simulation of leakages . . . 40
5.4 Features examination for leakage detection in a case-study node of the under study distributed water supply system using energy, entropy and DWD pressures features extraction . . . 44
5.4.1 Introduction . . . 44
5.4.2 SmartWaters GUI parameters and experiments description . . . 44
5.4.3 Extracted features from the under study node pressure signals, results and discussion . . . 47
5.4.4 Proposed leakage detection algorithm description . . . 52
5.5 Results and discussion . . . 53

6 Summary and future work 55
6.1 Thesis summary . . . 55
6.2 Conclusions . . . 55
6.3 Future work . . . 56

References 57

Appendices 59

A Vlites pumping station curves 59

B Proposed control algorithms total simulation results 63

1 Introduction

1.1 General

Water is the most essential chemical substance for the human being. Without water the existence of people and societies would be impossible. The water is transferred from the water sources to the consumers, by using a distributed water supply system. A significant amount of electrical energy is spent in distributed water supply systems and especially in pumping stations. This fact creates the need to control the operation of the pumping stations in order to achieve reduction of the consumed electrical energy. Another major problem in distributed water supply systems is the existence of leakages, especially when the systems are old. In this case, the percentage of the leaking water can reach up to 40 % of the water which is incoming to the network [1]. This creates the need for leakage detection algorithms implementation, in order to detect possible leakages in a fast way.
This Thesis deals with those two subjects. It examines a set of pumping station control algorithms and an algorithm for big leakage detection, greater than 20-25 m^3/h, based on features extraction, in a real distributed water supply system, which was modelled in Epanet [2] and simulated in SmartWaters framework [1].

1.2 SmartWaters Scientific project [1]

This Thesis is based on scientific project Design of an intelligent system for sustainable management of water networks: application to Crete (SmartWaters) [1], which was submitted for the purposes of the program GR02.03 - "Integrated marine and inland water management - Good environmental status in European marine and inland waters" and was funded by the European Economic Area grants 2009 - 2014 (EEA grants 2009 -2014). The partners of the scientific project are, the Technical University of Crete, the Organization for the Development of of Crete S.A. (OAK.AE), the Institute of Geology and Mineral Exploration (IGME), the Mediterranean Agronomic Institute of Chania (MAICh) and the Regional Development Fund of Crete (RDFC).
The main aim of the project is to improve the management of distributed water supply system of OAK.AE, which is located in the region of Chania, by using a smart decision making environment which takes into account every parameter of the system. This environment can sustains the water demand of the network, minimizes water losses and reduces the operating costs.
For the purposes of the scientific project, a framework, called SmartWaters, was developed. This framework consists of Epanet, which makes the hydraulic analysis and the simulations of the distributed water supply system, some algorithms that have been developed in Matlab, in order to control the operation of the simulated network and making decisions and a Matlab GUI, in which the parameters of the simulations are configured and the results are shown.

1.3 Thesis goals

As mentioned above, this Thesis deals with the subject of controlling the operation and the flow of the main pumping station of distributed water supply system of OAK.AE. and the subject of leakages detection in the same system.
The first aim of the Thesis focuses in Vlites pumping station of the under study system. The objectives are, to examine the operation and the behavior, in an extended set of simulations in SmartWaters framework, of i) an algorithm based on pumping station's pumps scheduling control (ON/OFF) under constant speed operation and tank level control, ii) an algorithm based on pumping station's pumps scheduling control under variable speed operation and tank level control, iii) an algorithm based on PI controller and tank level control iv) an algorithm based on PID controller and tank level control. The first 2 algorithms were implemented by the team of the scientific project SmartWaters [1], for the purposes of the project. The other 2 algorithms were implemented in the present Thesis.
The second goal of this Thesis is to examine the possibility of creating a decision making algorithm, based on features extraction from nodes pressure signals, for big leakage detection. The examined features are, the energy, the entropy and the energy of detail coefficients of Daubechies 2, 3^{d} level discrete wavelets decomposition. The examination of those features can be achieved by creating an extended set of simulations in SmartWaters framework and evaluating their behavior and the possibility of setting thresholds, when leakages appear in water supply system nodes.

1.4 Thesis structure

This Thesis consists of 6 chapters. Apart from the introductory chapter, the rest of them are:

Chapter 2 describes the structure and the basic components of a distributed water supply system. It describes the path of the water from the water sources to the consumption nodes. It also makes an introduction to the problem of water leakages in those systems. Finally, it includes the basic fundamentals for pumps and pumping station.

Chapter 3 describes the structure of the distributed water supply system under study, the basic regions of the network and also the basic parts of it. Furthermore, it includes a description of Epanet and SmartWaters Matlab GUI, which was created for the purposes of the scientific project [1].

Chapter 4 focuses on the main pumping station of the distributed water supply system under study and especially the operation of the included pumps, named as Vlites. It contains a short brief about the control methods which were implemented for the purposes of the scientific project [1]. Furthermore, in this chapter a new control algorithm is implemented, based on PI and PID controllers. Finally, an investigation about all the described algorithms takes place by testing these algorithms in a set of extended simulations in SmartWaters framework.

Chapter 5 refers to a proposed algorithm for leakage detection in the under study distributed water supply system. In this chapter, an experimental investigation about leakage simulations in SmartWaters framework in a testing network model takes place. Furthermore, it includes a basic short theory about the under study features and introduces an experimental methodology in order to determine which of them are suitable for leakages of dozen of cubic meters per hour in the under study distributed water supply system by making experimental extended simulations, in a case - study node of the under study system, by using SmartWaters framework.

Chapter 6 includes a short summary about the conclusions and the results that came up from this Thesis. It also includes suggestions about feature work.

Appendix A includes the network of Vlites pumping station and the characteristics of the included pumps.

Appendix B includes the total simulation results of Vlites pumping station's control algorithms, as described in Chapter 4.

2 Distributed water supply systems

2.1 Introduction

The aim of a distributed water supply system is to provide a region with water by transferring the water from the aquifers to the consumers of the system. A typical distributed water supply system consists of sources of water, water purification facilities, pipes, connection nodes, consumption nodes and pumping stations [3]. The transfer of the water, from water sources to the consumers, is accomplished by using distributed water supply systems. A typical system consists of water sources, pipes, connection nodes, consumption nodes and pumping stations. Initially raw water, which is found in the environment, is collected to the sources. After that, it is transferred, by using a network of pipes, to water purification facilities in order to be treated for harmful substances. Afterwards, the water is driven to the consumers or stored in specific facilities, such as tanks and reservoirs, located on positions with high power of gravity. The transfer of the water inside the pipes, is achieved by the power of gravity which gives the water the necessary kinetic energy in order to circulate among the pipes. If the power of gravity is not enough, pumps are installed to give the required kinetic energy.

2.2 Water supply Systems modeling and simulation

A lot of programs are implemented in order to model and simulate the behaviour of a distributed water supply system. One of them is Epanet [2].
The model of the distributed water supply systems is designed in a graphical tool, when the user sets the connection and consumption nodes of the network, the pipes, the tanks and the pumps. Also the user sets the parameters for each component of the network, like the height of the nodes, the length and the roughness of the pipes and other basic things, the demand for each consumption node and general demand patterns.
The big advantages of Epanet, compared to other software, are that Epanet is free and open source. From the other side, Epanet is very simple and does not take into consideration extra variables, which exist in a real distributed water supply system. The management of a distributed water supply system, which can be simulated in Epanet, is very simple and is based in IF - ELSE logic.

2.3 Leakages in water supply systems

Distributed water supply systems, usually, present leakages. The timely detection of water leakages is very significant, because of the big amounts of water losses from the network. The percentage of the leakages in a typical water supply system is, usually, between 20 % and 30 % of the incoming water. Sometimes, this percentage can reach up to 40 % [1]. Water leaks can be categorized as physical or notional. Physical losses are due to leaks in tanks and pipeline connections, mainly due to strain on construction materials. Notional losses refer to the water

consumed without being paid. The notional losses are very difficult to be found, because the costs, in order to install a detect system for those leaks, are very high.
In recent years, many methods have been implemented for leakage detection in distributed water supply systems. Some of these methods, are based on acoustic waves [4, 5, 6], on node pressure signals and extracted metrics, like HLR method [7], on artificial intelligence and neural networks [8, 9, 10, 11] and on some metrics which are calculated from the pressures and the flows of the system [1].

2.4 Pumps

2.4.1 Pump fundamentals

A pump is a device that moves fluids by mechanical action. It takes energy from a specific source, such as electric, and converts that energy into hydraulic form. Pumping systems are a indivisible part of the water industry because they give to the water the necessary power to overcome forces like gravity and friction.
There are two basic types of pumps, the positive displacement pumps and the centrifugal pumps. Positive displacement pumps trap a fixed amount of fluid into their cavity and then force the trapped fluid into the discharge pipe. On the other side, centrifugal pumps cause the fluid to move by using an impeller. The inner components of a centrifugal pump are shown in Figure 1. An increase in the fluid pressure from the pump inlet to its outlet is created. This pressure difference drives the fluid to the discharge pipe. Centrifugal pumps are the most widely used pumps in the world. This Thesis focuses on this type of pumps. When we discuss centrifugal pumps, there are some basic terms based on their operation. The definitions of the terms and their symbols are listed in Table 1 [12].

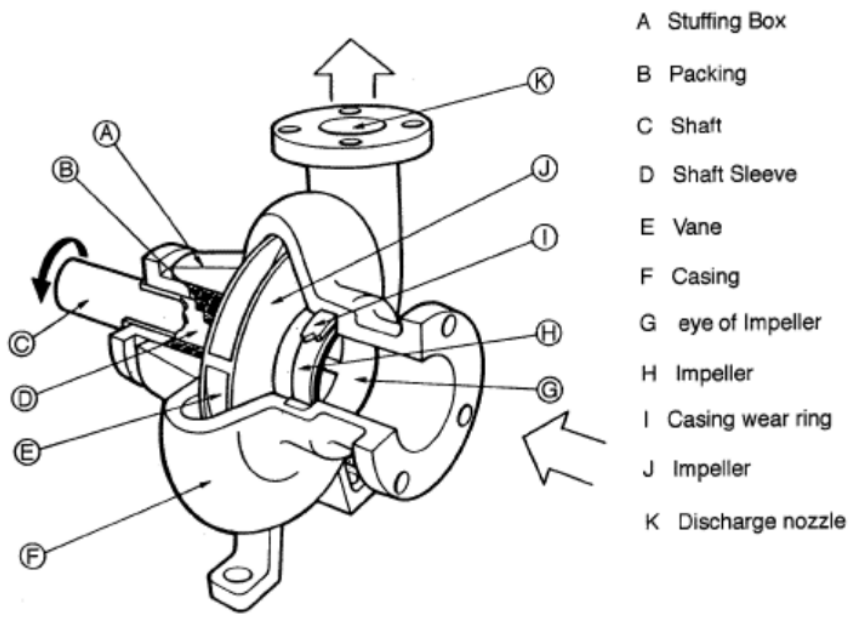

Figure 1: Inner components of a centrifugal pump [1].

	Term	Definition	Symbol	Units
1	Total Head	The high which a pump can lift a liquid	H	m
2	Flow rate	The amount of fluid delivered by the pump to the discharge per unit of time	Q	m^3/h
3	Shaft rotational speed	The rotations of the impeller per minute	N	RPM
4	Shaft power	The required power from the motor to the shaft of the pump	P	$Watts$
5	Diameter	The diameter of the pump impeller	D	m

Table 1: Basic pump terms

2.4.2 Pump affinity laws

For a further study of pumps, it is necessary to approach their operation using a set of mathematical equations. Let us have two pumps. If these pumps are geometrically and dynamically similar, operate at similar operational points, then a set of equations, which are called affinity laws, can be applied to recalculate their operation, if a variable changes. Let us define the performance variables of the above two pumps. H_1, Q_1, N_1, P_1, D_1 are the variables for pump one and H_2, Q_2, N_2, P_2, D_2 refer to pump two. According to affinity laws the relationship between the above variables are [12]:

$$\frac{Q_1}{Q_2} = \frac{N_1 D_1}{N_2 D_2} \tag{1}$$

$$\frac{H_1}{H_2} = \frac{N_1^2 D_1}{N_2^2 D_2} \tag{2}$$

$$\frac{P_1}{P_2} = \frac{N_1^3 D_1}{N_2^3 D_2} \tag{3}$$

$$\frac{N_1}{N_2} = \sqrt[3]{\frac{P_1}{P_2}} \tag{4}$$

The Affinity laws can be applied to the same pump. In this case the diameter of the impeller of the two pumps is equal, $D_1 = D_2$. Using this case, a satisfactory prediction of the operation of the pump can be produced if the speed of the impeller changes. This prediction exists only for small changes in pump's speed, at maximum, approximately, 20%. Equation 4 relates the changes of the speed with the changes of the pump's power.

2.4.3 Pump curves

Affinity laws, by themselves, can not describe the operation of a specific pump. It is vital to declare for each pump the relationship between the flow and some variables. Some terms are necessary before we discuss the curves.

Net Positive Suction Head Available (NPSHa) depends on the conditions of the installation and is declared as the total suction head of liquid absolute minus the absolute vapor pressure in meters of the liquid at a specific rate of flow expressed in meters of liquid.

Another useful term about pumps is their efficiency. Pump efficiency declares the percentage of the mechanical power which the pump converts to hydraulic power. Another useful term is the Net Positive Suction Head Required (NPSHR). NPSHR is given by the pump manufacturer and is related with the minimum head in which the pump operates normally, without any problem.

Total head, efficiency and NPSHa depend on the flow rate. Pump curves declare the modification of those variables when the flow of the pump changes. Rotodynamic are pumps that have a curve where the head falls gradually with increasing flow.

A set of curves for a specific rotodynamic pump is shown in Figure [12].

Another significant curve is the system curve. This curve is related to the water network system by showing the hydraulic energy required to move water into the system. The required hydraulic energy increases as flow increases.

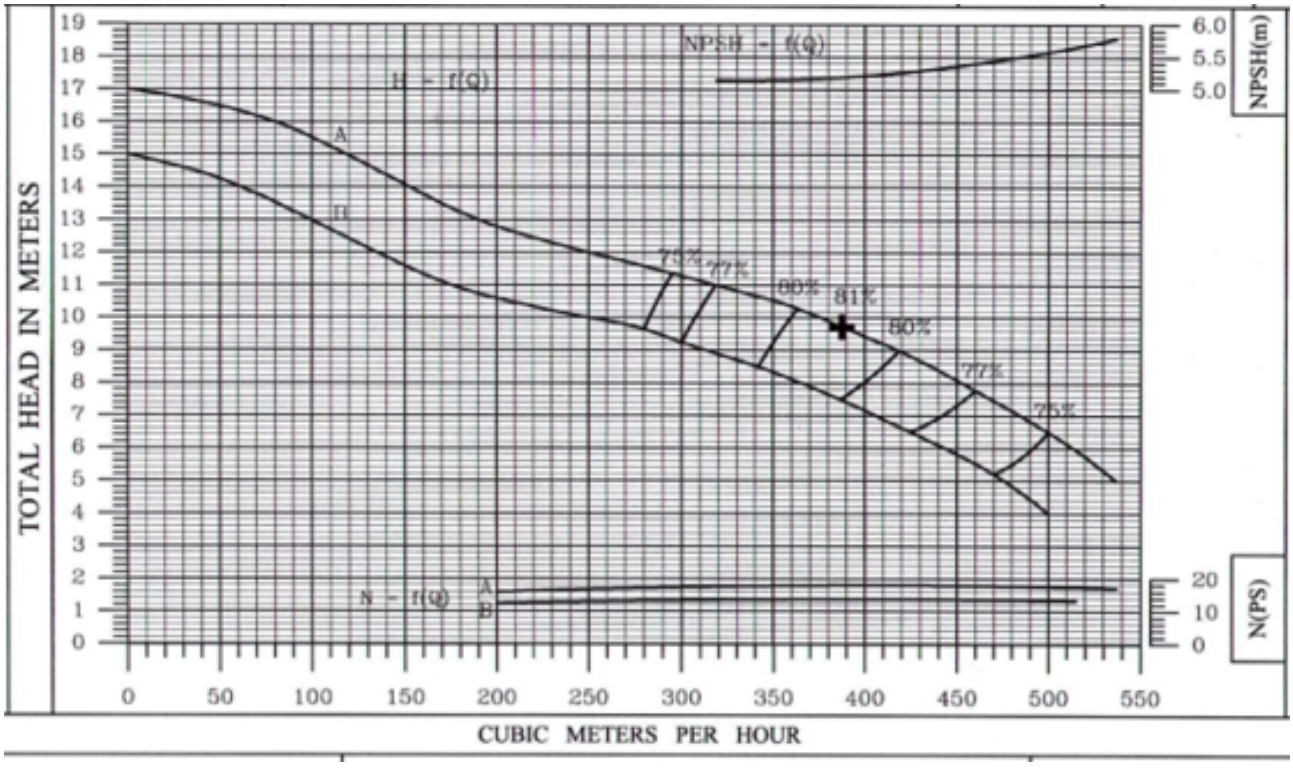

Figure 2: A set of pump curves from Tamesis Pumps [1].

2.4.4 Series pump operation

Pumping stations usually have to deal with high differential head [12]. That makes necessary to use more than one pump in a pumping station in a series configuration. Series configuration is used when the pumps deal with a high differential head,usually in combination with small flows. When two pumps are connected in series the resulting Head - Flow curve is obtained by adding the individual heads, for each value of flow. The series pump configuration of two pumps and the resulting Head -Flow curve are shown in Figure 3.

2.4.5 Parallel pump operation

Except from series pump configuration, pumps can connect in a parallel way [12]. Parallel pump configuration is very useful when pumps deal with large and varying flows. When a parallel configuration exists, the resulting Head-Flow curve is obtained by adding the actual flows for each head value. The parallel pump configuration of two pumps and the resulting Head -Flow curve are shown in Figure 4.

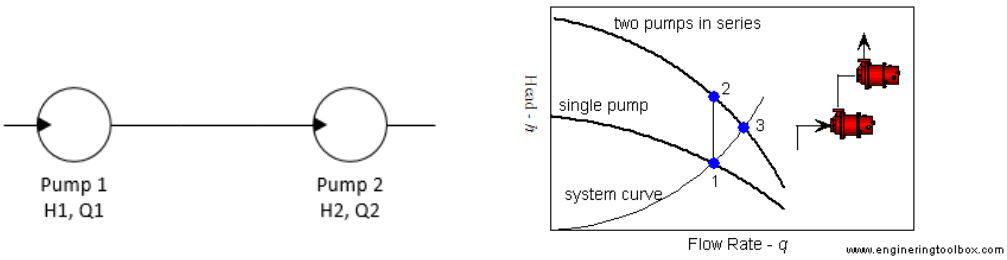

(a) Series pump configuration (b) Resulting Head - Flow curve.

Figure 3: Series pump configuration example and resulting Head - Flow curve. Figure 3b downloaded from www.engineringtoolbox.com.

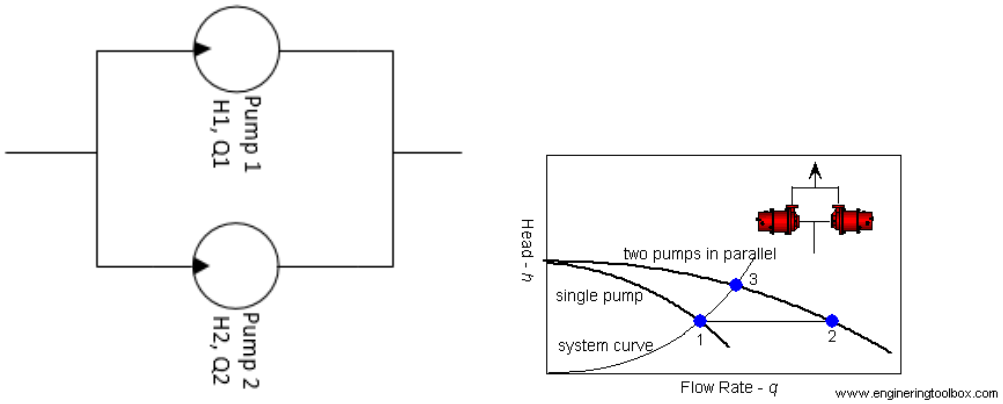

(a) Parallel pump configuration. (b) Resulting Head - Flow curve.

Figure 4: Parallel pump configuration example and resulting Head - Flow curve. Figure 4b downloaded from www.engineringtoolbox.com.

2.4.6 Causes of water hammer

When a pump reduce it's speed or closes, the flow of the water changes very fast. The water is forced to stop or to change direction. This causes an instant high pressure wave which propagates in the outlet pipe of the pump. Water hammer can cause major problems in the system, like strong vibrations, damages, leakages and even a pipe explosion. Normally the pressure wave inside the inlet pipe is very small because pumps change their state gradually but, when we discuss pump controlling in a big water network system, the hammer effect must be examined. There are some situations where water hammer is susceptible. For example an automatic re-start of a pump, which rotates backwards after a power failure or an acoustic resonance effect due to positive displacement pump flow variations [12].

2.4.7 Pumps speed control

The relation between the speed of a pump and it's required power, is also known as the cubic law, because the required power is the cube of the speed, as shown in Equations 3 and 4. This fact means, that a small reduction in pump's speed results a significant reduction in required pump's power and consumed energy. As well, by controlling the speed of a pump, the outflow of the pump is controlled. Pump's speed controller are divided into 2 main categories, mechanical and electric. Mechanical controllers include hydraulic clutches, wet coupling, and adjustable belts and pulleys. Electric controllers include eddy current clutches, rotor adjusters, and frequency controllers [1].

3 Description of the under study distributed water network, Epanet and SmartWaters Matlab GUI

3.1 Under study water network description

This Thesis deals with the distributed water network of the Organization for the Development of Crete S.A. (OAK.AE). The water network starts from the western sid of sub-region of Chania and finishes on the eastern side of Chania sub-region. Also the water network is expanding in Akrotiri cape of Chania. The under study distributed water network is shown in Figure 5.

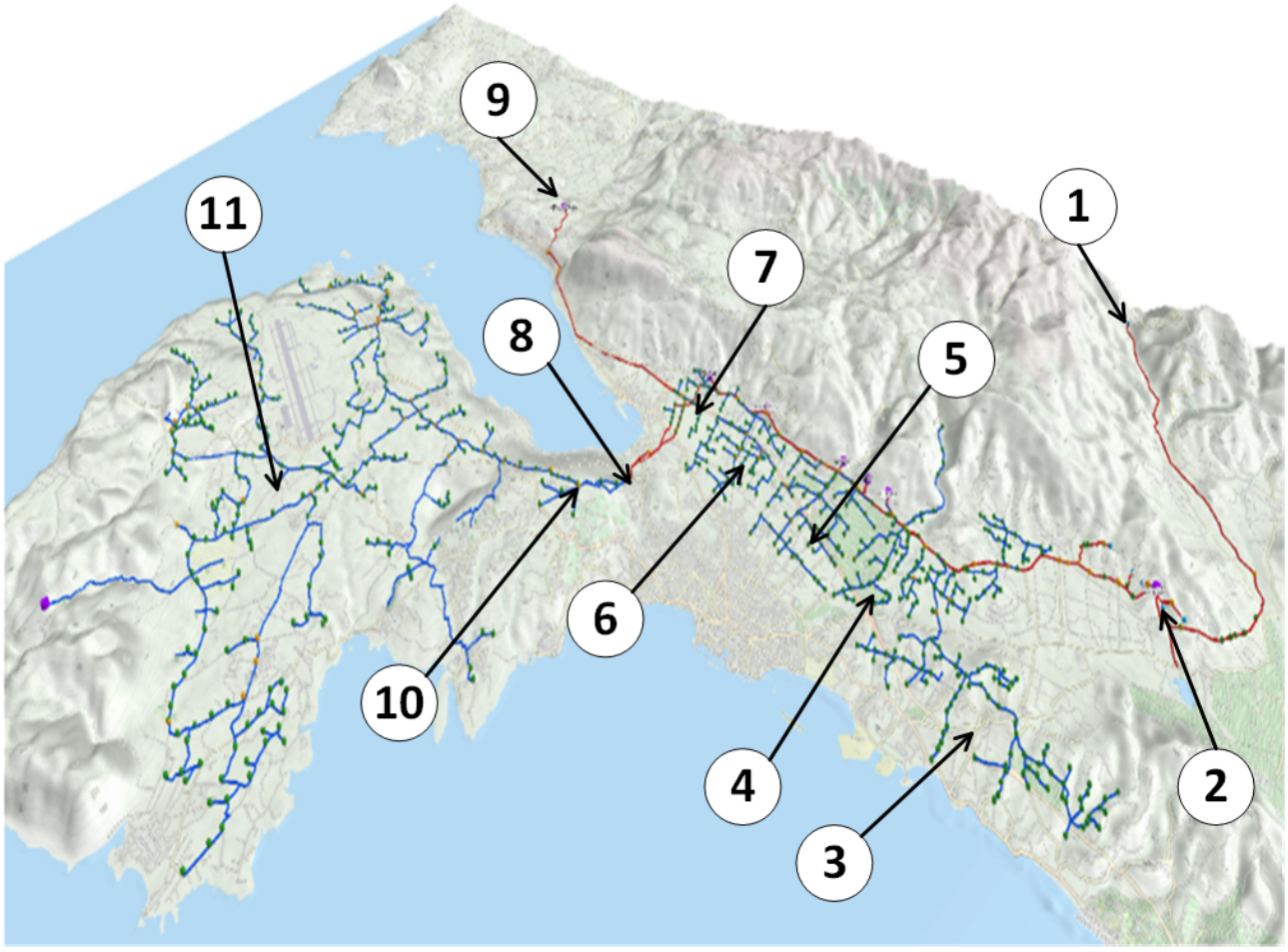

Figure 5: Under study distributed water network [1]. 1: Meskla village, 2: Myloniana tanks, 3: Daratso region, 4: Perivolia region, 5: Mournies region, 6: Nerokouro region, 7: Tsikalaria region, 8: Vlites pumping station, 9: Megala Chorafia region, 10: Korakies tanks, 11: Akrotiri region. Red color: main supply pipe, blue color: sub-networks pipes.

The network is supplied with fresh water by sources which are located near Meskla village. The sources high is between 197 m and 212 m. From those sources the water is transferred, using the force of gravity, into two tanks where are located in Myloniana territory. The capacity of both tanks is about 6500 m^3 and the altitude is about 135 m. Furthermore, in Myloniana there

are 5 boreholes which are also connected with the base tanks. The main pipe of the network starts from Miloniana tanks and supplies 4 other tanks, along the pipe. The main pipe ends up to Vlites booster pump station where the water is concentrated to a relief well. Vlites is located 83 m above MSL. The pump station boosts the water from the relief well to the two main Akrotiri tanks territory. Those two tanks which are located in Korakies territory, about 215 m above MSL, have a capacity of 8500 m^3 and supply the whole Akrotiri cape. A second pipe is also used to transfer water to Akrotiri via Vlites booster station. This pipe starts from a tank in Megala Chorafia territory and with a local booster pumping station, the pipe drives the water from the Tank to Vlites pumping station which supplies the two tanks in Korakies. Vlites booster pumping station is the main station of the network. This Thesis focuses on this pumping station. This station has nine pumps which serve water supply and irrigation needs. The characteristics and the curves of Vlites pumping station are included in Appendix A.

3.2 SmartWaters Matlab GUI and Epanet

SmartWaters GUI, as a part of SmartWaters framework, is a Matlab GUI, which uses Epanet[2] and was implemented by the team of [1] for the purposes of the Scientific project: Design of an intelligent system for sustainable management of water networks: application to Crete. The basic operation of SmartWaters framework is shown in Figure 6. A part of the SmartWaters framework, Epanet, perform an extended period simulation for the hydraulic and water quality behavior of a distributed water network, like the under study network in this Thesis. Epanet can simulate permanent or transient flows, in under pressure supply networks of any size and topology. Epanet calculates the amenities and pressures in nodes and pipes, the demand pressures, the water levels in tanks, the speed of the pumps and the position of the valves. The method that computes the hydraulic behavior of a water network in Epanet, is based on the principle of mass conservation and law of conservation of energy. Those are the two base equations to examine as to whether a water network is in a hydraulic stability. Let us define a water network with N crossed nodes and NF fixed grade nodes.

$$\sum_j Q_{i,j} - D_i = 0, i = 1, ..N \tag{5}$$

$$H_i - H_j = h_{i,j} = rQ_{i,j}^n + mQ_{i,j}^2 \tag{6}$$

$$h_{i,j} = -\omega^2(h_0 - r(\frac{Q_{i,j}}{\omega})^n) \tag{7}$$

SmartWaters framework calculates the pressures (loads) H_i for each node and $Q_{i,j}$ for each pipe, at every time-step, based on the above equations. Equations 5 and 6 describe the conservation of mass and energy in which, D_i is the demand of node N_i, H_i and H_j the loads in nodes N_i and N_j, $h_{i,j}$ the losses of the load between nodes N_i and N_j, r is a resistance factor which is analog to the roughness of the in-between pipe and m, is a factor for unimportant losses. Equation 7

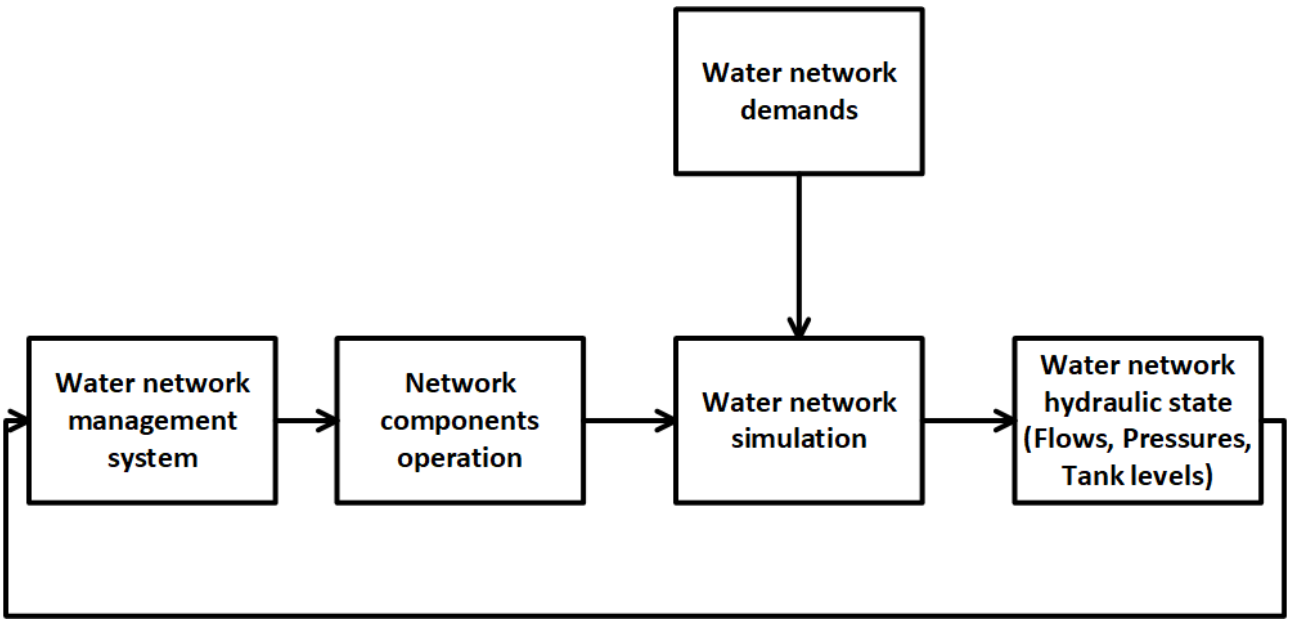

Figure 6: Block diagram of SmartWaters framework which was developed in [1].

is the corresponding equation for the operation of pumps, in which h_0 is the cutoff head of the pump, ω is the related speed of the pump and r, n are related with the curve of the pump.
The environment of SmartWaters Matlab GUI is shown in Figures 7, 8, 9 and 10. Figure 7 shows the initial window, where the user loads the topology of the under study network and sets the simulation parameters such as the total duration of the simulation, the time step which the program will analyze and calculate the hydraulic units of the network, the pattern time steps in which the consumption will remain the same and some other variables. After that, when the simulation starts, window in Figure 8 opens. This Figure shows the simulation progress of the under study distributed water supply network. This window also shows, graphically, the change of network tank levels. When the simulation finishes, the user can get basic metrics of the overall network parts, like pipe flows, pump flows, node pressures and others. A sample of the result windows is shown in Figures 9 and 10.

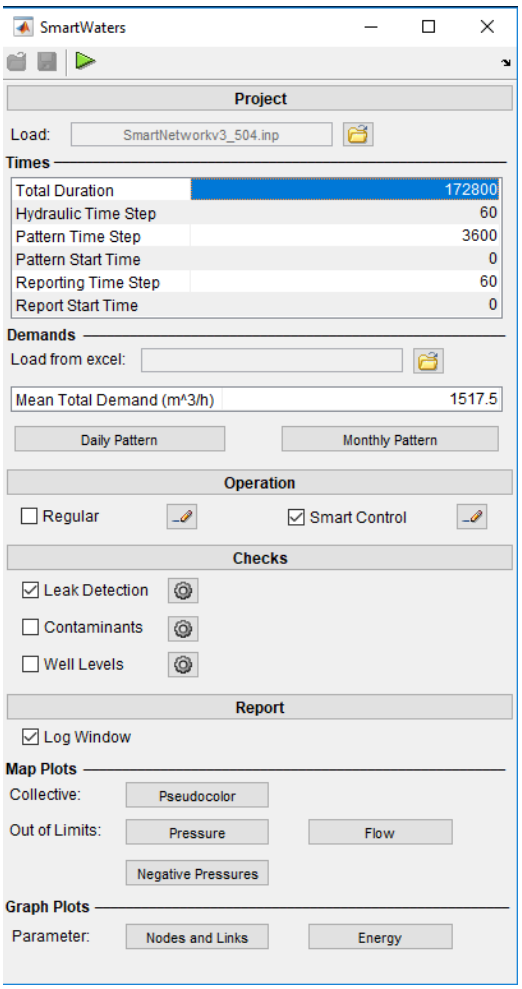

Figure 7: SmartWaters GUI. Network parameters window, as developed in [1].

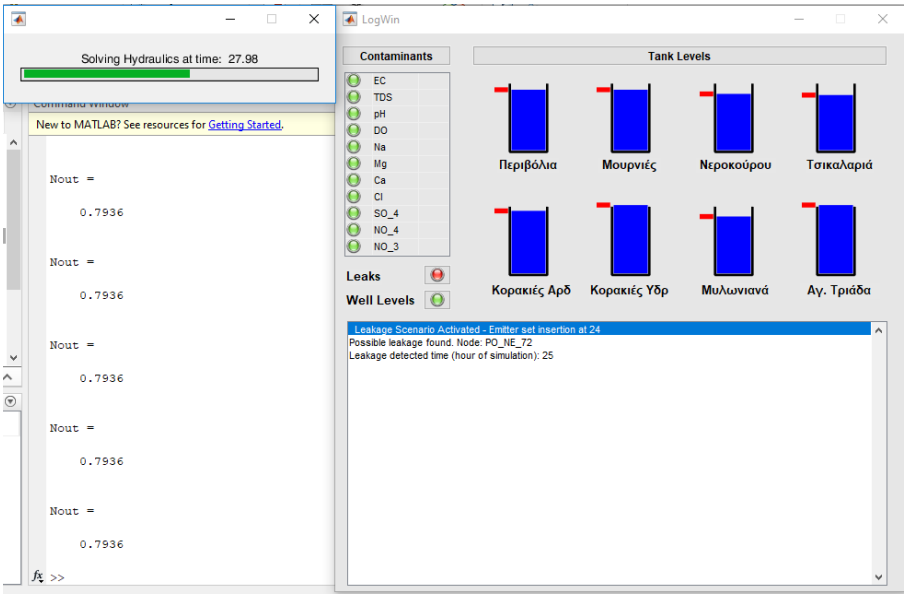

Figure 8: SmartWaters GUI. Network simulation window, as developed in [1].

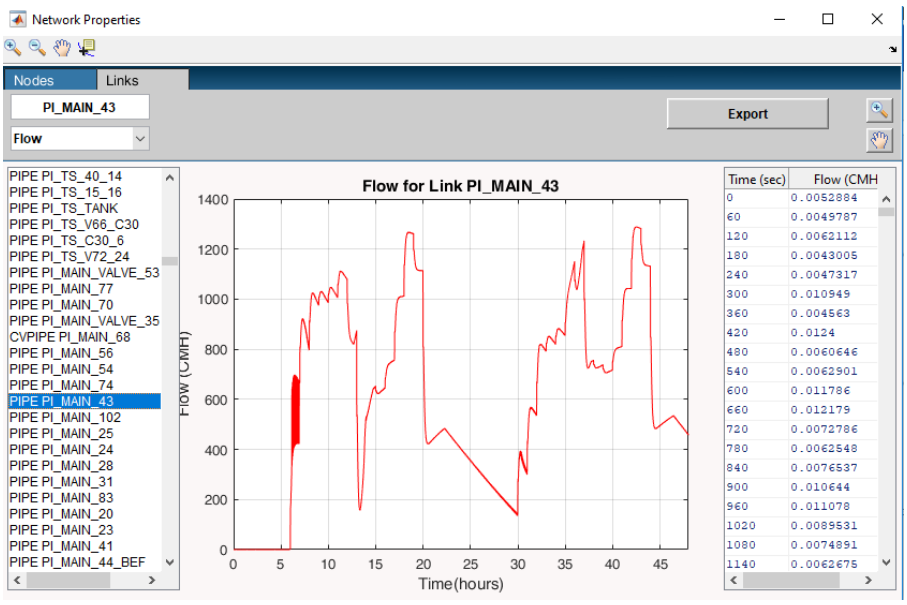

Figure 9: SmartWaters GUI. Example of flows results window, as developed in [1].

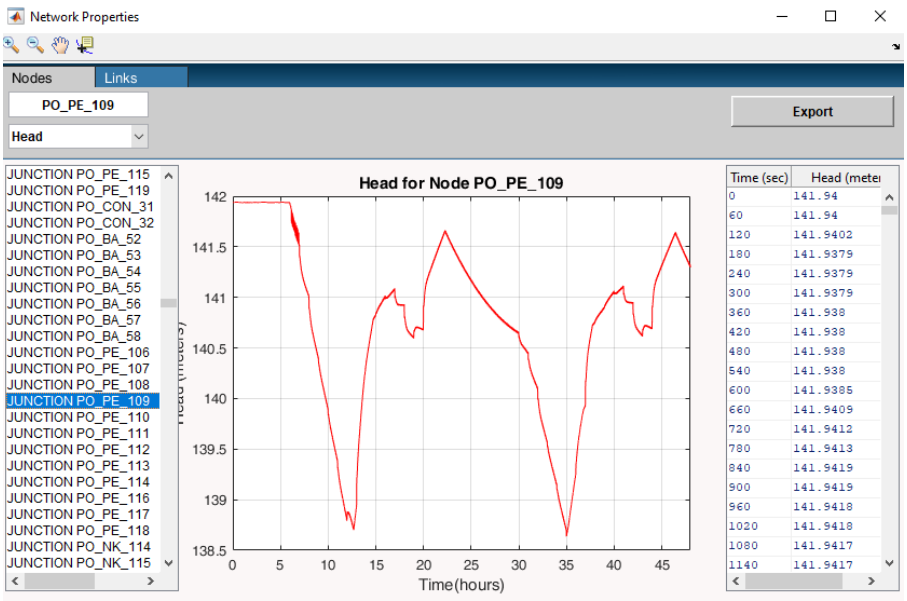

Figure 10: SmartWaters GUI. Example of pressures results window, as developed in [1].

4 Vlites pumping station proposed control algorithms

4.1 Under study main pumping station description

Vlites is the biggest pumping station of the under study irrigation water supply system, as described in Chapter 3. The elevation of the station is 83 m. The diagram of the pumping station is shown in Figure 11.

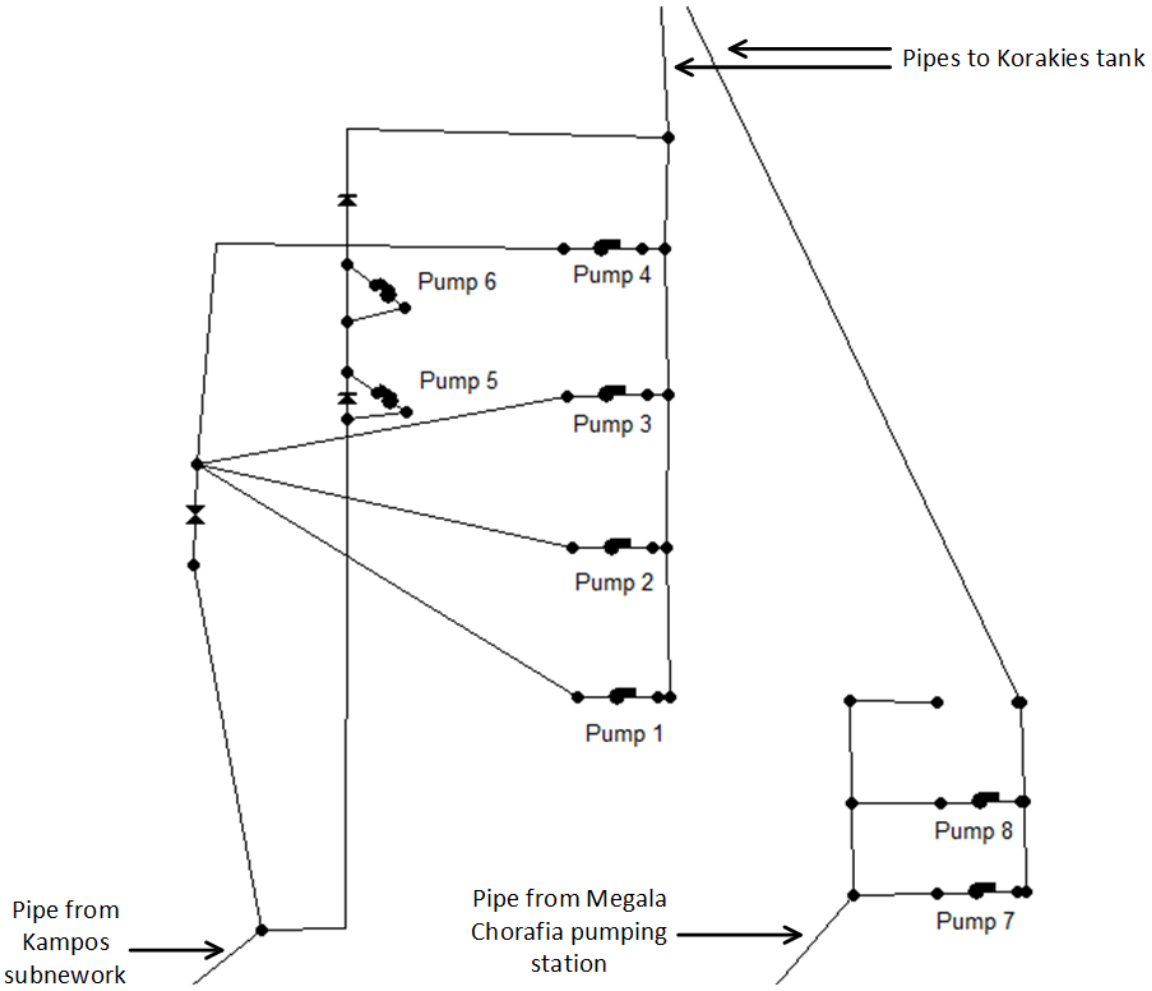

Figure 11: Vlites pumping station structure.

The pumping station is made up of 8 pumps, 7 of which can operate together due to demand requirements. Pump 4 exists for safety reasons if 1 of the other 3 similar pumps fails. Pumps 1 to 6 are inside Vlites pumping station building and the other 2 are outside. The basic characteristics of the pumps, as named in Figure 11 are shown in Table 2 and pump curves for each pump are figured in Appendix A.

Vlites station boosts the water to Korakies irrigation tank in order to feed the irrigation supply system of Akrotiri region. The elevation of Korakies irrigation tank is 212 m. The diameter of the tank is 37 m, the minimum tank level is 0.5 m and the maximum is 6 m. The total capacity of the tank is 6500 m^3. Figure 12 shows the whole region of Akrotiri, including the

location of Vlites pumping station and Korakies irrigation tank, Figure 13 shows the connection of the pumping station with Korakies Irrigation tank and Figure 14 shows the pipes which are connected with the tank.

Pump name	Installed power kW	Nominal flow m^3/h	Nominal rotational speed (RPM)	Type of pump
Pumps 1 to 6	250	350	1450	Deep well jet pumps
Pumps 5, 6	93	180	1450	Centrifugal pumps
Pumps 7, 8	186	300	2900	Booster pumps

Table 2: Main characteristics of Vlites pumps.

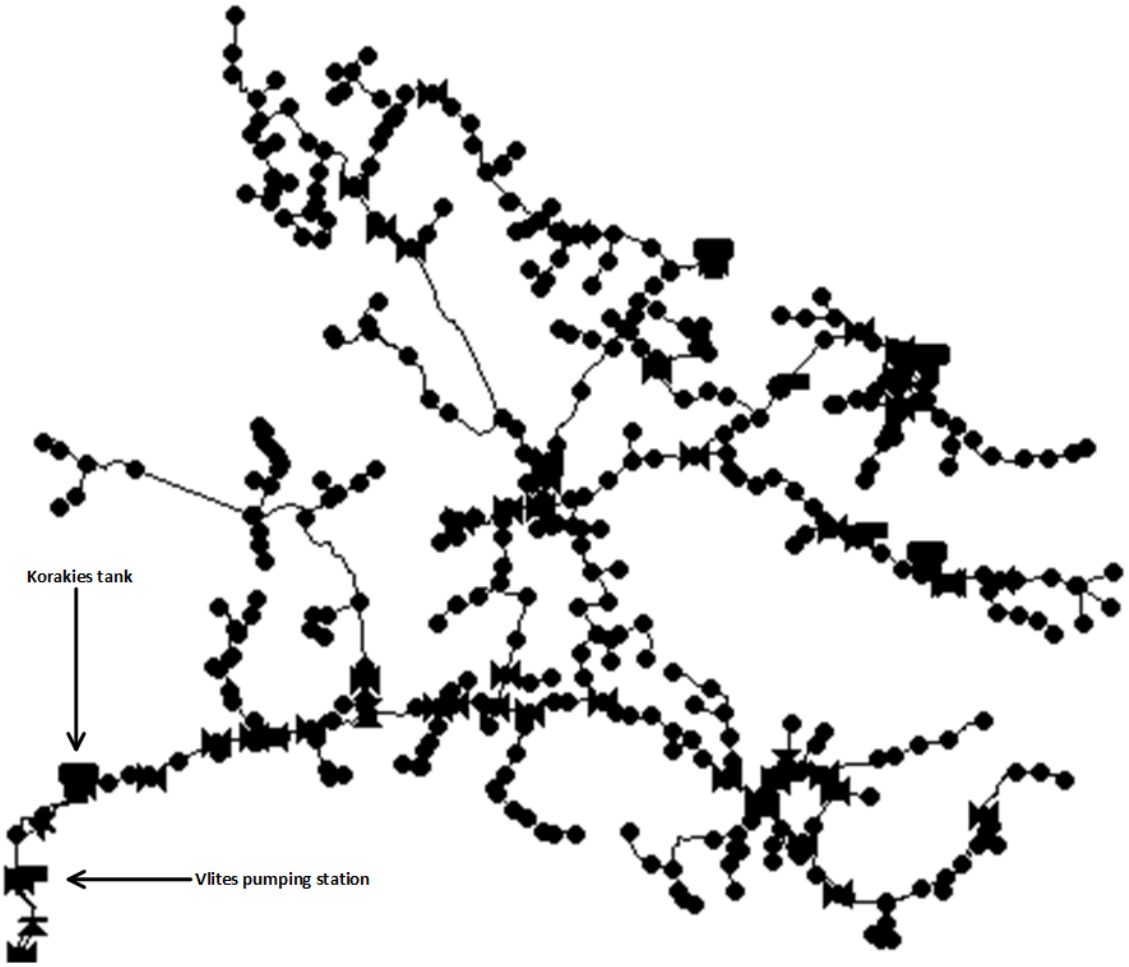

Figure 12: Akrotiri irrigation supply sub-network, consists of 547 nodes and 495 pipes.

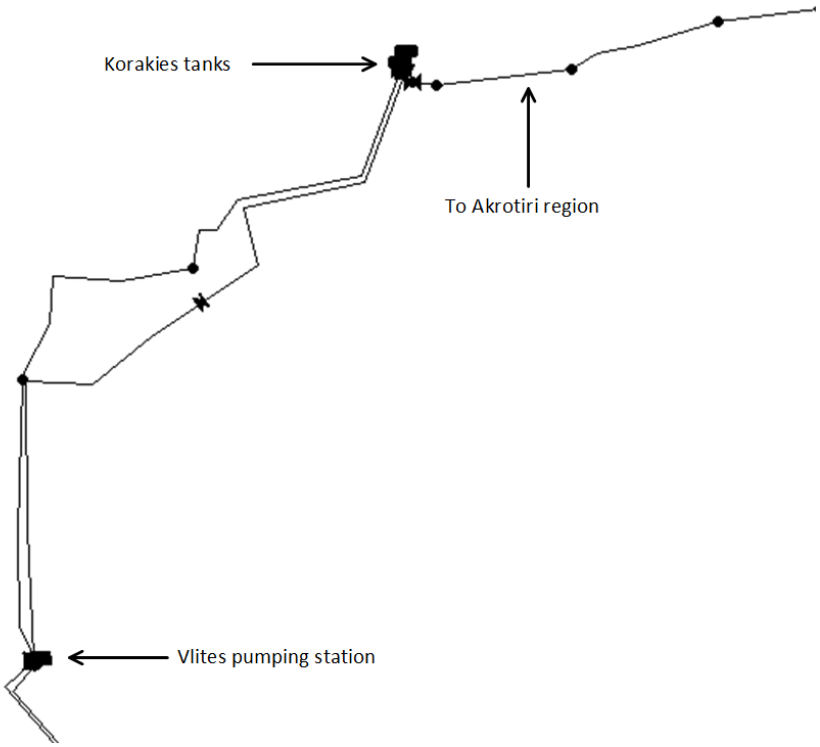

Figure 13: Connection of Vlites pumping station with Akrotiri tank. Vlites MSL is 83 m and Korakies tank is 212 m.

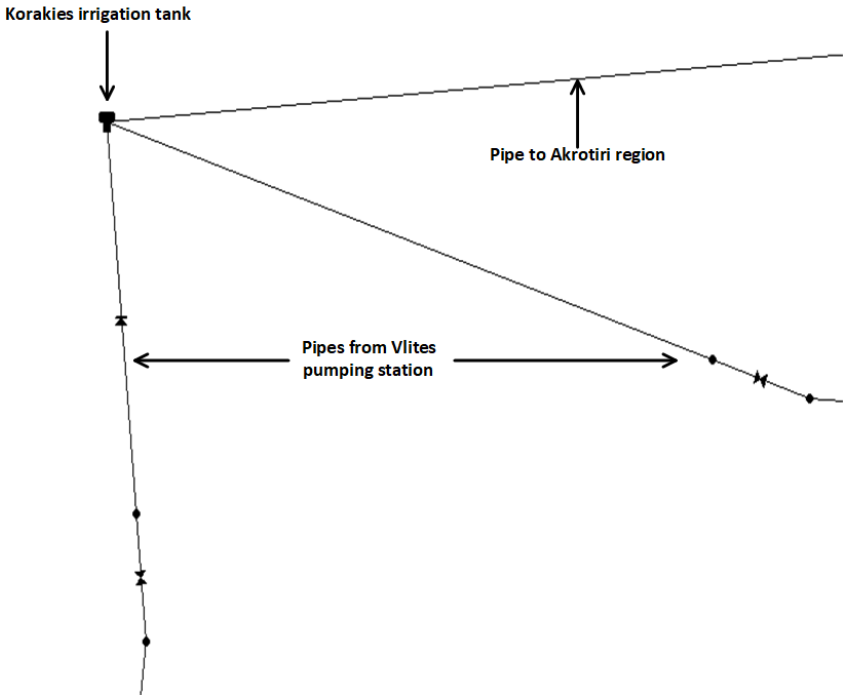

Figure 14: Korakies irrigation tank and connected pipes.

4.2 Proposed pumps scheduling control (ON/OFF) under constant speed operation based on boolean logic

A first approach to control the flow from Vlites pumping station to Korakies tank it's achieved by dividing the level of the tank in certain regions. Depending on the region where the tank level is, a combination of pumps operates, in order to deliver water to the tank of the system [1]. The input of the scheduling controller is the level of Korakies tank and the output is the pumps which will operate. Table 3 shows the tank level regions in m and the corresponding pumps which are operating. All pumps are operating in nominal speeds.

	Tank level region (m)	Pumps in operation
1	$Level > 5.5$	None
2	$5.3 < Level \leq 5.5$	Pump 1
3	$4.8 < Level \leq 5.3$	Pumps 1, 2
4	$3.9 \leq Level \leq 4.8$	Pumps 1, 2, 5
5	$3.1 \leq Level \leq 3.9$	Pumps 1, 2, 5, 7
6	$2.5 \leq Level \leq 3.1$	Pumps 1, 2, 5, 7, 8
7	$Level \leq 2.5m$	Pumps 1, 2, 3, 5, 7, 8

Table 3: Tank level regions and corresponding active pumps on pumps scheduling control.

4.3 Proposed pumps scheduling control under variable speed operation based on boolean logic

Variable speed operation can reduce the consumed energy of the pumping station. The aim of this control method is to keep the tank level within certain limits, by scheduling in real time the combination of Vlites pumps, which will be active and the speed of the pump would be operating in variable speeds [1]. In the present study, Pump 1 was selected to operate in variable speeds because it has one of the highest energy consumptions in the whole pumping station, and it is the first of the pumps, which will be active. The controller uses, as input, the current level of Korakies tank,$L(t_1)$, and the previous tank level, $L(t_2)$, in order to calculate the changing rate of the tank level, $DL(t_2 - t_1)$. The output of the present controller is the combination of the pumps which are operating and the speed of the pump which operates in variable speeds. In the under study system, the changing rate of the Korakies tank is calculated every minute. Depending on the changing rate, the variable speed pump operates in a specific discrete speed. The minimum shaft speed of Pump 1, in order to lift the water to Korakies tank is set 80 % of Pump 1 nominal rotational speed. Due to affinity laws, the maximum reduction of the power by reducing the speed of the pump to 80 % is approximately 128 kW.

The combination of the operating pumps at each time depends on the level of Korakies tank and it is the same as pumps scheduling control under constant speed operation.

4.4 Proposed PI(D) pumps control method based on tank level control

4.4.1 Tank level system

Another way to control the water flow of Vlites pumping station and the level of Korakies tank, is by using a PI and a PID controller. A water tank level controller can be implemented to control the tank level by keeping that in a specific reference point. This approach is presented in Figure 15. This idea can be applied to the under study pumping station, because Vlites pumping station supplies Korakies tank with water.

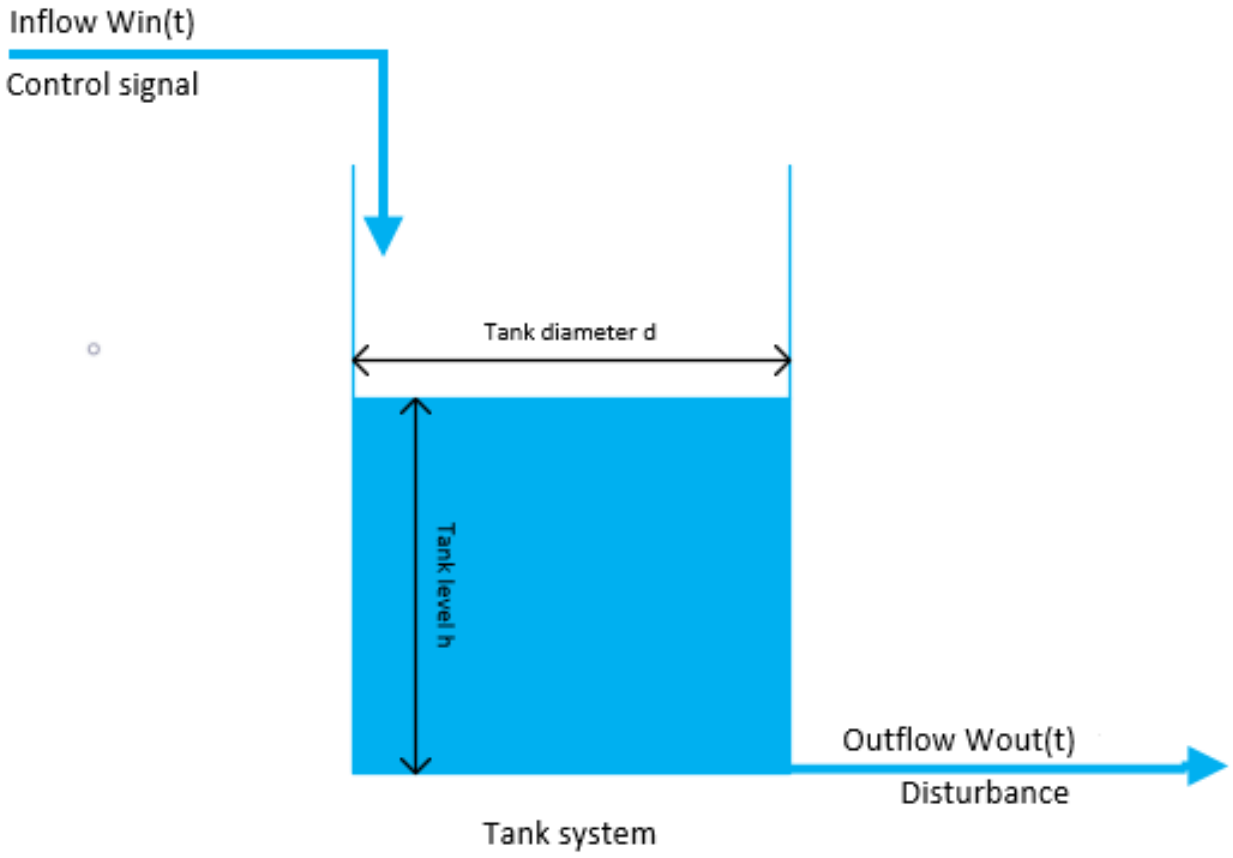

Figure 15: Tank level control scheme

Using the automatic control theory, the tank represents the plant of the system, the outflow represents the disturbance because it is an unknown variable and the inflow represents the control signal of the under study system [1, 13].

4.4.2 Mathematical model

Let $w_{in}(t)$ to be the mass supply flow at time t, $w_{out}(t)$ the mass output flow at time t and $m(t)$ the mass of the liquid at time t. Due to law of conservation of mass:

$$m(t) = w_{in}(t) - w_{out}(t) \tag{8}$$

The mass of the liquid at time t is $m(t) = dAh(t)$ where d is the density of the liquid in kg/m^3, A is the tank section in m^2, and $h(t)$ the height of the liquid inside the tank in m at time t. In the above system the liquid is the water. Replacing the above relation in equation 8, equation 9 is produced [1, 14].

$$Ah(t) = w_{in}(t) - w_{out}(t) \tag{9}$$

In the case of constant flow (feeding through a pumping station) is equal to the output flow, the level of the water tank remains constant.

Based on Equation 9, where $Dh(t)$ is the controlled value and $u(t) = w_{in}(t)$ is the execution value, the transfer function for the variation of the supply flow, $w_{in}(t)$ to the water level variation $Dh(t)$ is:

$$h(s) = \frac{1}{sA} w_{in}(s) - \frac{1}{sA} w_{out}(s) + \frac{1}{s} h(0^-) \tag{10}$$

In equation 10, $h(0^-)$ represents the initial level of Korakies tank.

Considering that system's operation starts from a known initial condition, by using Equation 10, the transfer function of the tank level system, in which the input represents the inflow of the tank from Vlites pumping station minus the outflow of the tank to Akrotiri region, $w_{in}(s) - w_{out}(s)$ and the output represents the level of the tank, $h(s)$, is:

$$G_p(s) = \frac{h(s)}{w_{in}(s) - w_{out}(s)} = \frac{1}{As} e^{-Ts} \tag{11}$$

where T represents the delay of the system. For reasons of simplicity, the delay is not taken into account. The block diagram of the closed loop system, based on Equation 11, is presented in Figure 16.

The Controller decides the flow must be given from the pumping station to the tank in order to keep the tank level in a given reference height. The section of Korakies tank, A, is 1075 m^2. There are some basic constraints related with the operation of the controller which must be taken into account.

The tank has a specific height and capacity. Firstly the tank level should not overflow neither become empty.

The second constraint deals with the limits of the pumping station. The flow of the water from the pumping station to tank, can not be negative. Also the pumping station has an upper flow limit which it can reach.

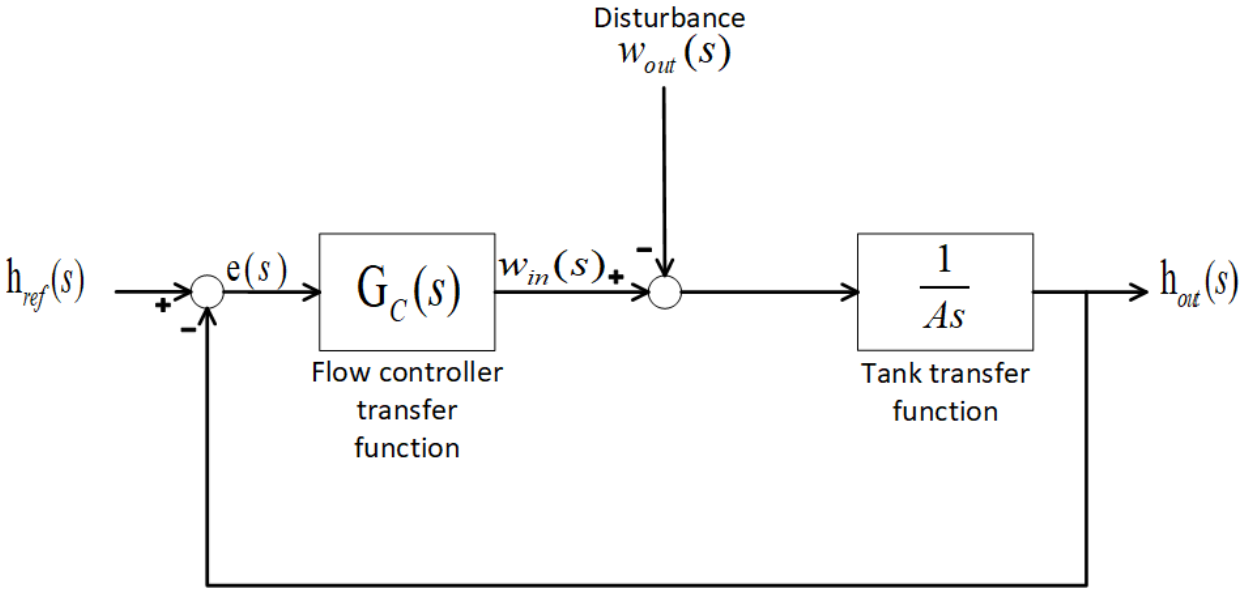

Figure 16: Tank level control closed loop system. w_{out} models the demand requirements of the network in Akrotiri region. The h_{out} is the level of the tank.

Taking into consideration those two basic constraints, the control of the flow of the pumping station can be achieved by using a PI controller as the specific process in Figure 16 is a first order system [15]. For examination purposes, a PID controller was also designed.

4.4.3 PI controller tuning for Korakies tank level control

The transfer function of a parallel PI controller is defined in Equation 12.

$$G_{C,PI}(s) = K_p + \frac{K_i}{s} \tag{12}$$

where K_p and K_i are the proportional and integral terms of the controller. By using the transfer function of the parallel PI controller in the closed loop system of Figure 16, the transfer function of the closed loop system is:

$$Gcl_{PI}(s) = \frac{K_p s + K_i}{1075s^2 + K_p s + K_i} \tag{13}$$

By using the transfer function of Equation 13, Routh–Hurwitz stability criterion is used [16], in order to be found the ranges of K_p and K_i in which the under study closed loop system is stable. The Routh's stability matrix is:

$$\begin{array}{c|cc} s^2 & 1075 & K_i \\ s^1 & K_p & 0 \\ s^0 & K_i & - \end{array} \tag{14}$$

By using the Routh–Hurwitz stability criterion and the matrix, as calculated in 14, the under study system is stable, if $K_p > 0$ and $K_i > 0$.

In order to apply the PI in SmartWaters framework and control the flow of the main pumping station, the parameter gains of the controller must be tuned. PI controllers are very popular, but tuning process is not something trivial.
To calculate sufficient values for the gains of the PI controller, the model of the tank level control system, as shown in Figure 16, was modeled and simulated in Matlab Simulation and Model Based Design (Simulink) in order to use PID Tuner graphical tool [17] which is very suitable for controllers tuning proposes. Also a disturbance time-series was created (Figure 17), in order to simulate the behaviour of the closed loop system and to tune the parameters of the PI controller. The selection of the disturbance time- series is based on the real consumption data of the under study network [1].
PID tuner provides controller gains in order for a good balance to be achieved between performance and robustness for PI and PID controllers.
Initially it creates a linearised model by taking into consideration the combination of all blocks between the input and the output of the controller block. The Matlab graphical interface of the PID tuner gives the opportunity to change two main variables, in order to find suitable gains for the controller. Those two variables are the response time and the transient behaviour of the controller. Changing the values of these two parameters, changes the gains of the PI controller. Also an input disturbance step plot exists, in order to give a graphical information about the rejection of the disturbance during the tuning of the controller.

	Model parameter	Value
1	Total simulation duration	72 h
2	Simulation time-step	1 min
3	Tank reference height	5.5 m
4	Tank upper bound	6 m
5	Tank lower bound	0.5 m

Table 4: Matlab tuning procedure. Simulink simulation parameters.

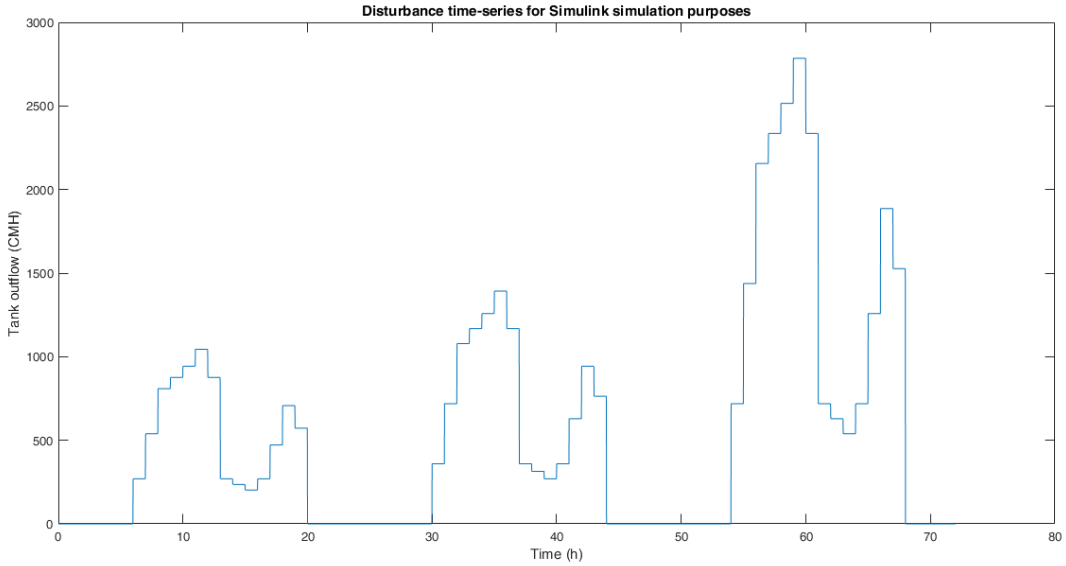

Figure 17: Simulink model disturbance time-series ($w_{out}(t)$) for the tuning processes of the PI and PID controllers, which models the demand requirements in Akrotiri region, as shown in Figure 16.

By using the above method to tune the PI controller and making many trials, by changing the parameters of the PID tuner tool in order to minimize the overshoot of the system response and taking into consideration the restrictions of the tank level problem, as mentioned above, the extracted PI gains are presented in Table 5. The results of the closed loop system, after the tuning of the PI controller are shown in Figure 18.

	PI controller parameter	Gain (unitless)
1	Proportional gain (K_p)	3175.45625
2	Integral gain (K_i)	12

Table 5: Results of PI tuning process. Tuned PI controller gains.

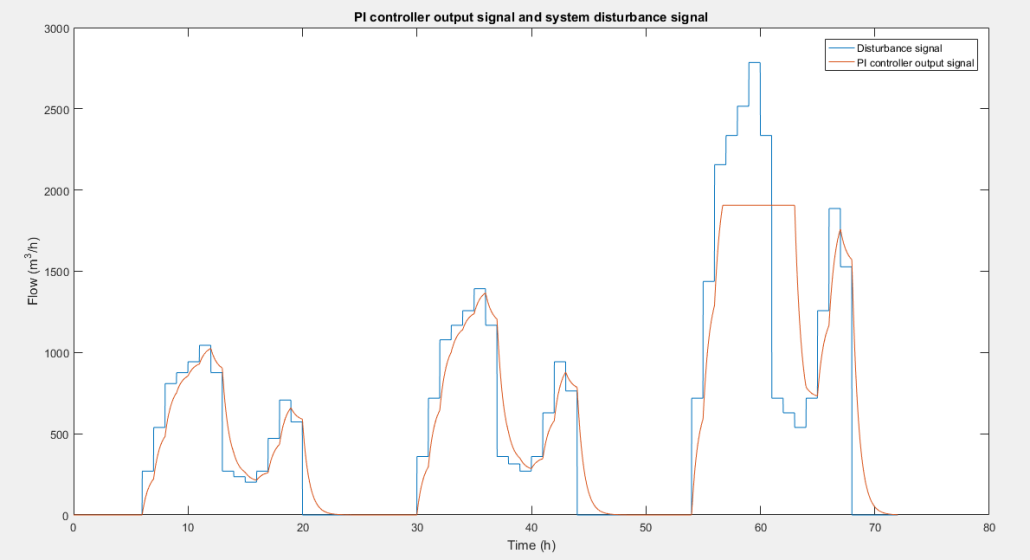

(a) PI controller signal time series, represents tank inflow and disturbance time series, represents tank outflow (system's demand). Settling time is 1 h.

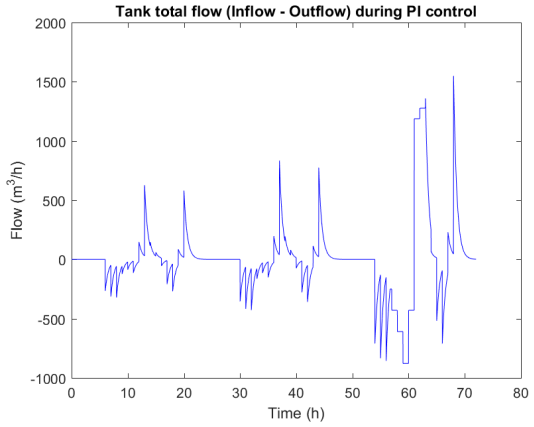

(b) Tank total feed flow time series represents the tank inflow minus outflow.

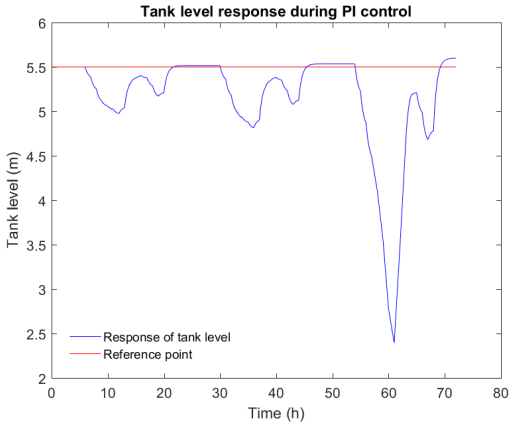

(c) Tank level time series. Red line represents the reference level of the tank.

Figure 18: Matlab simulink simulation testing results for tuned PI controller.

4.4.4 PID controller examination

The transfer function of a parallel PID controller is defined in Equation 15.

$$G_C(s) = K_p + \frac{K_i}{s} + K_d s \tag{15}$$

By using the transfer function of the parallel PID controller in the closed loop system of Figure 16, the transfer function of the closed loop system is:

$$Gcl_{PID}(s) = \frac{K_d s^2 + K_p s + K_i}{(K_d + 1075)s^2 + K_p s + K_i} \tag{16}$$

By using the transfer function of Equation 16, Routh–Hurwitz stability criterion is used [16], in order to be found the ranges of K_p, K_i and K_d in which the under study closed loop system is stable. The Routh's stability matrix is:

$$\begin{array}{c|cc} s^2 & K_d + 1075 & K_i \\ s^1 & K_p & 0 \\ s^0 & K_i & - \end{array} \tag{17}$$

By using the Routh–Hurwitz stability criterion and the matrix, as calculated in 17, the under study system is stable, if $K_p > 0$, $K_i > 0$ and $K_d > -1075$.

Except for the PI controller, which is sufficient for first order systems, a D parameter is inserted in the above PI controller, by keeping P and I gains the same as in the PI controller, in order to examine the behaviour and the effects of the derivative gain to the system. For small gains, the D parameter does not affect the system. The gains are calculated by simulating and increasing the value of the derivative gain until it affects the system. The parameters of the examined PID controller are presented in Table 6. The examination results of the PID controller gains are shown in Figure 19. Also an effort was made in order for suitable gains to be found by using PID Tuner tool. Each tuning trial failed because some of the problem restrictions were violated.

	PID controller parameter	Gain (unitless)
1	Proportional gain (K_p)	3175.45625
2	Integral gain (K_i)	12.00000
3	Derivative gain (K_d)	390.00000

Table 6: Results of PID tuning process. Tuned PID controller gains.

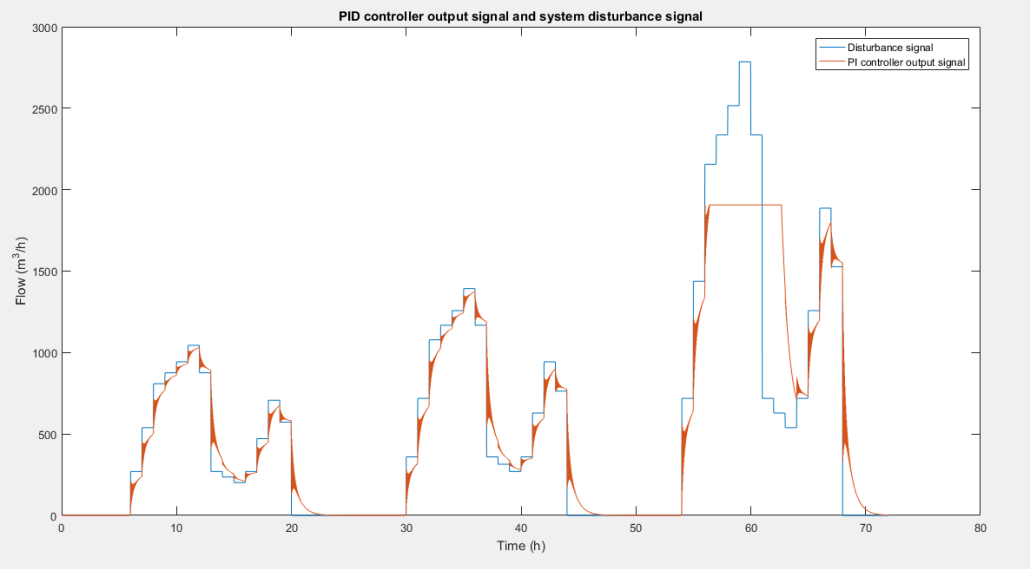

(a) PID controller signal time series, represents tank inflow and disturbance time series, represents tank outflow (system's demand). Worst settling time is 1 h.

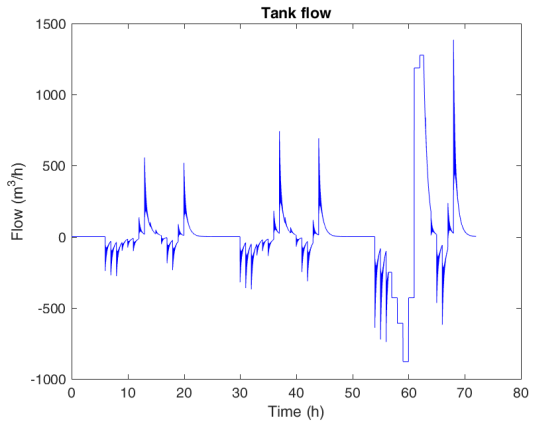

(b) Tank total feed flow time series represents the tank inflow minus outflow.

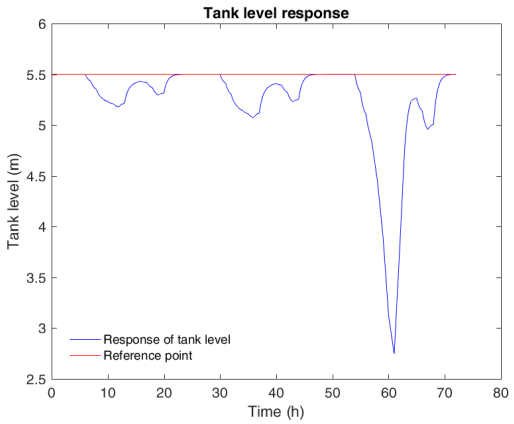

(c) Tank level time series. Red line represents the reference level of the tank.

Figure 19: Matlab simulink simulation testing results for tuned PID controller.

4.4.5 Pumping station flow matching

The PI and PID controllers, as designed above, decide indirectly the required flow must be given from the main pumping station to the tank, by keeping the tank level in a specific level. The main pumping station has 8 operating pumps. According to this, there is a need of matching the operation of the pumps with the decided flow. This pairing is shown in Table 7. The speed of Pump 1, which is set to operate in variable speeds, has a minimum permitted speed limit, 80 % of pump's nominal speed, in order to operates in Best efficiency Point (BEP) region in which affinity laws can be applied.

	Flow Q (m^3/h)	Pumps in operation (Var. speeds)
1	$Q \leq 0$	All pumps off
2	$0 < Q \leq 350$	Pump 1
3	$350 < Q \leq 530$	Pumps 1, 5
4	$530 < Q \leq 700$	Pumps 1, 2
5	$700 < Q \leq 880$	Pumps 1, 2, 5
6	$880 < Q \leq 1180$	Pumps 1, 2, 5, 7
7	$1180 < Q \leq 1480$	Pumps 1, 2, 5, 7, 8
8	$1480 < Q$	Pumps 1, 2, 3, 5, 7, 8

Table 7: Vlites pumping station pumps proposed operation, based on pumps flow capacity and tank level regulation.

4.4.6 Stability, controllability and observability of the tank level control closed loop system after PI and PID controllers tuning

In order to characterize the closed loop system of Figure 16 after the tuning of the controllers, the transfer functions of the closed loop system, when the tank is controlled by the PI and the PID controllers, were calculated. Equation 18 shows the transfer function of the closed loop system, $Gcl_{PI}(s)$, when the PI controller is used and Equation 19 shows the corresponding transfer function,$Gcl_{PID}(s)$ when the PID controller is applied.

$$Gcl_{PI}(s) = \frac{3175s + 12}{1075s^2 + 3175s + 12} \tag{18}$$

$$Gcl_{PID}(s) = \frac{390s^2 + 3175s + 12}{1465s^2 + 3175s + 12} \tag{19}$$

From the transfer function of Equation 18 turns out that the poles of the closed loop system, when the PI controller is set, are $p_{1,PI} = -2.9496$ and $p_{2,PI} = -0.0038$. The transfer function has one zero, which is $z_{1,PI} = -0.0038$. The pole - zero map of this transfer function is shown in Figure 20. As for the transfer function of the closed loop system, when the PID controller is applied, the poles are $p_{1,PID} = -2.1635$ and $p_{2,PID} = -0.0038$ and the zeros are $z_{1,PID} = -8.1384$ and $z_{2,PID} = -0.0038$. The pole - zero map of the transfer function of PID case is shown in Figure 21.

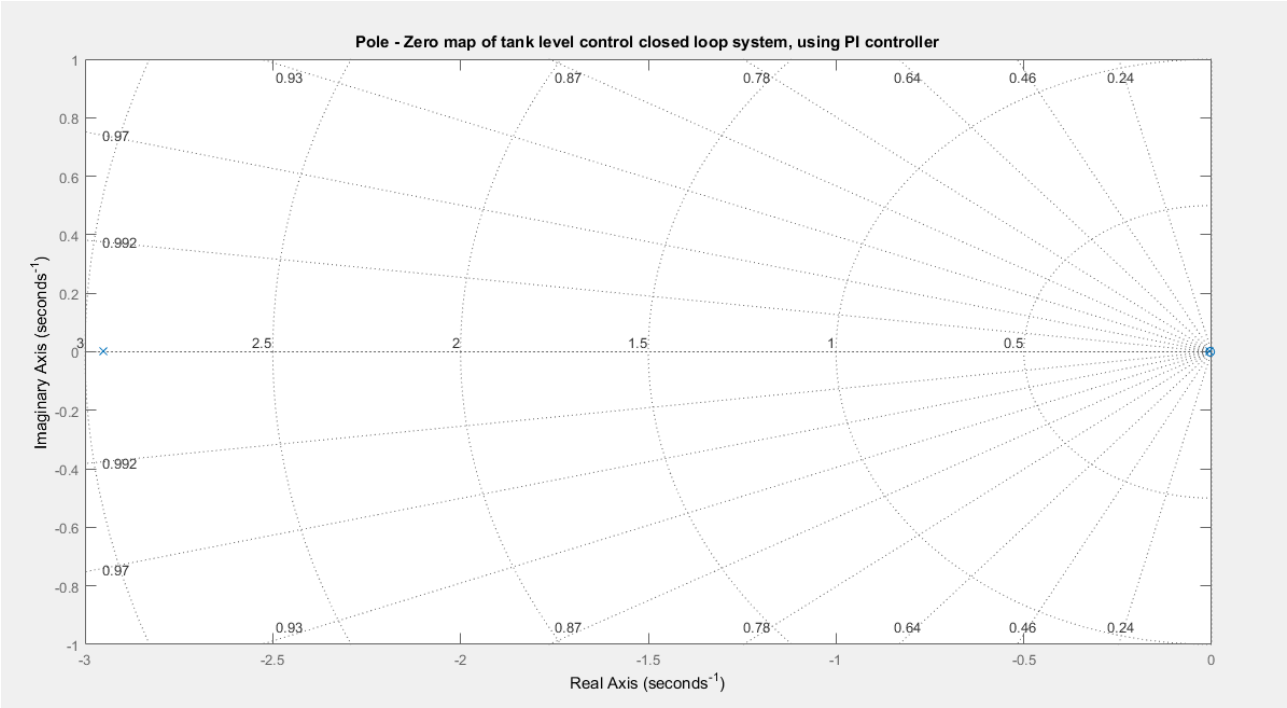

Figure 20: Pole - zero map (s-plane) of tank level closed loop system, when the PI controller is applied. Poles are symbolized as x and zeros as o.

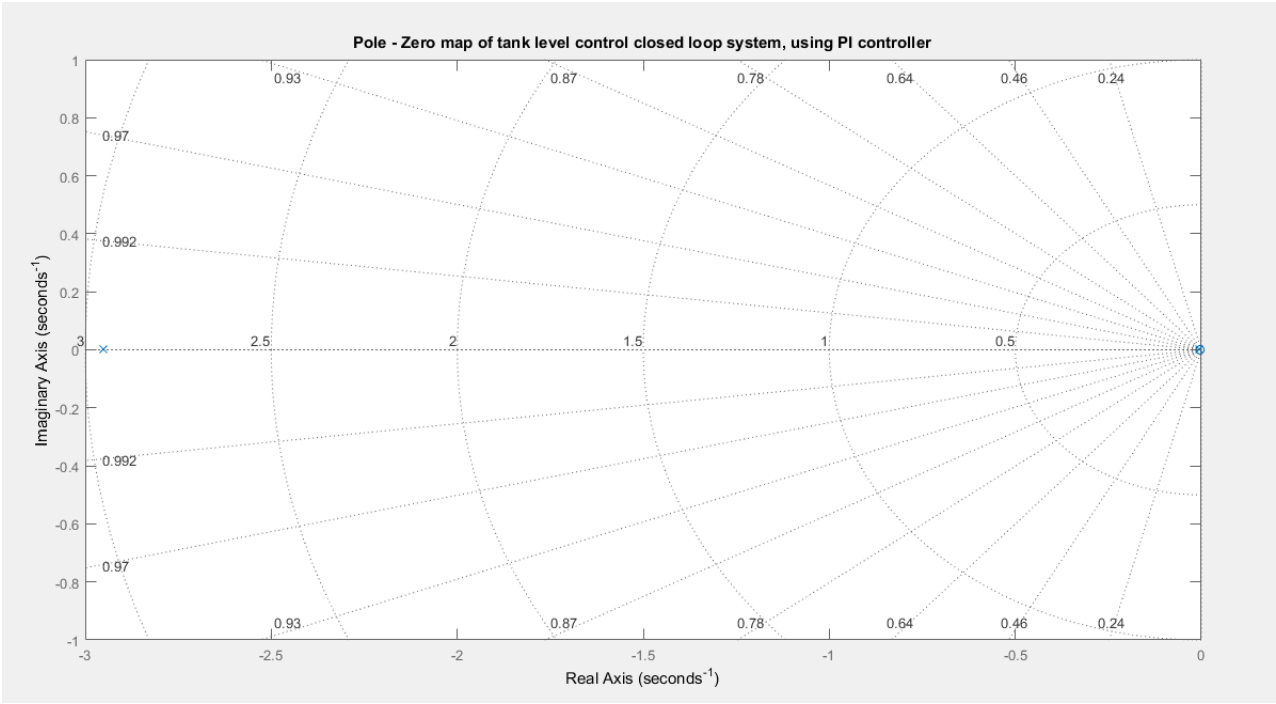

Figure 21: Pole - zero map (s-plane) of tank level closed loop system, when the PID controller is applied. Poles are symbolized as x and zeros as o.

From the position of the system's poles in both PI and PID cases, is concluded that both closed loop systems are stable, because the poles are on the left semi-plane of the poles - zeros s-plane map [18].

In order to examine the controllability and the observability of the closed loop system the system must be represented in the state space. The state space matrices, after thee transformation of the system [19], when the PI controller is used, are shown in Equations 20, 21, 22 and 23 and when the PID controller is used, are shown in Equations 24. 25, 26 and 27.

$$\mathbf{A_{PI}} = \begin{pmatrix} -2.9535 & -0.0112 \\ 1.0000 & 0 \end{pmatrix} \tag{20}$$

$$\mathbf{B_{PI}} = \begin{pmatrix} 1 \\ 0 \end{pmatrix} \tag{21}$$

$$\mathbf{C_{PI}} = \begin{pmatrix} 2.9535 & 0.0112 \end{pmatrix} \tag{22}$$

$$\mathbf{D_{PI}} = \begin{pmatrix} 0 \end{pmatrix} \tag{23}$$

$$\mathbf{A_{PID}} = \begin{pmatrix} -2.2.1672 & -0.0082 \\ 1.0000 & 0 \end{pmatrix} \tag{24}$$

$$\mathbf{B_{PID}} = \begin{pmatrix} 1 \\ 0 \end{pmatrix} \tag{25}$$

$$\mathbf{C_{PID}} = \begin{pmatrix} 1.5903 & 0.0060 \end{pmatrix} \tag{26}$$

$$\mathbf{D_{PID}} = \begin{pmatrix} 0.2662 \end{pmatrix} \tag{27}$$

In order to examine if a system is controllable, the controllability matrix must be calculated. The controllability matrix of a system is defined in Equation 28 [20].

$$\mathbf{Co}(\mathbf{A}, \mathbf{B}) = \begin{pmatrix} \mathbf{B} & \mathbf{AB} & \mathbf{A^2B} & \dots & \mathbf{A^{n-1}B} \end{pmatrix} \tag{28}$$

In Equation 28, $\mathbf{Co}(\mathbf{A}, \mathbf{B})$ represents the controllability matrix, $\mathbf{A}$ and $\mathbf{B}$ the matrices of the system and n, the order of the system. The controllabily matrix of the under study closed loop system, when the PI controller is applied, is shown in Equation 29 and when the PID controller is used, is shown in Equation 30.

$$\mathbf{Co_{PI}}(\mathbf{A_{PI}}, \mathbf{B_{PI}}) = \begin{pmatrix} 1.0000 & -2.9535 \\ 0 & 1.0000 \end{pmatrix} \tag{29}$$

$$\mathbf{Co_{PID}}(\mathbf{A_{PID}}, \mathbf{B_{PID}}) = \begin{pmatrix} 1.0000 & -2.1672 \\ 0 & 1.0000 \end{pmatrix} \tag{30}$$

In order to be a system controllable, the order of the system must be equal to the rank of controllability system's matrix. In both cases, the ranks of the controllability matrices are the same with the order of the systems. This fact proves, that the under study closed loop system

in both PI and PID control methods, is controllable, because the rank of $\mathbf{Co_{PI}}$ and $\mathbf{Co_{PID}}$ is 2, the same as the corresponding system's order.
The examination of the system's observability is required the observability matrix, which is defined in Equation 31 [21].

$$\mathbf{O}(\mathbf{A},\mathbf{C}) = \begin{pmatrix} \mathbf{C} \\ \mathbf{AC} \\ \mathbf{A^2C} \\ \vdots \\ \mathbf{A}^{n-1}\mathbf{C} \end{pmatrix} \tag{31}$$

In Equation 31, $\mathbf{O}(\mathbf{A},\mathbf{C})$ represents the observability matrix, $\mathbf{A}$ and $\mathbf{C}$ the matrices of the system and n, the order of the system. The observability matrix of the under study closed loop system, when the PI controller is applied, is shown in Equation 32 and when the PID controller is used, is shown in Equation 33.

$$\mathbf{O_{PI}}(\mathbf{A_{PI}},\mathbf{C_{PI}}) = \begin{pmatrix} 1.9535 & -0.0112 \\ -8.7119 & -0.0330 \end{pmatrix} \tag{32}$$

$$\mathbf{O_{PID}}(\mathbf{A_{PID}},\mathbf{C_{PID}}) = \begin{pmatrix} 1.5903 & -0.0060 \\ -3.4405 & -0.0130 \end{pmatrix} \tag{33}$$

In order to be a system observable, the order of the system must be equal to the rank of observability system's matrix. In both cases, the ranks of the observability matrices are the same with the order of the systems. This fact proves, that the under study closed loop system in both PI and PID control methods, is observable, because the rank of $\mathbf{O_{PI}}$ and $\mathbf{O_{PID}}$ is 2, the same as the corresponding system's order.

4.5 Test of the proposed control algorithms by using SmartWaters framework for the OAK.AE simulated model

4.5.1 SmartWaters simulation scenario

For the tests of the proposed control algorithms, is used the framework SmartWaters [1]. The simulation parameters used for the hydraulic simulation, via Epanet, of the OAK.AE distributed water supply system, are set as shown in Table 8.

	SmartWaters's GUI parameter	Value
1	Total simulation duration	12 days
2	hydraulic analysis time-step	1 minute
3	Pattern time step	1 hour
6	Flow units (Q)	m^3/h
7	Pressure units (P)	m

Table 8: SmartWaters simulation parameters.

4.5.2 Water demand scenario

The multipliers and the demand data for each node are based on real consumption data of OAK.AE. network.

The water demand profile, which is used for testing, the proposed control algorithms, is based on real data, as they are calculated by the SmartWaters team [1]. Every consumption node of the network has a base demand. The total base demand of the under study system is 1514 m^3/h. The total base demand of Akrotiri sub-network is 561.48 m^3/h. To change the consumption of the system during the simulation, two demand patterns were implemented, a daily demand pattern which provides hourly multipliers and it is the same for each simulation day (Figure 22) and a total pattern which provides multipliers for every day (Figure 23). The demand of each consumption node at a given simulation hour is calculated by multiplying the base demand of the node with the corresponding multipliers from Figures 22 and 23. The consumption data for each simulation day represents a typical day of each month of the real under study network [1].

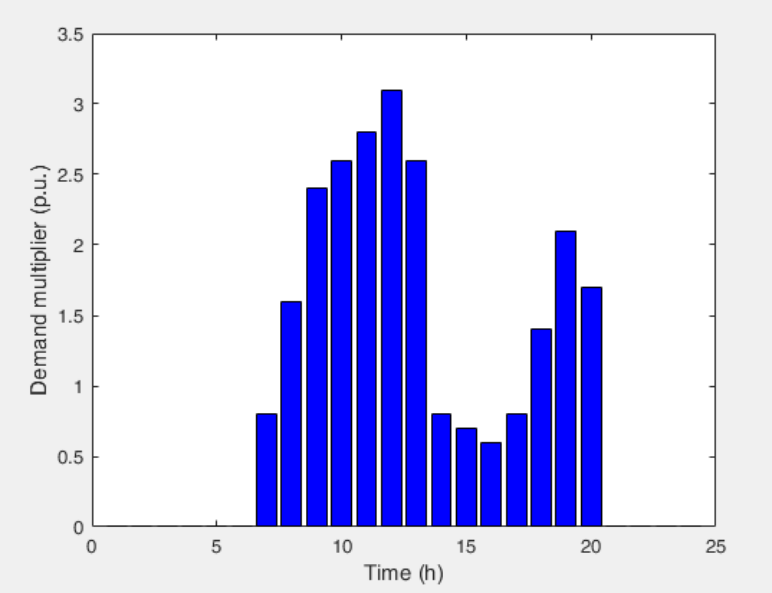

Figure 22: Standard daily demand multipliers, based on real data [1].

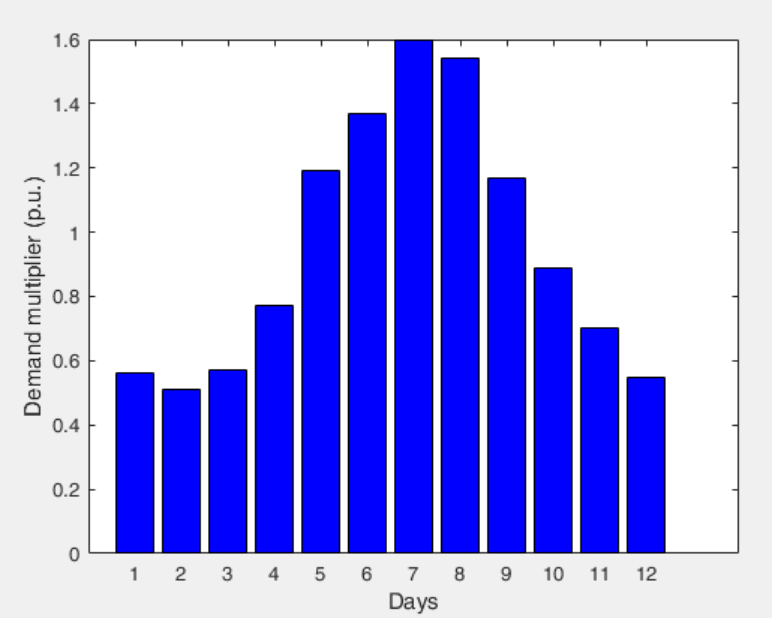

Figure 23: Demand multipliers for each day of simulation.

4.6 Testing simulation results and discussion

In order to examine and compare the efficiency of the PI, PID, pumps scheduling under constant speed operation based on boolean logic and pumps scheduling under variable speed operation based on boolean logic tank level controllers, two basic types of graphs are exported, for each controller. The first is the Korakies tank level response during the simulation of each method and the second is the outflow of Vlites pumping station. Also the total energy consumption of the pumping station was calculated and is presented in Table 9.

The figures for all the control methods for the overall duration of simulation can be found in Appendix B.

In the following figures the results for each control method for 2 simulation days,3^{d} and 7^{th} days are presented.

Figure 24 refers to Proposed pumps scheduling control (ON/OFF) under constant speed operation based on boolean logic, Figure 25 refers to Proposed pumps scheduling control under variable speed operation based on boolean logic, Figure 26 refers to PI control based on tank level control results and Figure 27 refers to PID control based on tank level control results.

Also an important metric, in order to compare the proposed and the examined control methods, is the total consumed energy of the pumping station at each control method.

	Control method	Energy consumption (kW)	Percentage energy reduction (%)
1	Proposed pumps scheduling control (ON/OFF) under constant speed operation based on boolean logic	84204.78	Reference method
2	Proposed pumps scheduling control under variable speed operation based on boolean logic	81193.66	3.58
3	PI pumps control method based on tank level control	82581.59	1.93
4	PID pumps control method based on tank level control	81847.36	2.80

Table 9: Vlites energy consumption for all control methods.

By comparing the energy results, it can be noted that pumps scheduling control under variable speed operation based on boolean logic has the minimum energy consumption. All the above examined control methods reduce the energy consumption in relation with the pumps scheduling control (ON/OFF) under constant speed operation based on boolean logic method. The PID control method has smaller energy consumption than the PI control method. Examining the tank level response during the operation of the controllers, it is observed, in Figures 26 and 27, that PI and PID controllers have the fastest response and the minimum error for all simulation days. Also the decision flow of the PI controller is very smooth. PID control method shows small oscillations when the demand of the systems changes. Those oscillations arise from the effect of the PID derivative gain. It seems that PI and PID controllers exploit better the variable speed operation of the variable speed pump compared with Smart control method. Finally it is observed that PI controller presents a small steady state error compared with PID controller which eliminates this error in all simulation days.

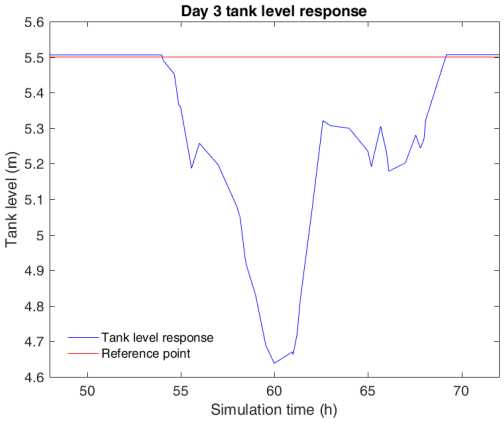

(a) Third day tank level response.

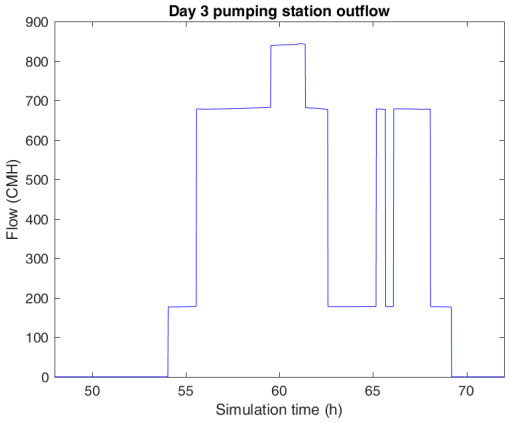

(b) Third day given flow from Vlites pumping station to Korakies tank.

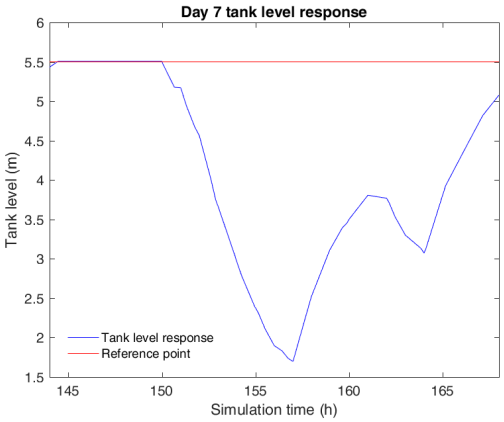

(c) Seventh day tank level response.

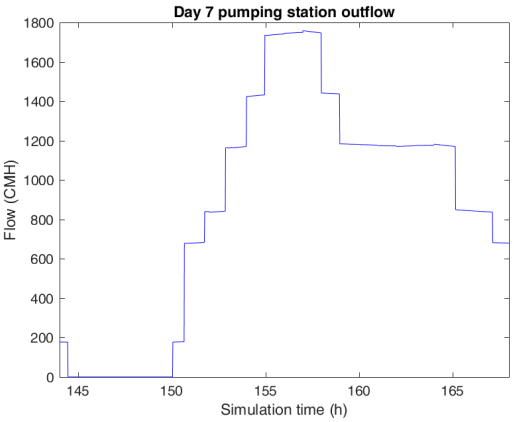

(d) Seventh day given flow from Vlites pumping station to Korakies tank.

Figure 24: Pumps scheduling control (ON/OFF) under constant speed operation based on boolean logic simulation results for third and sixth day.

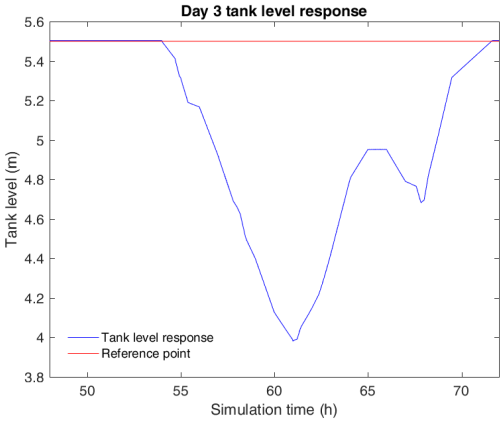

(a) Third day tank level response.

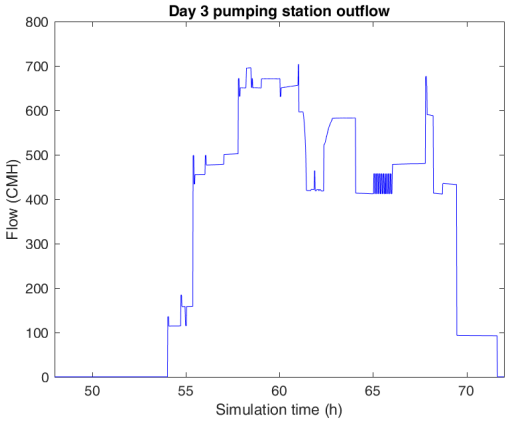

(b) Third day given flow from Vlites pumping station to Korakies tank.

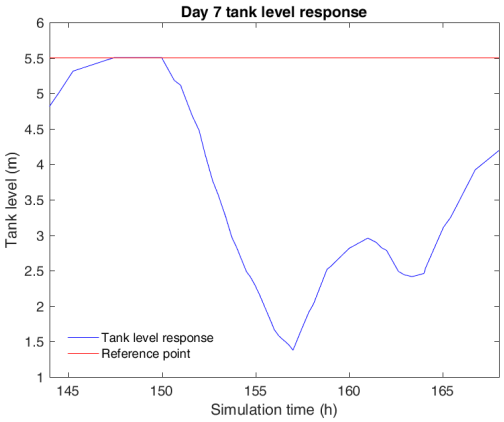

(c) Seventh day tank level response.

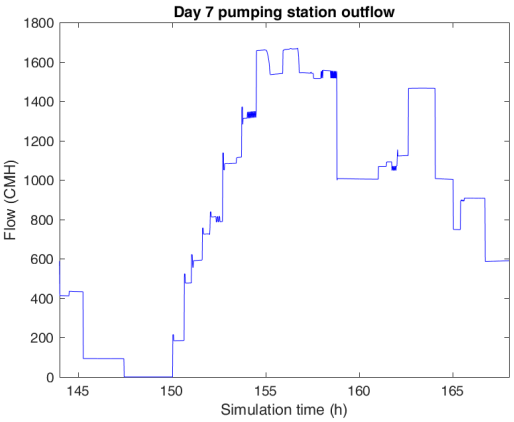

(d) Seventh day given flow from Vlites pumping station to Korakies tank.

Figure 25: Pumps scheduling control under variable speed operation based on boolean logic simulation results for third and sixth day.

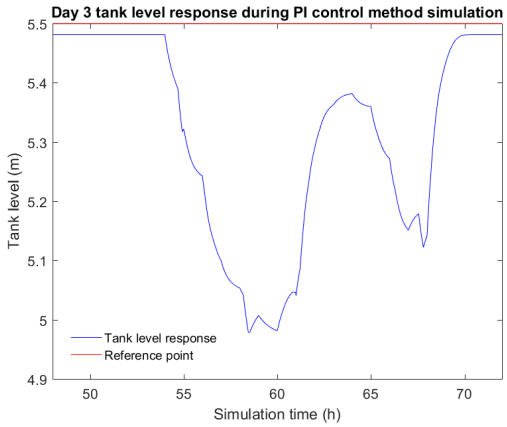

(a) Third day tank level response.

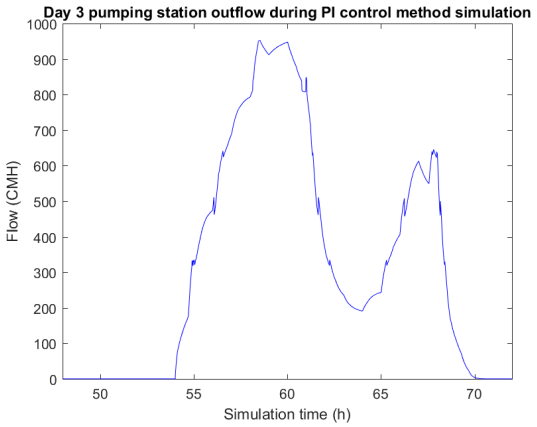

(b) Third day given flow from Vlites pumping station to Korakies tank.

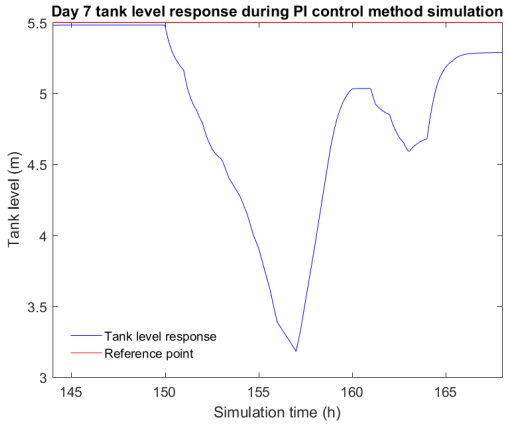

(c) Seventh day tank level response.

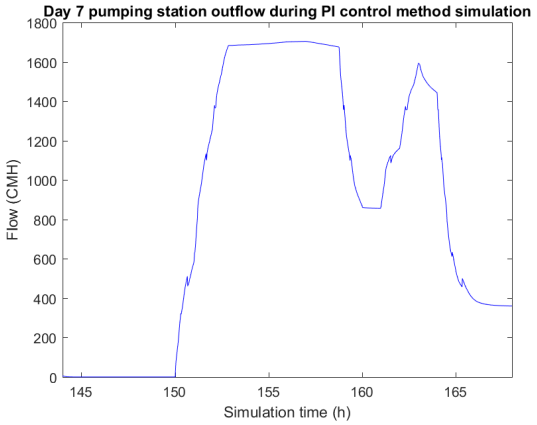

(d) Seventh day given flow from Vlites pumping station to Korakies tank.

Figure 26: PI pumps control method based on tank level control simulation results for third and sixth day.

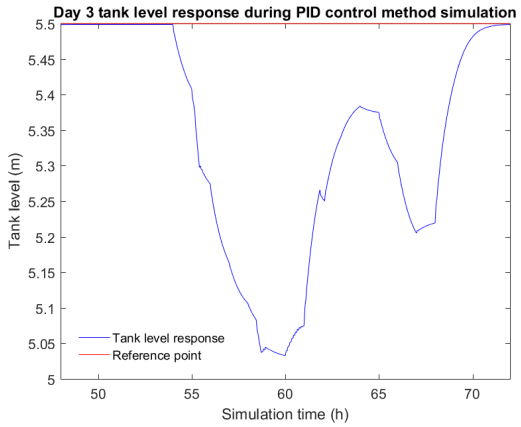

(a) Third day tank level response.

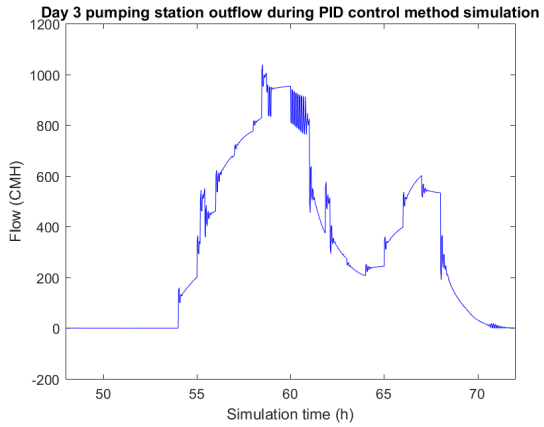

(b) Third day given flow from Vlites pumping station to Korakies tank.

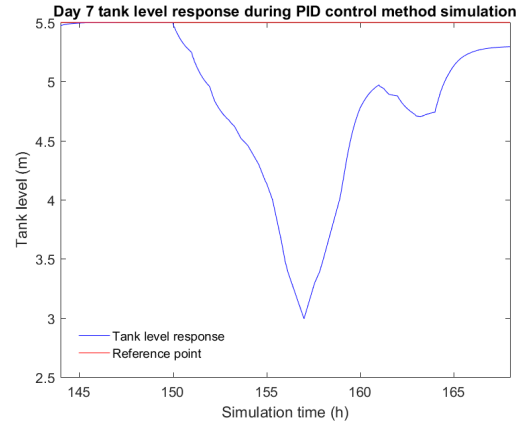

(c) Seventh day tank level response.

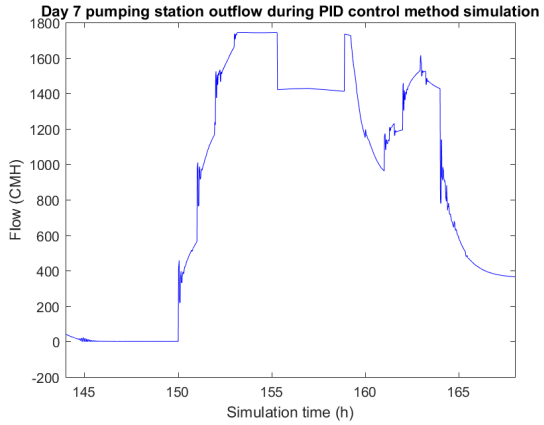

(d) Seventh day given flow from Vlites pumping station to Korakies tank.

Figure 27: PID pumps control method based on tank level control simulation results for third and sixth day.

5 Proposed leakages detection algorithm

5.1 Introduction

During the transfer of the water from water sources to consumption nodes, there are significant water losses in the pipes and the connection nodes of a water supply system because of the leakages. The timely detection of a leakage is very important in water supply systems because it can prevent water losses. A satisfactory method, in order to detect big leakages, greater than 20-25 m^3/h, can be based on extraction of features of nodes pressure signals. Features extraction method transforms an input set of values, like time-series, to another set, depending on extracted feature, in order to get indirect information about the behavior of the under study signal and classify the signal into some categories. In the present Thesis 3 features are examined which are extracted from the measured pressures of the under study water supply system connection and consumption nodes. Those features are

- the discrete time interval energy of the pressure signals of the node which is examined for leakages,
- the entropy of the pressure signals and
- the discrete Wavelet decomposition of the pressure signals

All the above features are examined in an experimental simulation of the under study network, in order to find which of the above features can be used for big leakage detection.

5.2 Examined features from node pressure signals

5.2.1 Energy

For a given discrete time interval $[n_1, n_2]$ the energy of the discrete signal is defined in Equation 34 [22].

$$E_x = \sum_{n=n_1}^{n_2} x^2[n] \tag{34}$$

In Equation 34, $x[n]$, represents the values of the under study signal. Energy declares how far are the values of a vector for their mean.

5.2.2 Entropy

Entropy is a generic measure of uncertainty. Entropy was initially introduced as a thermodynamic state variable, but was associated with signal processing. In information theory, entropy is a measure of randomness, the information dispersion for the included information in a vector. The entropy of a vector is defined in Equation 35 [22].

$$H = -\sum_{i=1}^{n} P_i log_2(P_i) \tag{35}$$

In Equation 35, H is the calculated entropy of the signal and P_i is the probability function value for each element of the under study vector. The propability function, which is used in the present Thesis, is defined in Equation 36 [22].

$$P_i = \frac{x_i^2}{\sum_{n=1}^{n} x_n^2} \tag{36}$$

In Equation 36, P_i is the probability value and x_i the ith value of the under study vector, x.

5.2.3 Discrete Wavelets decomposition (DWD)

Wavelets transformation becomes famous over the past years in many applications which are related with signal processing. Wavelets are used as base functions, in order to describe other signals, like sines and cosines in Fourier transformation. The most significant advantage of Wavelets analysis against Fourier analysis is the study of transient phenomena during a signal processing. By using Wavelets decomposition, information about transient phenomena can be extracted. Another advantage of Wavelets against Fourier analysis in a time-series is that Fourier analysis required stationary signals which maintain their properties among the time. Signals in Water supply systems are not stationary because the changing of the consumption in the system or leakage, causes changes in the properties of the pressure signals. This fact creates the need of localization, not only in the frequency domain, but also in the time domain. Wavelets transformations are built for those purposes, because they focus both on frequency and time domain analysis of the under study signal [23]. Initially is defined a finite discrete wavelet base function. By shifting and scaling this function, other similar functions are created. All those functions, are multiplied with the under analysis signal in order to achieve the wavelet decomposition of the signal.
Another way to achieve descrete wavelet decomposition, is by using high and low pass filters. This can be achieved by using the Mallat algorithm, a two channel fast Wavelets decomposition algorithm, based on the above filters [24]. The operation of Mallat algorithm is shown in Figures 28 and 29.

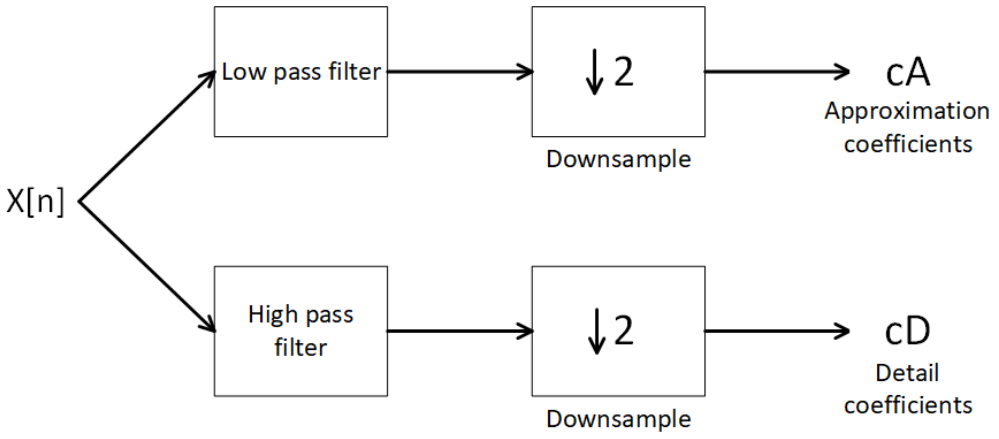

Figure 28: Block logic diagram of one dimension level Wavelets decomposition using Mallat algorithm. Downsample keeps the even indexed elements.

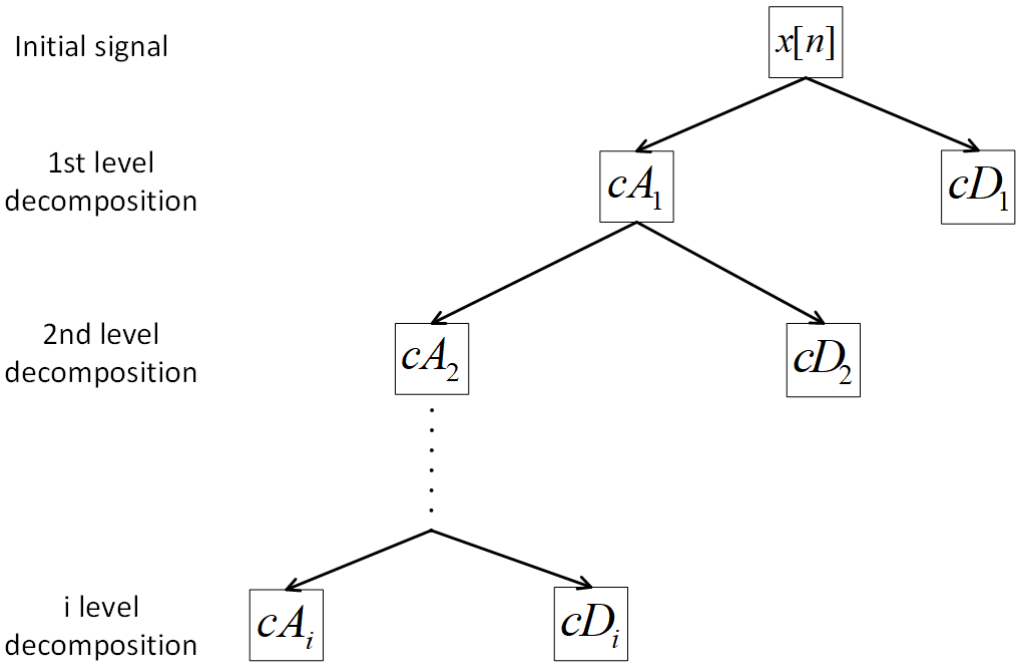

Figure 29: One dimensional discrete Multi level Wavelets decomposition using Mallat algorithm.

As shown in Figures 28 and 29, Mallat algorithm decomposes the signal into two base components, the approximation coefficients which arise from the low pass filter and are symbolized with A_i and the detailed coefficients which produced from the high pass filter and symbolized with D_i. Approximation coefficients show the behaviour of the signal in different from the initial scale. Detailed coefficients focus in rapid changes of the signal. The maximum level decomposition depends on the length of the initial signal and the selected wavelet family.
There are several wavelet families, with different properties, which can be used in signal analysis and decomposition. One of those families are Daubechies (db) [25], which introduced by Ingrid Daubechies [25]. Wavelets of Daubechies family are bi-orthogonal, asymmetric and orthogonal. There are several orders of Daubechies family. For the purposes of this Thesis, the 2 order of this wavelets family (db2) filter are used for pressure signals decomposition, because the length of the under examination signals consists of 60 samples, which is relatively small. Those filters are shown in Figure 30.

5.3 Modeling and simulation of leakages

Leakages in EPANET program are modelled by an emitter function which depends on the instant pressure of the node where the leakage exists [1, 2]. The definition of the emitter is shown in Equation 37.

$$Q(t) = K_e P_e(t)^{\gamma} \tag{37}$$

In Equation 37, $Q(t)$ in m^3/h, represents the outflow rate of the leak at time t in min, K_e in $\frac{m^3/h}{m^{\gamma}}$ is an emitter coefficient which declares the size of the leak, $P_e(t)$ in m represents the pressure of the leak node at time t and γ, a unitless factor, is an emitter exponent

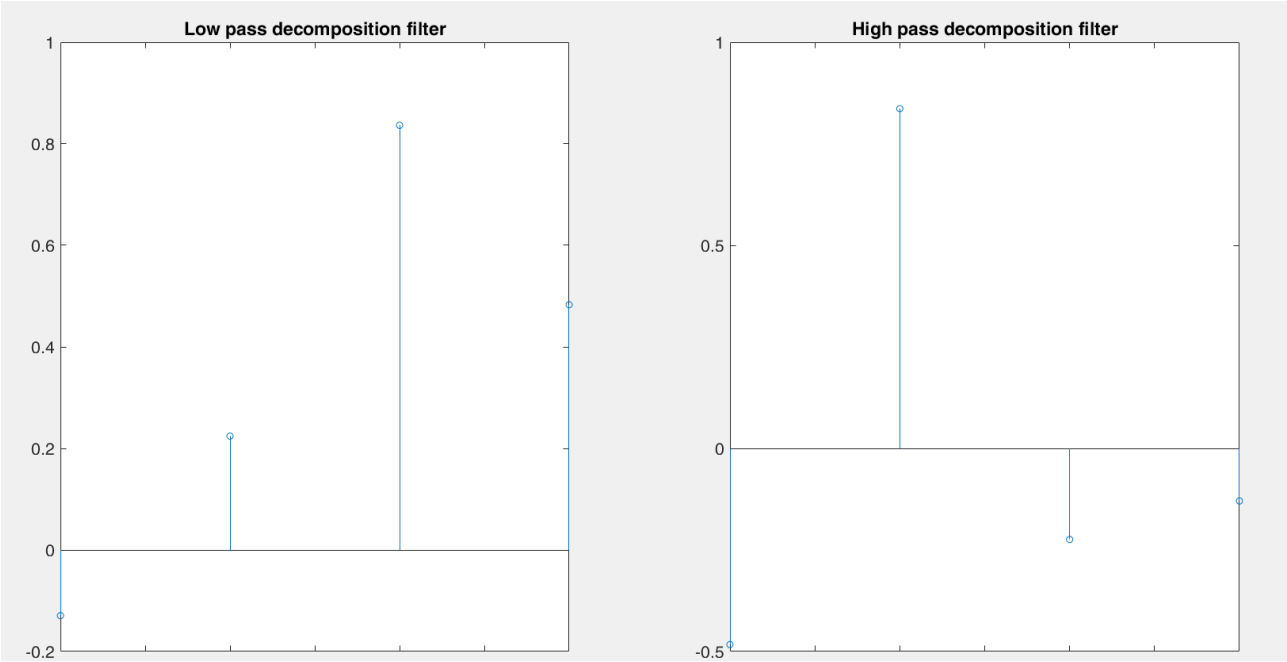

Figure 30: Daubechies 2 wavelets family (db2) low pass and high pass decomposition filters. Horizontal axis: discrete time (n). Vertical axis: Amplitude.

which depends on the material and the age of the node.
In order to test the accuracy of leakages modelling in SmartWaters framework, a prototype water supply network was created and is shown in Figure 31. The role model network consists of seven nodes, a tank and a throttle control valve. The radial of the tank is r=16 m and the initial water level is 4 m.
The characteristics of the simulation of the test model network we used are shown in Table 10.

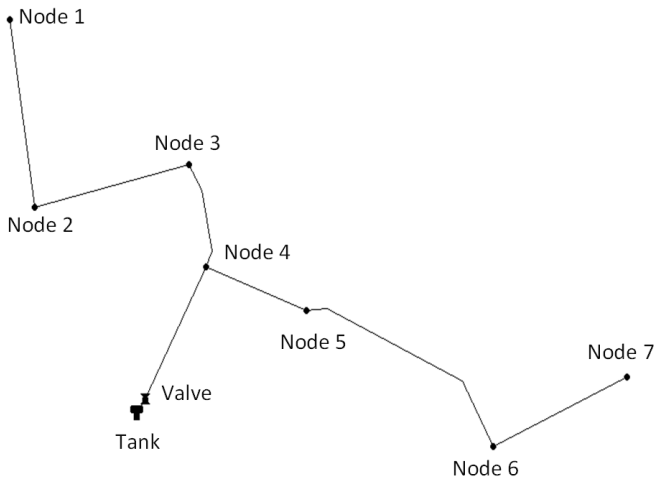

Figure 31: Prototype water supply network model used for SmartWaters's framework leakages testing.

	SmartWaters's GUI parameter	Value
1	Total simulation duration	48 h
2	Hydraulic analysis time-step	1 min
3	Flow units	m^3/h
4	Pressure units	m
5	Network consumption	null
6	Leaking node	Node 2
7	Leakage insertion time	24th h
8	Emitter coefficient	3
9	Emitter exponent	0.5

Table 10: Simulation parameters in order to test the correct simulation of leakages in SmartWaters program by using the prototype water network of Figure 31.

The results of the simulated testing network model in SmartWaters framework are shown in Figure 32. When a leakage of is applied, the level of the tank begins to decrease. Considering that the tank is vertical cylinder, the capacity of the water, which was lost due to leakage, can be calculated by the volume equation of a cylinder which is defined in Equation 38.

$$V = \pi r^2 h \tag{38}$$

In Equation 38, V represents the volume of the tank, r is the radius of the tank, and h is the height of water in the tank. By used the above equation, the capacity of lost water, during leakage simulation, is 506.2 m^3 (tank water level is reduced by 0.6294 m). To be ascertained the correct simulation of leakages in SmartWaters framework, the pressure of the leaking node is exported and then, by using Equation 37, the total amount of lost water is calculated. The total amount, as calculated, is 506.9 m^3. The amount of lost water from the leakages model and the experimental amount of the lost water in the prototype network are very close. The results, are also included in Table 11. This fact, proves the very accurate simulation of leakages in SmartWaters framework.

	Type of result	Value
1	Tank level reduction	0.6294 m
2	Expected total water leakage volume, as calculated from the model	506.2 m^3
3	SmartWaters framework simulation's total water leakage volume	506.9 m^3

Table 11: Leakages modeling and simulation results of the prototype water network, in order to examine the accuracy of leakages simulations in SmartWaters framework.

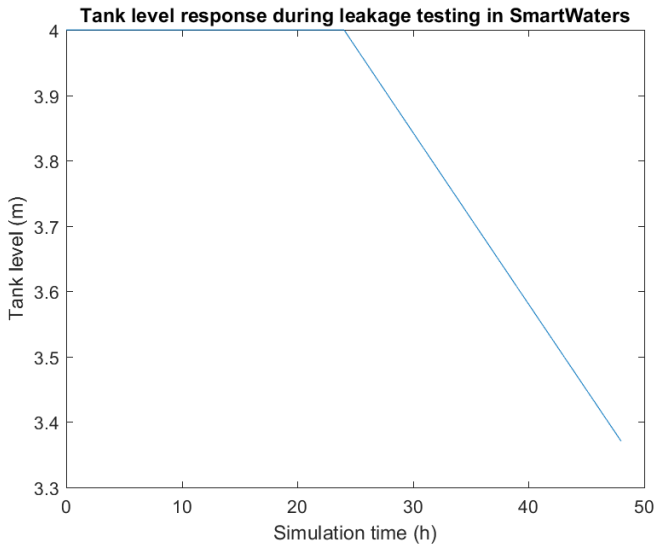

(a) Network's tank level.

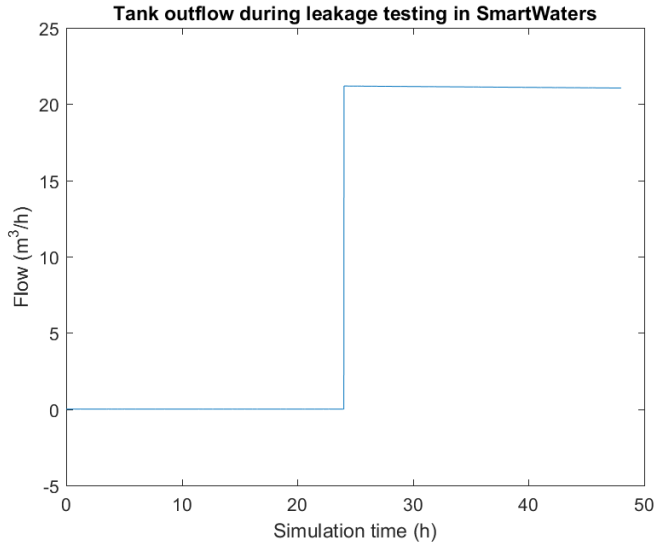

(b) The flow from the network's tank to the network, due to leakage affect.

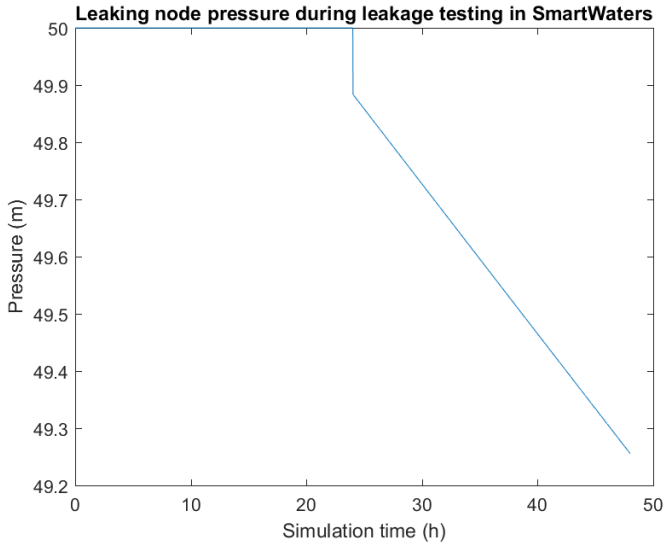

(c) The pressure of the node, where the leakage is located.

Figure 32: Testing network model simulation result, in order to test SmartWaters framework, when a leakage is applied.

5.4 Features examination for leakage detection in a case-study node of the under study distributed water supply system using energy, entropy and DWD pressures features extraction

5.4.1 Introduction

The above mentioned features are examined in a set of experimental extended simulations, in SmartWaters framework, in order to determine which of these features can be used to check if a possible leak exists. For the purposes of the experiment, a case-study node is selected, from the set of the examined for leakage nodes in the scientific project [1]. Especially the name of the node in the under study distributed water supply system is `PO_NE_5`, which is located at Nerokouro region of the under study distributed water supply system. The emitter coefficient which is used for the present experiments is the same as it is set in the scientific project.

5.4.2 SmartWaters GUI parameters and experiments description

The parameters set to SmartWaters's GUI for the experiments are shown in Table 12. Figure 33 shows the daily demand pattern and Figure 34 shows the coefficients, which the corresponding coefficient of each day multiplies the daily demand pattern.

	SmartWaters's GUI parameter	Value
1	Total simulation duration	12 days
2	Hydraulic analysis time-step	1 minute
3	Flow units	m^3/h
4	Pressure units	m
5	Network consumption	Figures 15 and 17
6	Leaking node	`PO_NE_5`
7	Emitter coefficient	4.5
8	Emitter exponent	0.5

Table 12: Simulation parameters in order to examine and compare the behavior of the mentioned features in a set of normal and leaking pressure signals.

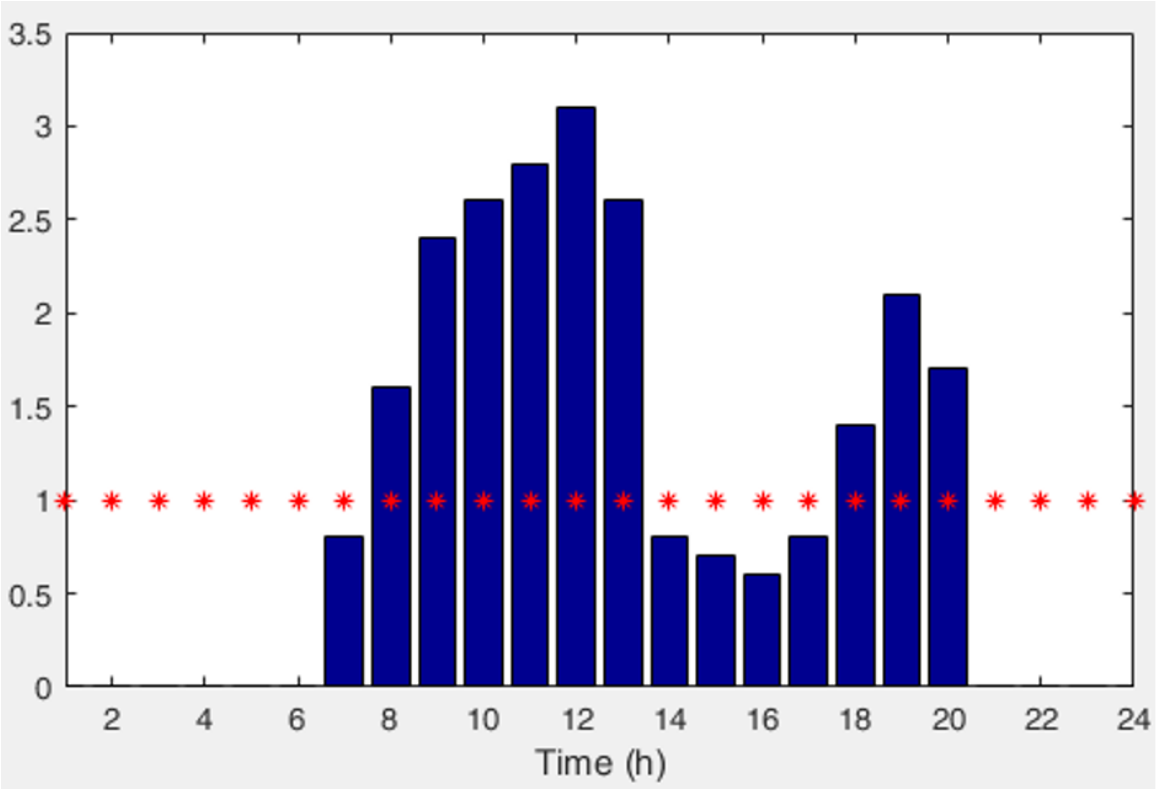

Figure 33: Daily demand pattern for the experimental simulation in order to examine and compare the behavior of the mentioned features in a set of normal and leaking pressure signals.

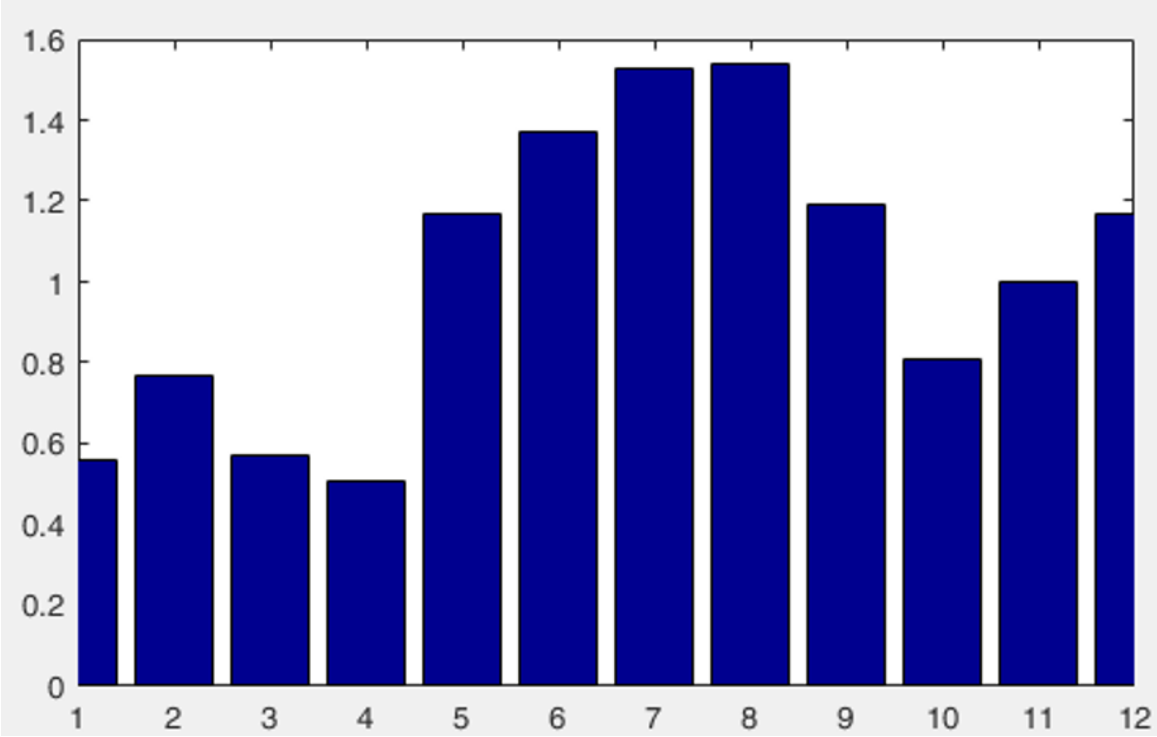

Figure 34: Coefficients, which multiply the daily demand pattern of the experimental simulation in order to examine and compare the behavior of the mentioned features in a set of normal and leaking pressure signals.

In order to find which features are useful for leakage detection five experiments were done. The first experiment was done without any leakage and represents the normal operation of the node, which depends on the water consumption of the under study node.
The other four experiments deal with leakages which were inserted in different simulation times. In all leakage experiments the node emitter coefficient remains the same. The labels of the experiments and the leakage insertion time in each experiment is shown in Table 13. At each experiment, the pressure signal of the under study node was extracted for the overall simulation time. Those signals are shown in Figure 35. In this Figure it is observed, that the pressure in leakage experiments drops when the leak starts. Another observation is that when the leakage starts, the drop of the pressure is very sharp for a short time period compared with the normal experiment, in which the transition of the pressure during the changes of the consumption is smoother.

	Experiment label	Type of experiment	Leak insertion time (hour)
1	Experiment 1	Experiment without leak	
2	Experiment 2	Experiment under leak	50
3	Experiment 3	Experiment under leak	103
4	Experiment 4	Experiment under leak	190
5	Experiment 5	Experiment under leak	235

Table 13: Experiments labels and leakages insertion times.

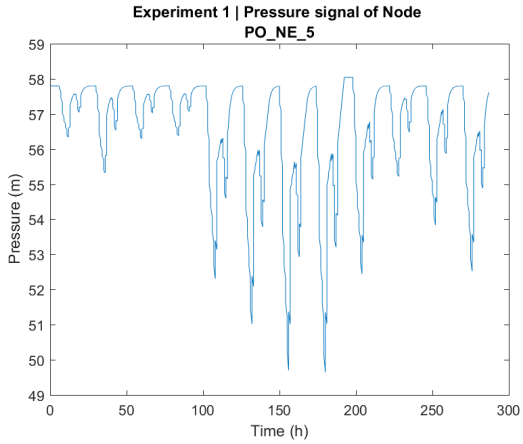

(a) Experiment 1 pressure signal.

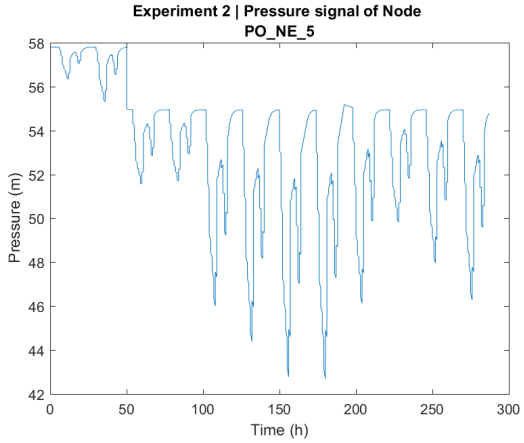

(b) Experiment 2 pressure signal.

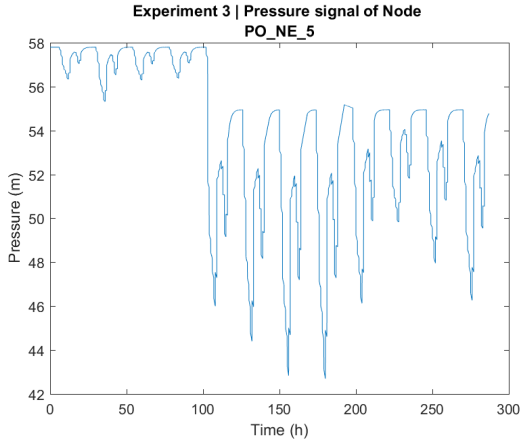

(c) Experiment 3 pressure signal.

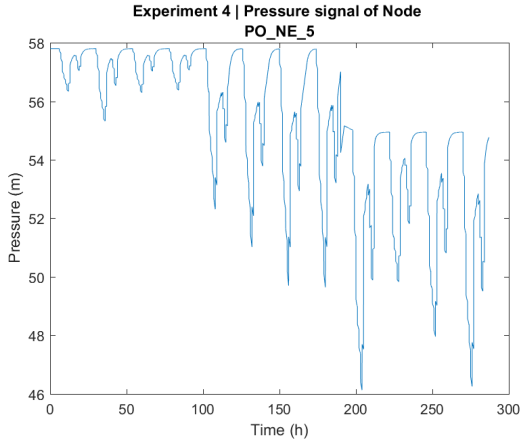

(d) Experiment 4 pressure signal.

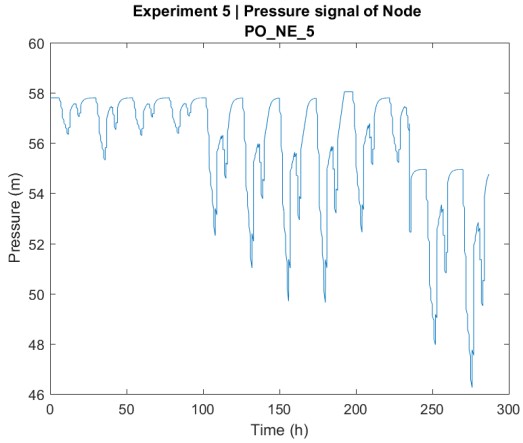

(e) Experiment 5 pressure signal.

Figure 35: Under study node pressure signals.

5.4.3 Extracted features from the under study node pressure signals, results and discussion

From the above pressure signals, as presented in Figure 35, energy, entropy and energy of detail coefficients of Daubechies 2 3^{d} level wavelets decomposition are calculated. The features are extracted every hour, by using the last hour pressure measurements, which are 60 values.

Figure 36 shows the hourly energy of all experiments, Figure 37 shows the hourly entropy of all experiments and 38 shows the hourly energy of detail coefficients of Daubechies 2 3^{d} level wavelets decomposition. The aim of the extracted features, is to find if they have significant changes in their behaviour when a leakage is inserted. It is observed that energy signal drops when a leak event takes place and after that, the signal continues to be reduced until the end of the simulation.

In order to examine the appropriateness of energy in leakage detection, a lower bound was set and is presented in energy figures. This bound is based on the minimum energy value of experiment 1. This bound is very strict and was set only for examination purposes. It is observed in Figure 36 that the energy in experiment 2 decreases when the leakage starts, but the values remain above the lower bound. Only when consumption grows considerably do the energy values drop below the lower bound.

This fact proves that energy features can not help to find out, relatively fast by using thresholds, if a leakage exists. On the other side, entropy and especially energy of detail coefficients of Daubechies 2 3^{d} level wavelets decomposition seem to be useful measurements for leakage detection. It is observed in Figures 37 and 38, that those features change significantly the hour when the leakage starts in all leakage experiments.

For the entropy experiments, a threshold to classify the leak and not leak events was experimental calculated (trial and error), based on the experiment 1 where there is not any leakage and is presented in entropy figures. The value of entropy threshold was set to be the previous fourth decimal of the entropy values.

Wavelets decomposition energy has the greatest change at the leak starting hour. When the experimental leakage takes place, the wavelets energy increases 1000 to 10000 times. The values between leak and no leak events have very big differences and it is easy to use this feature for leakage and no leakage events classification.

A threshold was calculated, as in previous features. The threshold is defined as twice the maximum value of experiment 1, in which there is not any leakage event. This threshold seems to be very suitable for leakage detection in the under study water supply network and is also used in the proposed leakage detection algorithm.

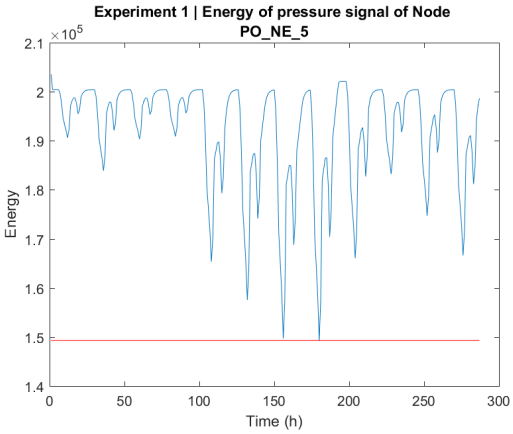

(a) Experiment 1 hourly energy.

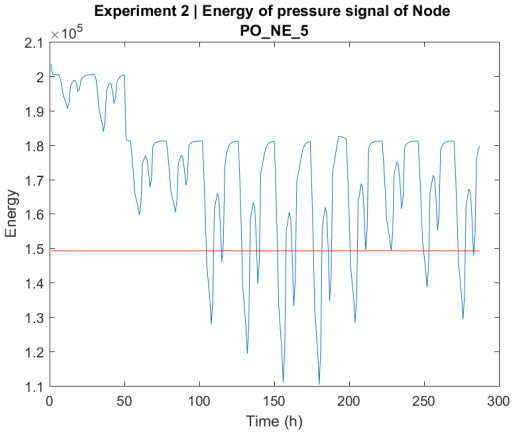

(b) Experiment 2 hourly energy.

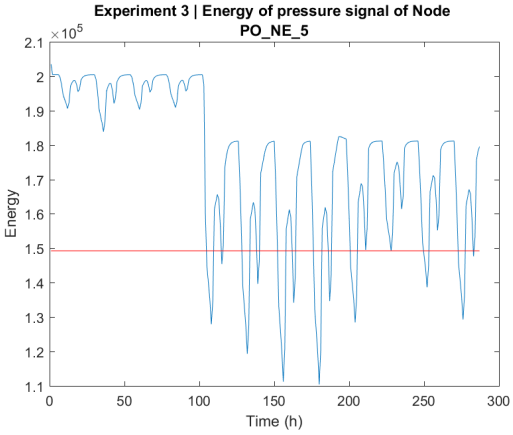

(c) Experiment 3 hourly energy.

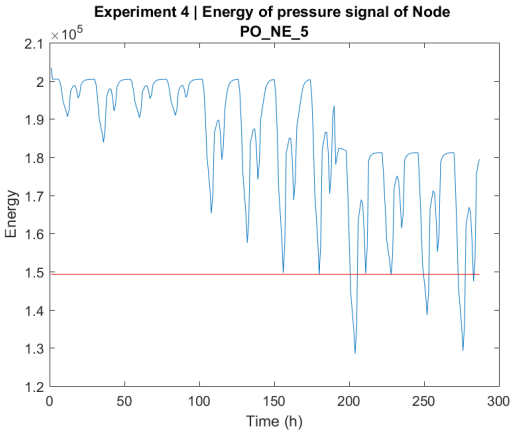

(d) Experiment 4 hourly energy.

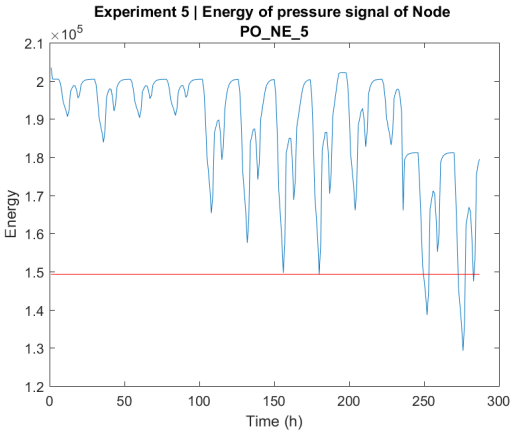

(e) Experiment 5 hourly energy.

Figure 36: Hourly energy of under study node pressure signals.

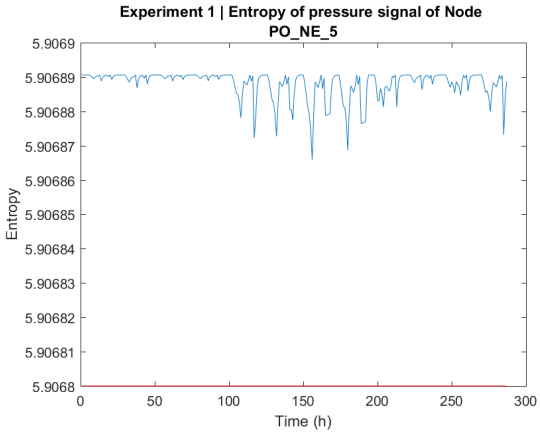

(a) Experiment 1 hourly energy.

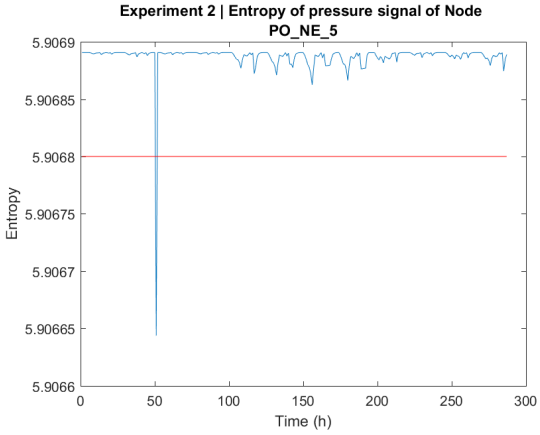

(b) Experiment 2 hourly energy.

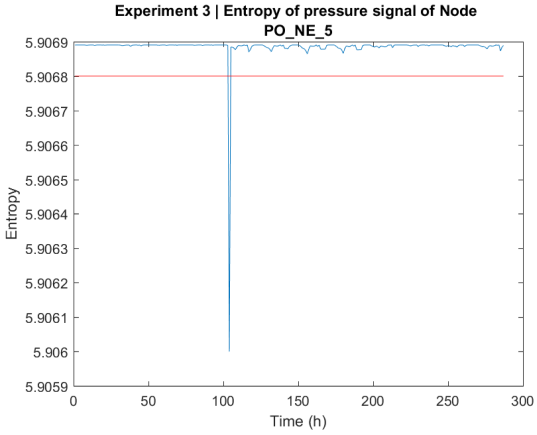

(c) Experiment 3 hourly energy.

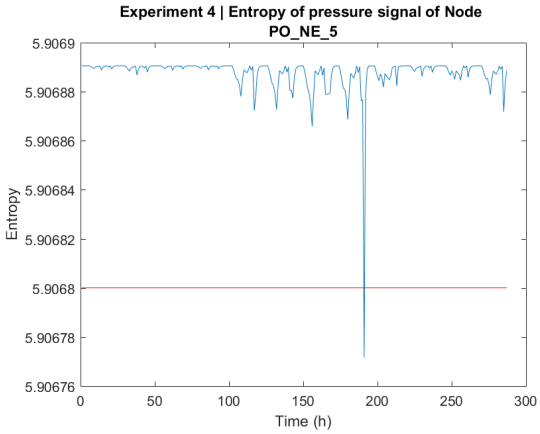

(d) Experiment 4 hourly energy.

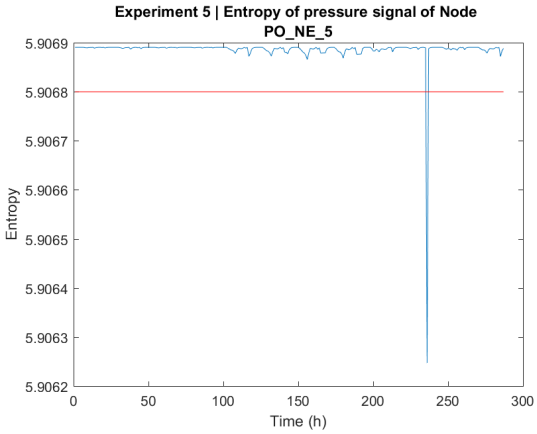

(e) Experiment 5 hourly energy.

Figure 37: Hourly entropy of under study node pressure signals.

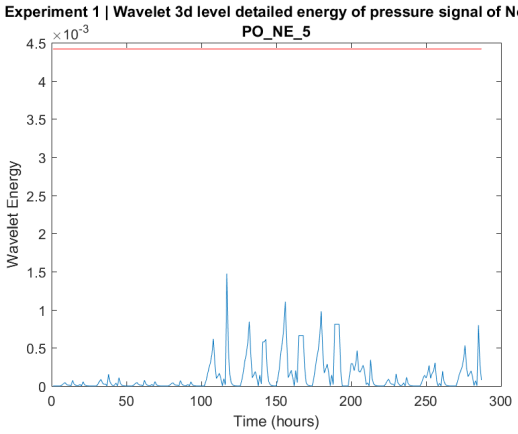

(a) Experiment 1 hourly under study wavelets energy.

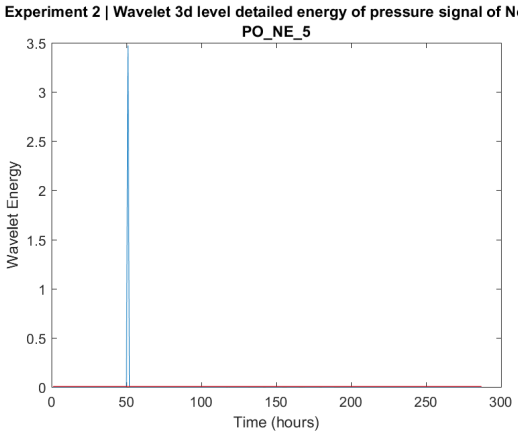

(b) Experiment 2 hourly under study wavelets energy.

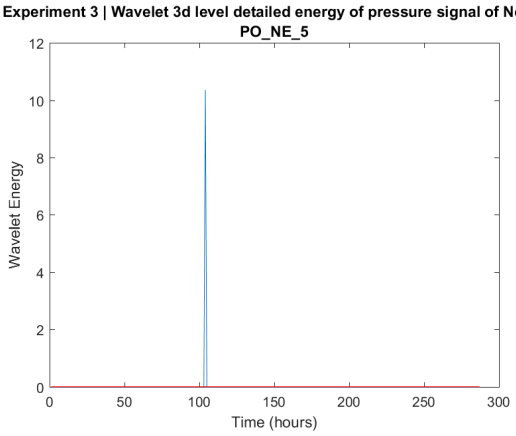

(c) Experiment 3 hourly under study wavelets energy.

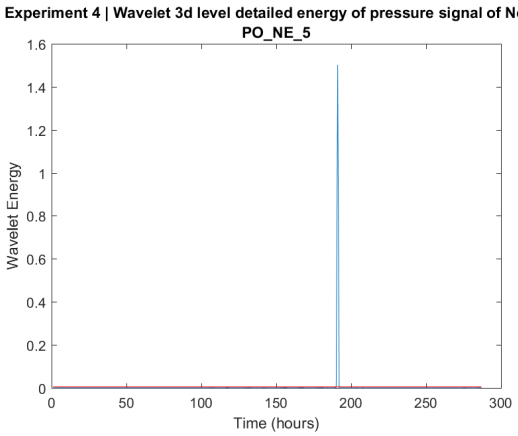

(d) Experiment 4 hourly under study wavelets energy.

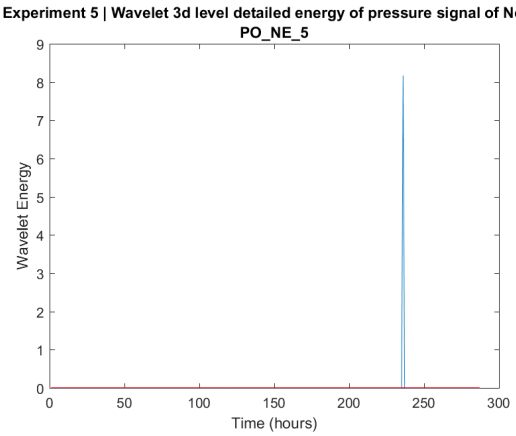

(e) Experiment 5 hourly under study wavelets energy.

Figure 38: Hourly energy of detail coefficients of Daubechies 2 3d level wavelets decomposition of under study node pressure signals.

5.4.4 Proposed leakage detection algorithm description

The proposed leakage detection algorithm is based on the previous features examination. It uses the energy of detail coefficients of Daubechies 2, 3^{d} level wavelets decomposition and a local threshold for every examined node in order to find possible leakages in the under study water supply system. The examined nodes are from the set of nodes in the scientific project examined for leakages [1]. The algorithm calculates the energy of the wavelets decomposition every hour by using the last 60 measurements of the under study node pressure signals. The sampling interval is 1 minute. At the end of every hour, the above feature is calculated for the 9 under study nodes and is compared with the corresponding threshold. If the value of a node is above the threshold, then a possible leak trigger for this node is activated. The thresholds for the examined nodes of the scientific project [1] were calculated, as calculated in Experiment 1 of the above subsection, and are twice the maximum value of the feature for each node in the case of no leakages. These thresholds can be found in Table 14. The block diagram of proposed leakage detection algorithm is shown in Figure 39.

	Node name	Node location	Feature threshold
1	PO_BA_51	Daratso region	4.0596
2	PO_NK_16	Daratso region	4.9453
3	PO_NK_67	Daratso region	4.9453
4	PO_PE_41	Perivolia region	5.7785
5	PO_NE_71	Nerokouro region	0.0115
6	PO_NE_5	Nerokouro region	0.0340
7	PO_NE_59	Nerokouro region	0.0225
8	PO_TS_18	Tsikalaria region	0.0851
9	PO_TS_31	Tsikalaria region	0.0100

Table 14: Energy of detail coefficients of Daubechies 2 3^{d} level wavelets decomposition thresholds for leak events classification.

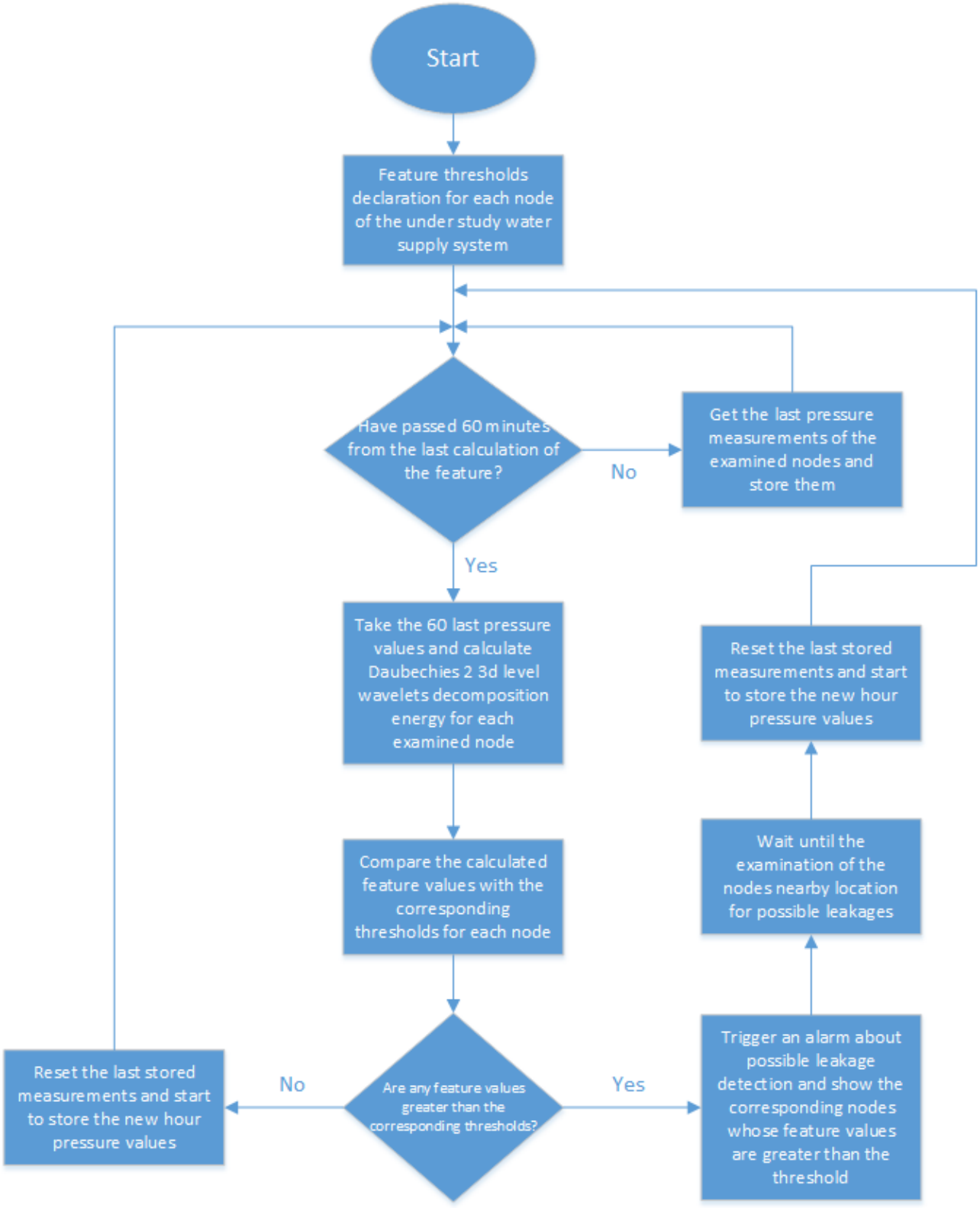

Figure 39: Proposed leakage detection algorithm block diagram.

5.5 Results and discussion

Big leakages, greater than $25 - 30m^3/h$, can be detected by extracting features and using threshold to classify normal and leak events. From the examined features, energy of detail

coefficients of Daubechies 2 3^d level wavelets decomposition, seems to be the most suitable feature for leakage detection, when the time length from one to another feature extraction is one hour. The distance of the values of this feature, between normal and leak events is very big. Also by using entropy, it seems that a classification by using thresholds can be achieved, but the distance between leak and no leak feature values is minimal and the change of the value when a leakage starts, appears in the fifth decimal of the value. Setting thresholds in energy measurements for leakage detection purposes is not very useful for leakage detection in big water supply networks with significant amount of consumptions. Finally, the proposed algorithm was tested in SmartWaters framework without any problem.

6 Summary and future work

6.1 Thesis summary

In this Thesis, a real distributed water supply system was studied. More specifically, a set of simulations was done, by using SmartWaters framework, which was implemented for the purposes of the project "An Intelligent system for sustainable management of water supply networks: application in the island of Crete", which was submitted for the purposes of the program GR02.03 - "Integrated marine and inland water management - Good environmental status in European marine and inland waters" and was funded by the European Economic Area grants 2009 - 2014 (EEA grants 2009 -2014) [1], in order to examine and compare the operation of Vlites pumping station which feeds "Korakies" tank. The "Vlites" pumping station control methods were based on the water tank level control of "Korakies" tank which supplies the water network of "Akrotiri" region. The latter supply is achieved by the use of gravity only (no pumps). Also an algorithm for big leakages detection was implemented, based on features extraction from system's nodes pressure signals. For the purposes of algorithm implementation, a set of simulations were done, in a case - study node, in order to examine which of the under study features are suitable for this kind of problem.

6.2 Conclusions

The examination and the simulation of the pumping station control algorithms has led to some useful conclusions. The installation of a speed controller, in one of the station pumps, leads to electrical energy reduction and smoother station response. The pumps scheduling control under variable speed operation based on boolean logic, which was implemented for the purposes of the project [1], has the least energy consumption, but the changes in the operation of the pumping station are steep. PI and PID controllers for tank level control, as tuned in the present Thesis, show a smoother response than pumps scheduling control under variable speed operation based on boolean logic, but have a little bigger energy consumption. For the part of leakage detection, SmartWaters framework has a very good algorithm for leakage simulations. Due to this fact, an extended set of simulations was done, in order to examine three features, based on node pressure signals, for leakages detection. Those three features were the hourly energy of pressure signals, the hourly entropy and the hourly energy of detail coefficients of Daubechies 2, 3^{d} level wavelets decomposition signal. By using hourly energy it can not be decided if a leakage exists. The value of hourly entropy, at leakage starting time, decreased by an order of 10^{-3} %, which makes entropy unremarkable for leak events detection. The corresponding value of energy of detail coefficients of Daubechies 2, 3^{d} level wavelets decomposition was increased by 1000 to 10000 times which makes this feature remarkable for leakages detection.

6.3 Future work

There are some open issues which can be studied in the future. A new, optimal, PI or PID controller for the operation and the flow control of the pumping station can be examined, by creating and minimizing an objective function, based on the costs of the consumed electrical energy. For leakage detection, more features and other wavelet families can be examined for leaking events detection. Also for the detection of the leakages, based on features extraction, a better set of thresholds can be achieved by using methods, such as k-means. Finally, a new algorithm can be implemented, based on neural networks and nodes categorization. Nodes with similarly hydraulic behaviour, can be examined if they can use the same threshold.

References

[1] *Design of an intelligent system for sustainable management of water networks: application to Crete*. Submitted for the program GR02.03 "Integrated marine and inland water management - Good environmental status in European marine and inland waters". Founded by the European Economic Area grants 2009 - 2014 (EEA grants 2009 -2014). 2016. URL: http://www.smartwaters.gr/en/.

[2] Lewis A. Rossman. *Epanet 2 Users manual*. U.S. Environmental Protection Agency. 2000. URL: https://nepis.epa.gov/Adobe/PDF/P1007WWU.pdf.

[3] A. Efstratiadis and D. Koutsoyiannis. *Lecture notes on Typical Hydraulic Works - Part 2: Water Distribution Networks*. Department of Water Resources, Hydraulic and Maritime Engineering – National Technical University of Athens, 2006.

[4] Hunaidi O. et al. "Acoustic methods for locating leaks in municipal water pipe networks". In: (2004). International Conference on Water Demand Management, pp. 1–14.

[5] Lockwood A. et al. "Locating leaks from water supply pipes using the passive acoustic method". In: *J Water SRT - Aqua* 54(8) (2005), pp. 519–530.

[6] McNulty J.G. "An acoustic-based system for detecting, locating and sizing leaks in water pipelines". In: *Proceeds. 4th Int. Conf. Water Pipeline Systems* (2001), pp. 217–225.

[7] Ishido Y. and Takahashi S. "A New Indicator for Real-time Leak Detection in Water Distribution Networks: Design and Simulation Validation". In: *Procedia Engineering* 89 (2014), pp. 411–417.

[8] Candelier A. et al. "Analytical leakages localization in water distribution networks through spectral clustering and support vector machines. The ice water approach". In: *Procedia Engineering* 89 (2014), pp. 1080–1088.

[9] Vítkovský J. P., Simpson A. R., and Lambert M. F. "Leak detection and calibration using transients and genetic algorithms". In: *Journal of Water Resources Planning and Management* 126(4) (2000), pp. 262–265.

[10] De Silva D., J. Mashford, and S. Burn. "Computer Aided Leak Location and Sizing in Pipe Networks". In: (). Urban Water Security Research Alliance Technical Publication No. 17.

[11] Gabrys B. and Bargiela A. "Neural network based decision support in presence of uncertainties". In: *Journal of Water Resources Planning and Management* 125(5) (1999), pp. 272–280.

[12] Nesbitt B. *Handbook of Pumps and Pumping*. Elsevier, 2006. ISBN: 9781856174763.

[13] Maria João Mortágua Rodrigues. *PID Control of Water in a tank (Bachelor thesis)*. 2011. URL: http://hig.diva-portal.org/smash/get/diva2:425782/FULLTEXT01.pdf.

[14] Anastasios Pouliezos. *Modern Control Theory*. Ed. by Hellenic Academic Libraries Link. 2015. URL: http://hdl.handle.net/11419/105.

[15] Åström Karl J. and Hägglund Tore. *PID Controllers - Theory, Design, and Tuning*. 2nd Edition. ISA, 1995. ISBN: 978-1-61583-599-7.

[16] Richard C. Dorf and Robert H. Bishop. *Modern Control Systems*. Upper Saddle River, NJ, USA: Prentice-Hall Inc., 2016. ISBN: 978-0134407623.

[17] MATLAB. *Control System Toolbox ™R2016a*. Natick, Massachusetts: The MathWorks Inc., 2018.

[18] Wilkie Jacqueline, Johnson Michael, and Reza Katebi. "Poles, zeros and system stability". In: *Control Engineering: An Introductory Course*. London: Macmillan Education UK, 2002, pp. 242–276. ISBN: 978-1-4039-1457-6. DOI: 10.1007/978-1-4039-1457-6_10. URL: https://doi.org/10.1007/978-1-4039-1457-6_10.

[19] Ogata Katsuhiko. *Modern control engineering*. 5th Edition. Prentice Hall, 2010. ISBN: 978-0-13-615673-4.

[20] Stanley M. Shinners. *Modern Control System Theory and Design*. 2nd Edition. Wiley, 1998. ISBN: 978-0-471-24906-1.

[21] G.C. Goodwin, S.F. Graebe, and Mario E. Salgado. *Control Systems Design*. Prentice Hall, 2001. ISBN: 0-13-958653-9.

[22] M.M. Gamboa-Medinaa, L.F. Ribeiro Reis, and R. Capobianco Guido. "Feature extraction in pressure signals for leak detection in water networks". In: *Procedia Engineering* 70 (2014). 12th International Conference on Computing and Control for the Water Industry, CCWI2013, pp. 688–697.

[23] Juuso T. Olkkonen. *Discrete Wavelet Transforms - Theory and Applications*. IN-TECH, 2011. ISBN: 978-953-307-185-5.

[24] STEPHANE G. MALLAT. "A Theory for Multiresolution Signal Decomposition: The Wavelet Representation". In: *IEEE TRANSACTIONS ON PATTERN ANALYSIS AND MACHINE INTELLIGENC* 11 (1989), pp. 674–693.

[25] Ingrid Daubechies. *Ten Lectures on Wavelets*. CBMS-NSF Regional Conference Series in Applied Mathematics, 1992. ISBN: 978-0-89871-274-2.

[26] MATLAB. *Wavelet Toolbox ™User's Guide*. Natick, Massachusetts: The MathWorks Inc., 2009.

Appendices

A Vlites pumping station curves

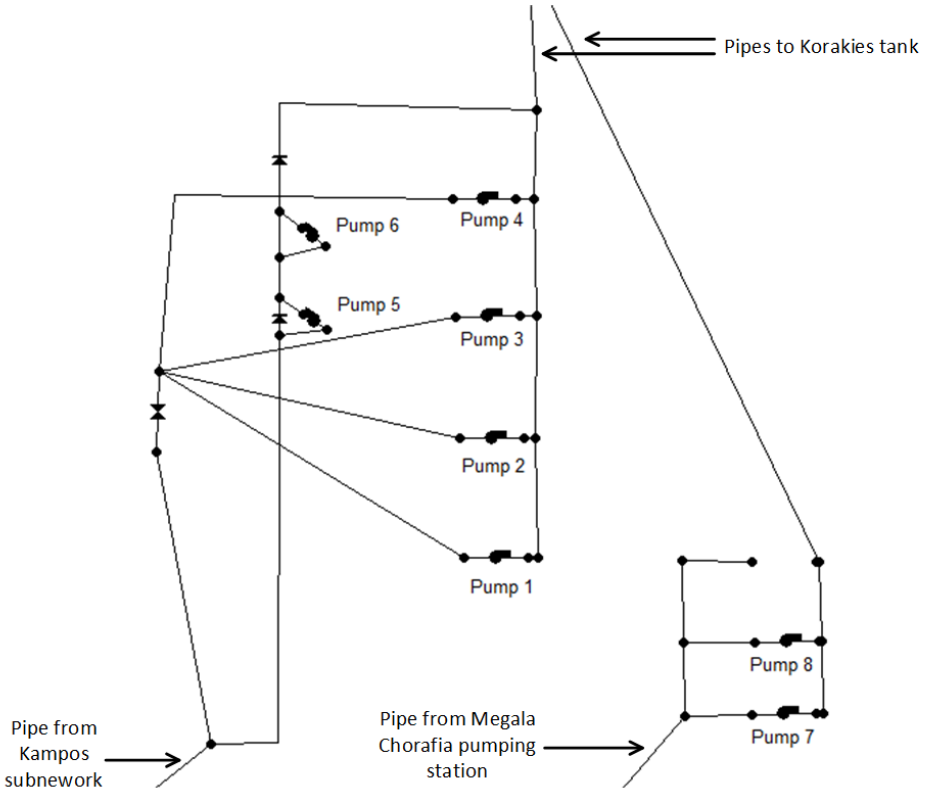

Figure 40: Vlites pumping station network.

Pump name	Installed power kW	Nominal flow m^3/h	Nominal rotational speed (RPM)	Group
Pumps 1 to 4	250	350	1450	Group 1
Pump 5, 6	93	180	1450	Group 2
Pump 7, 8	186	300	2900	Group 3

Table 15: Vlites pumping station pump groups and characteristics.

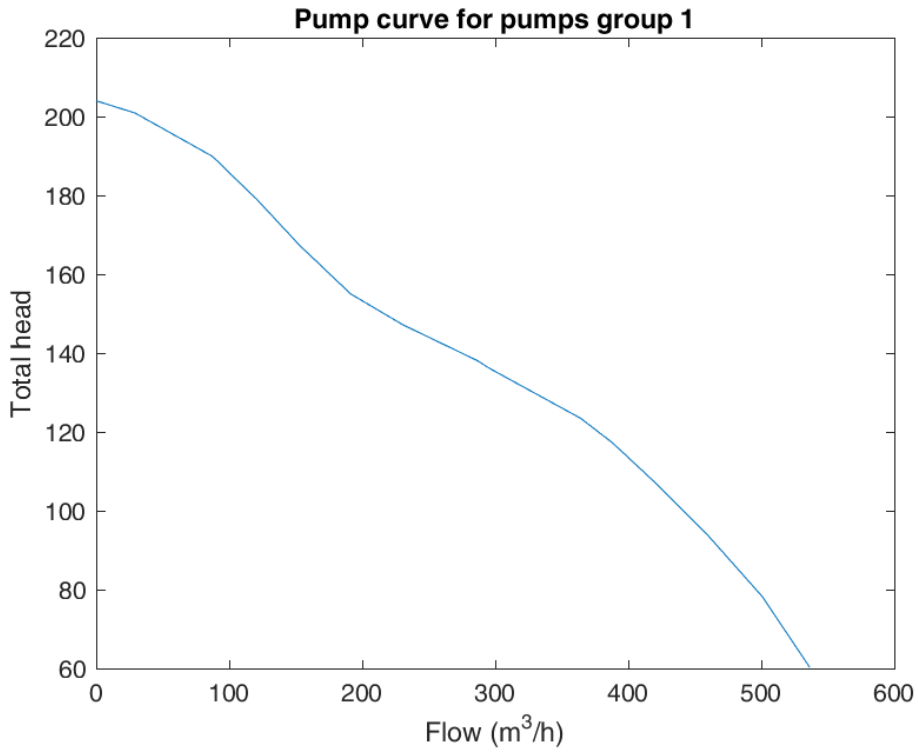

(a) Head - Flow curve

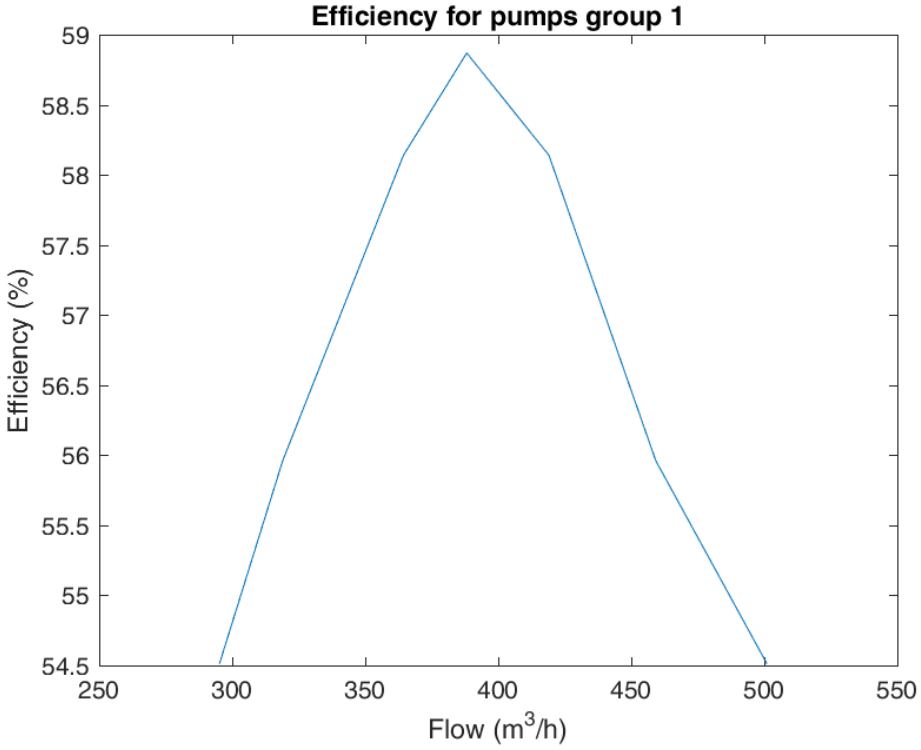

(b) Efficiency curve

Figure 41: Pump's Head - Flow and efficiency curves for pumps of Group 2

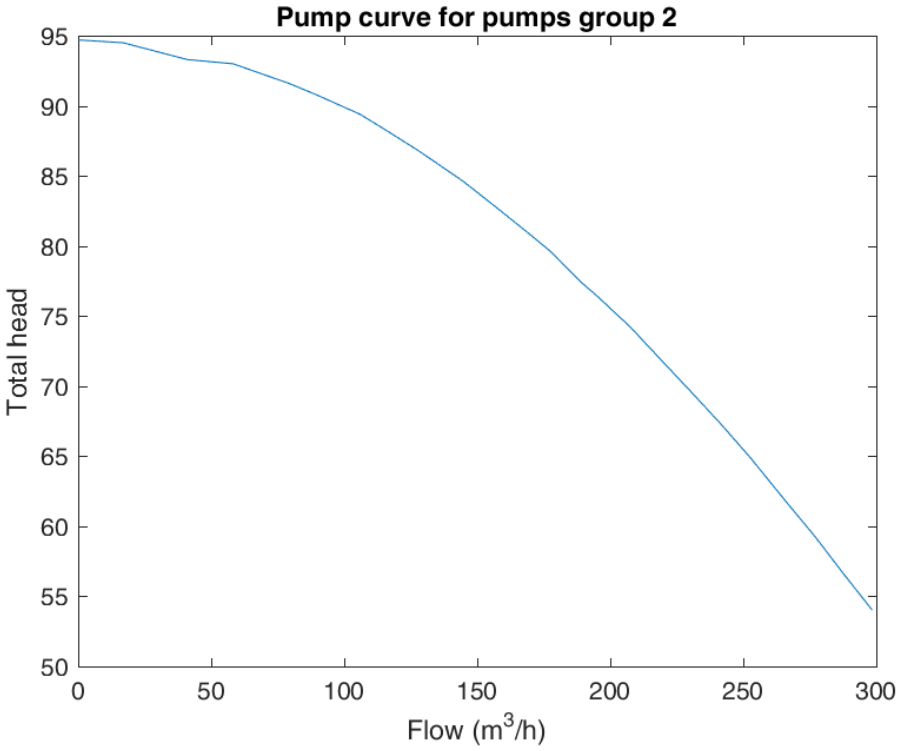

(a) Head - Flow curve

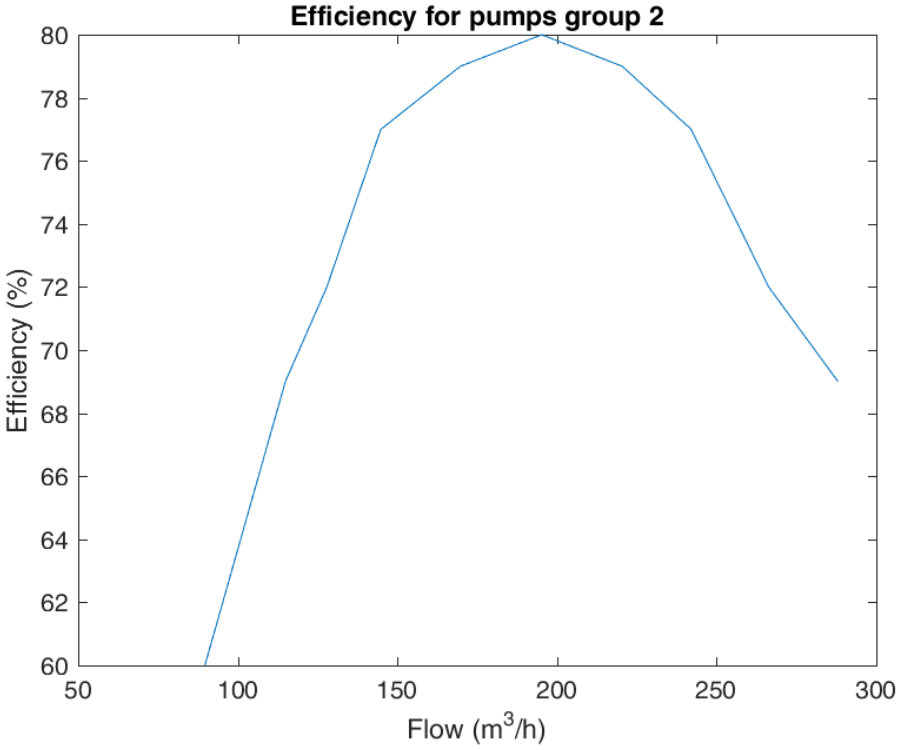

(b) Efficiency curve

Figure 42: Pump's Head - Flow and efficiency curves for pumps of Group 2

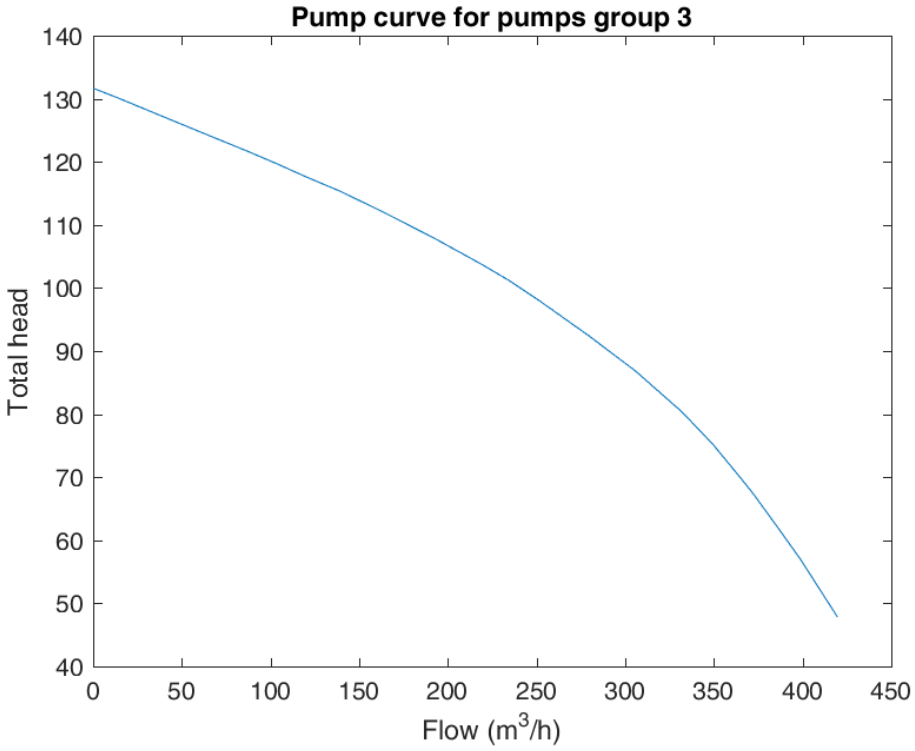

(a) Head - Flow curve

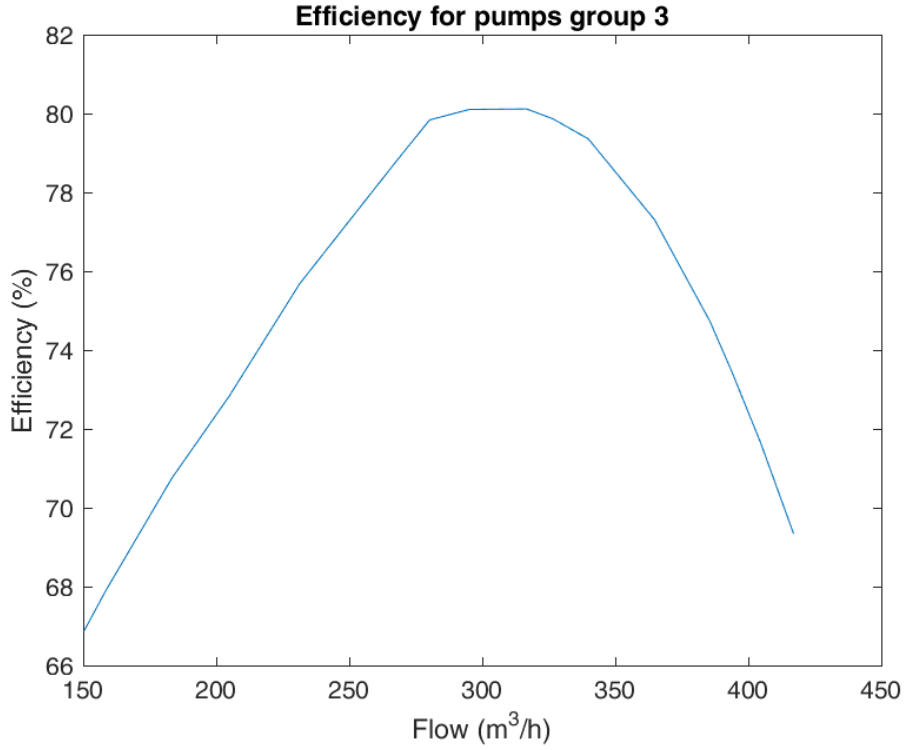

(b) Efficiency curve

Figure 43: Pump's Head - Flow and efficiency curves for pumps of Group 3

B Proposed control algorithms total simulation results

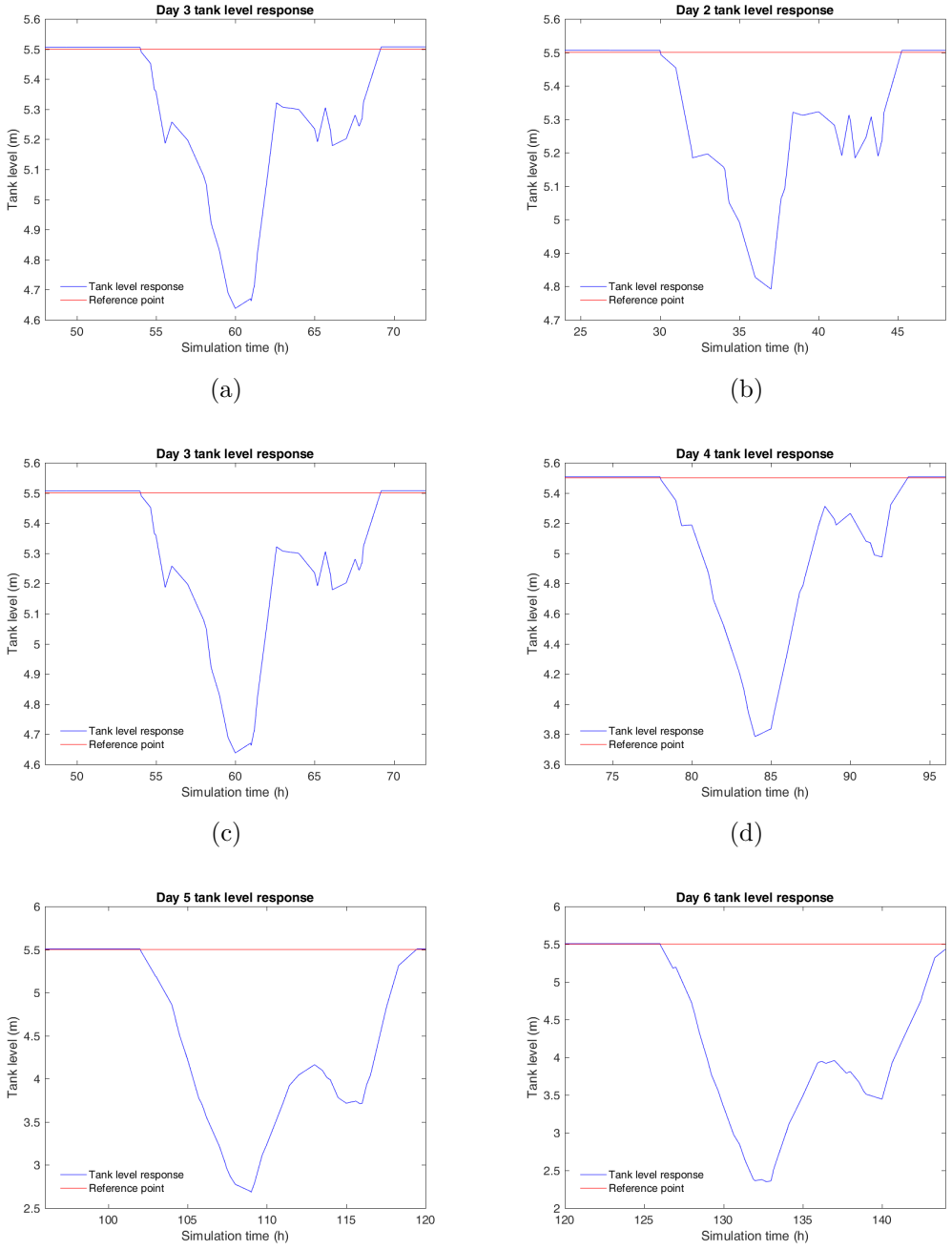

Figure 44: Pumps scheduling control (ON/OFF) under constant speed operation based on boolean logic results. Korakies tank level response for days 1 to 6.

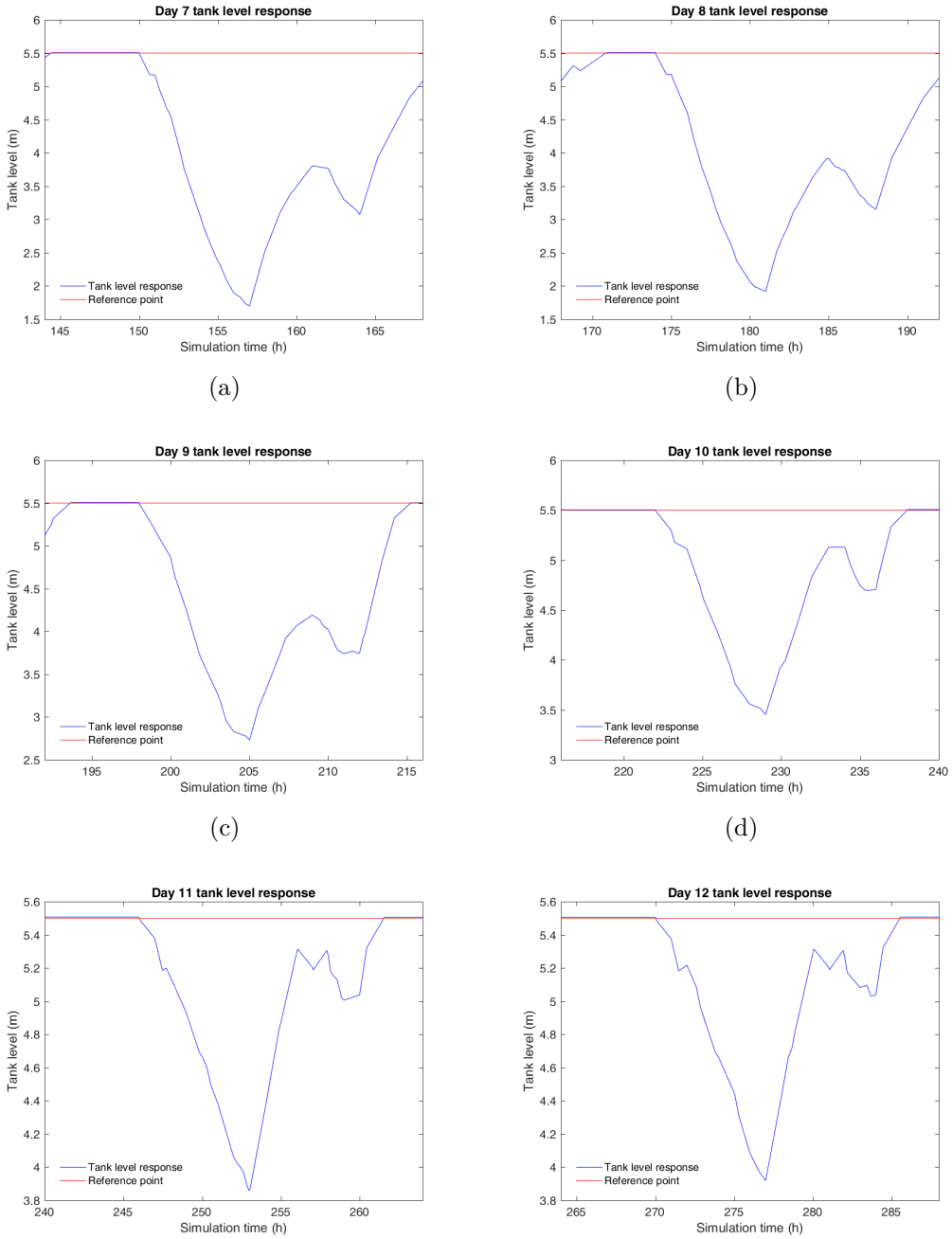

Figure 45: Pumps scheduling control (ON/OFF) under constant speed operation based on boolean logic results. Korakies tank level response for days 7 to 12.

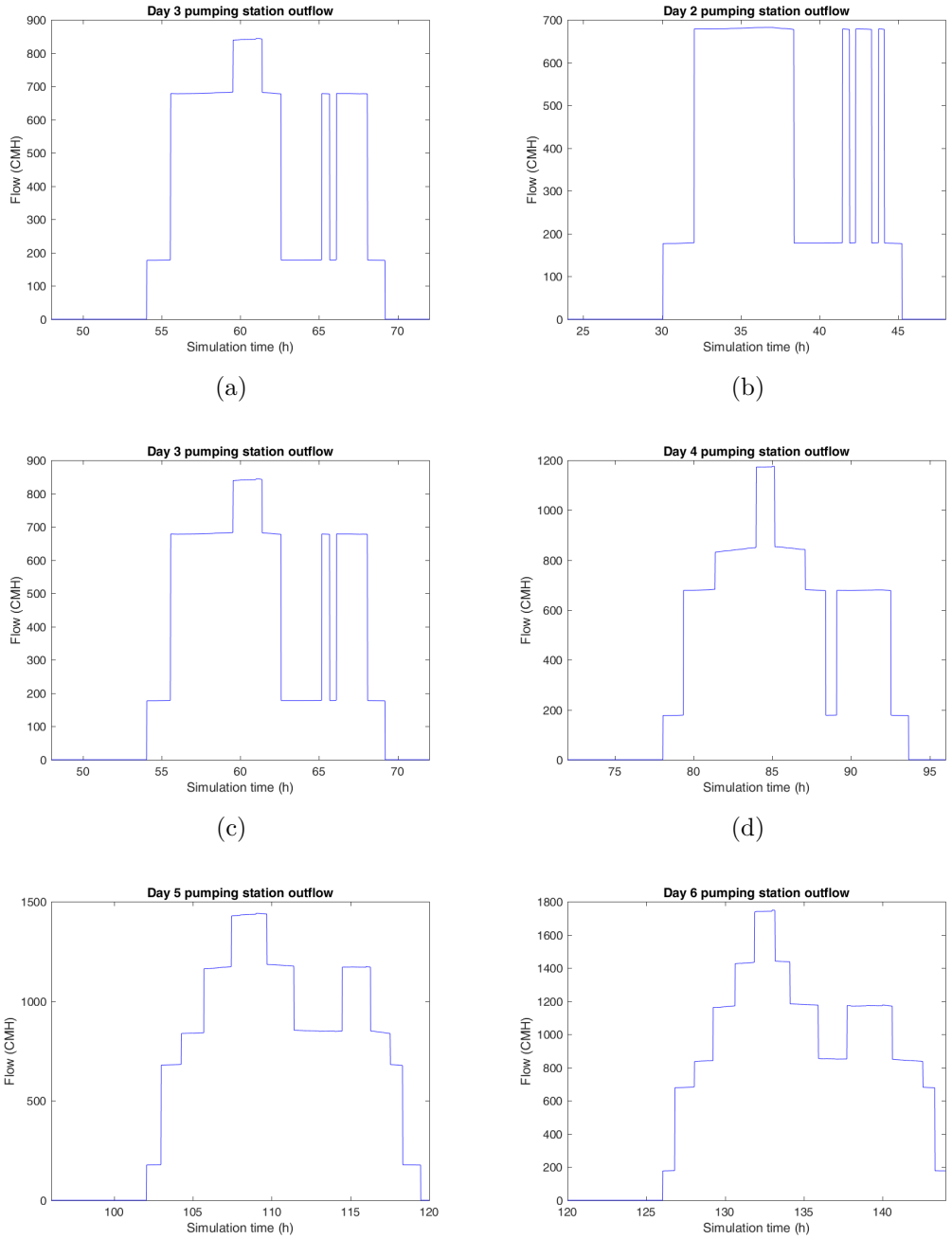

Figure 46: Pumps scheduling control (ON/OFF) under constant speed operation based on boolean logic results. Vlites pumping station outflow for days 1 to 6.

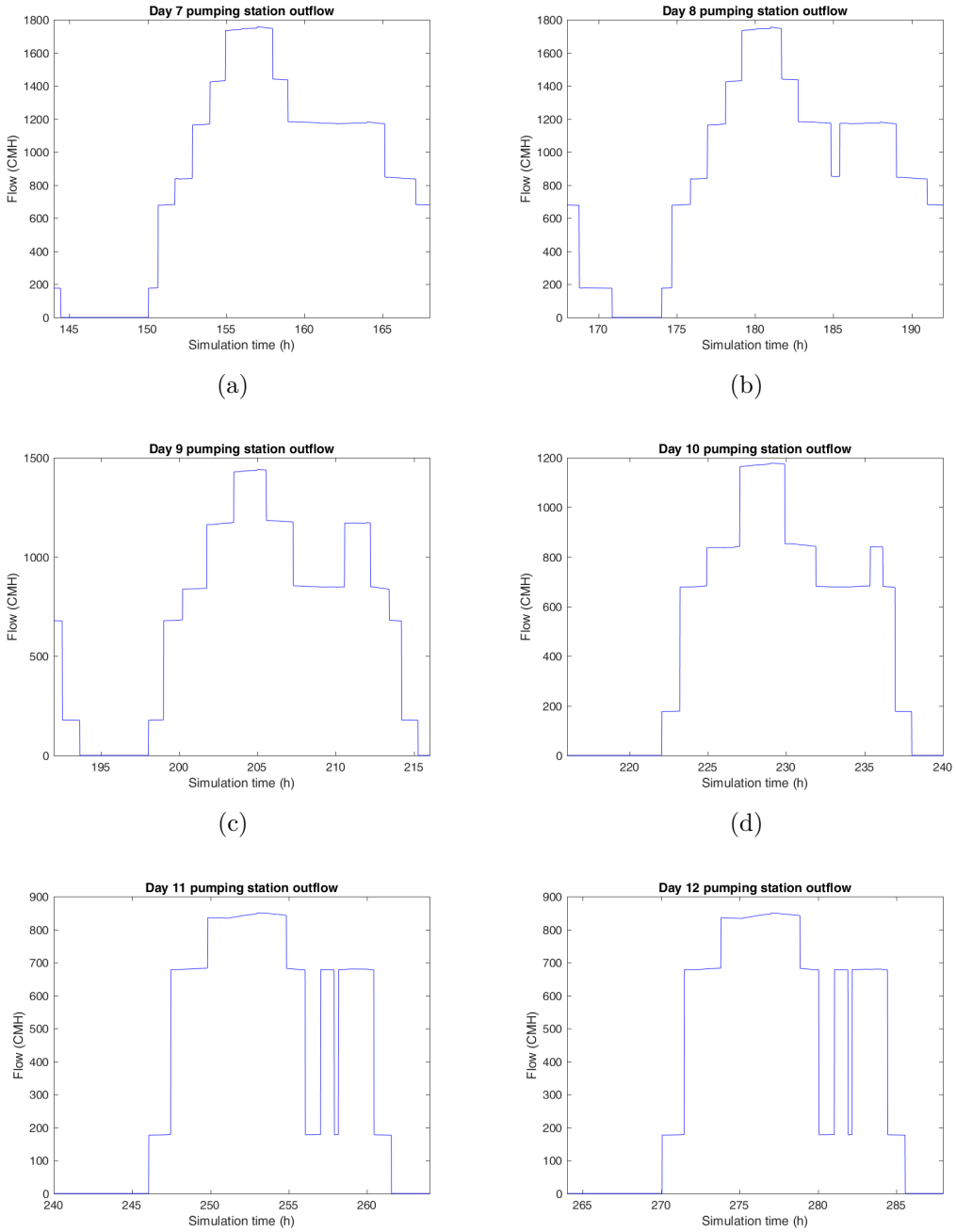

Figure 47: Pumps scheduling control (ON/OFF) under constant speed operation based on boolean logic results. Vlites pumping station outflow for days 7 to 12.

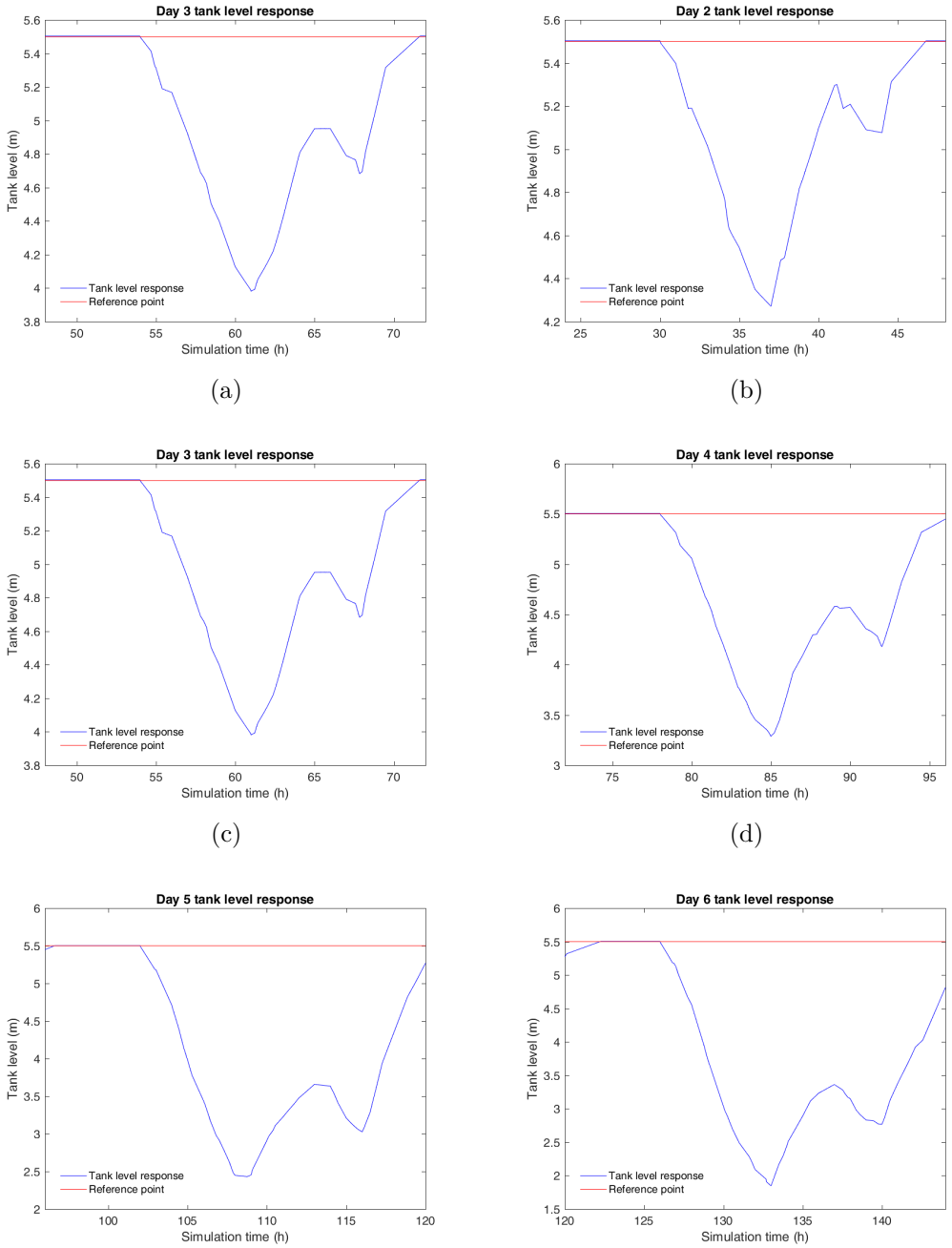

Figure 48: Pumps scheduling control under variable speed operation based on boolean logic simulation results. Korakies tank level response for days 1 to 6.

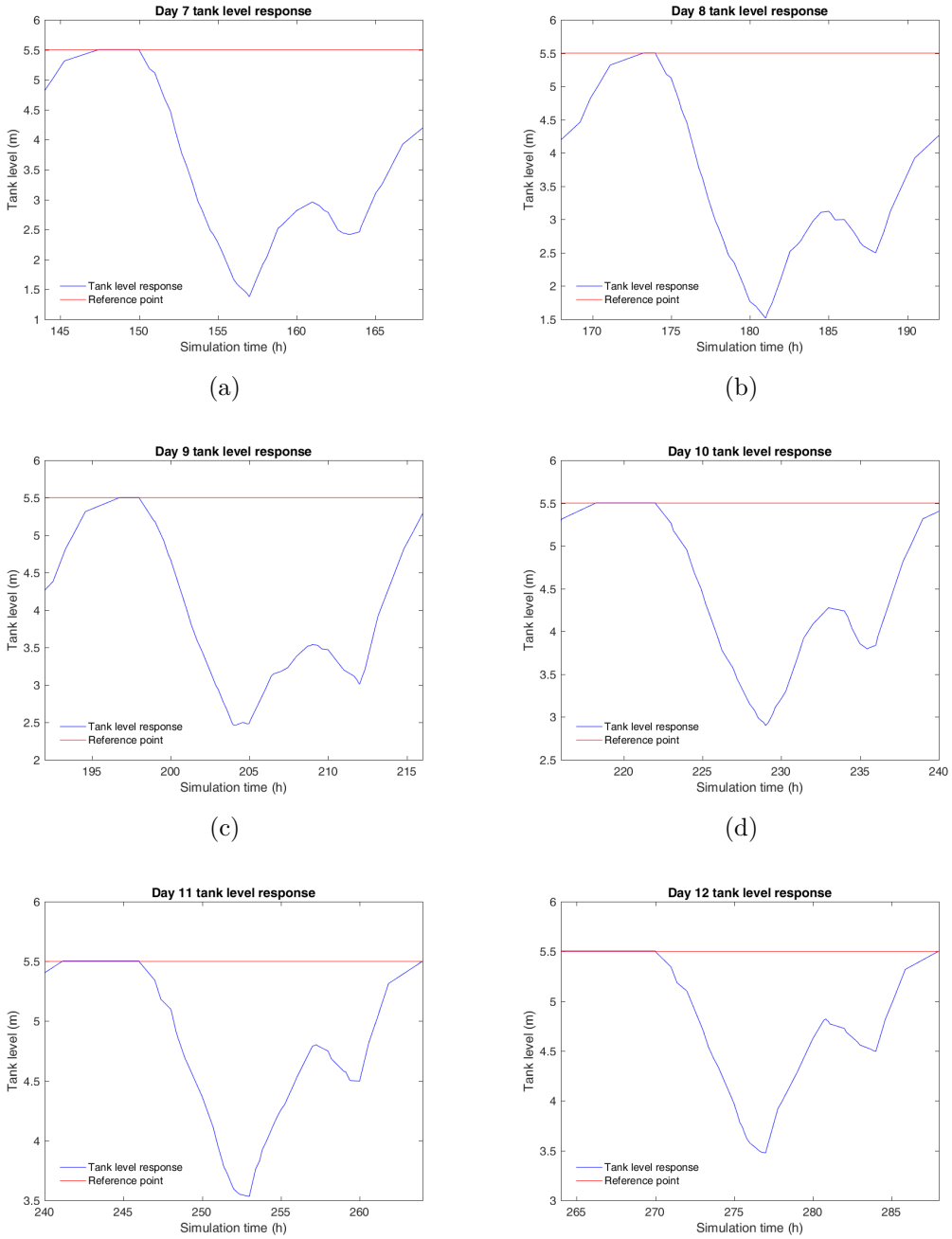

Figure 49: Pumps scheduling control under variable speed operation based on boolean logic simulation results. Korakies tank level response for days 7 to 12.

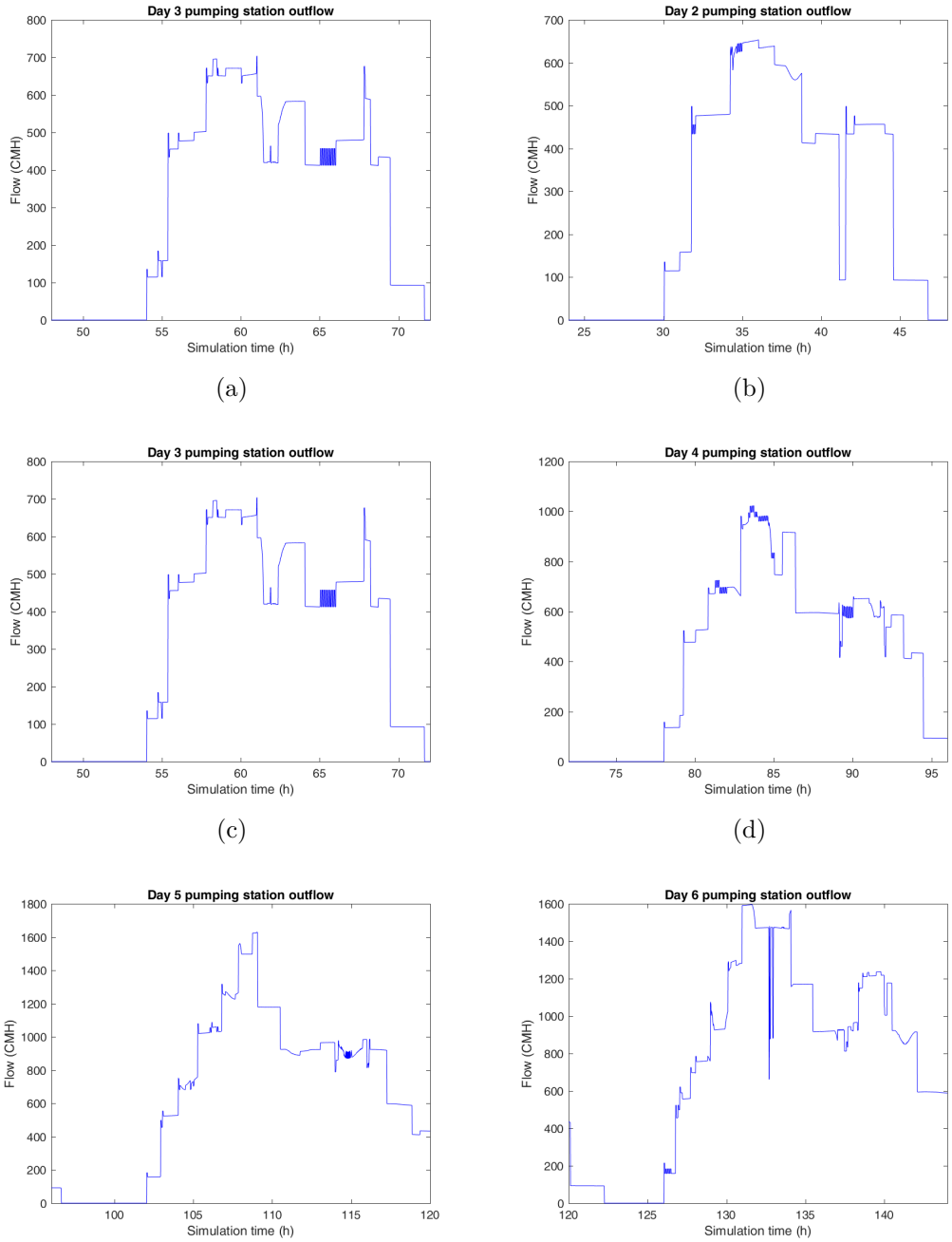

Figure 50: Pumps scheduling control under variable speed operation based on boolean logic simulation results. Vlites pumping station outflow for days 1 to 6.

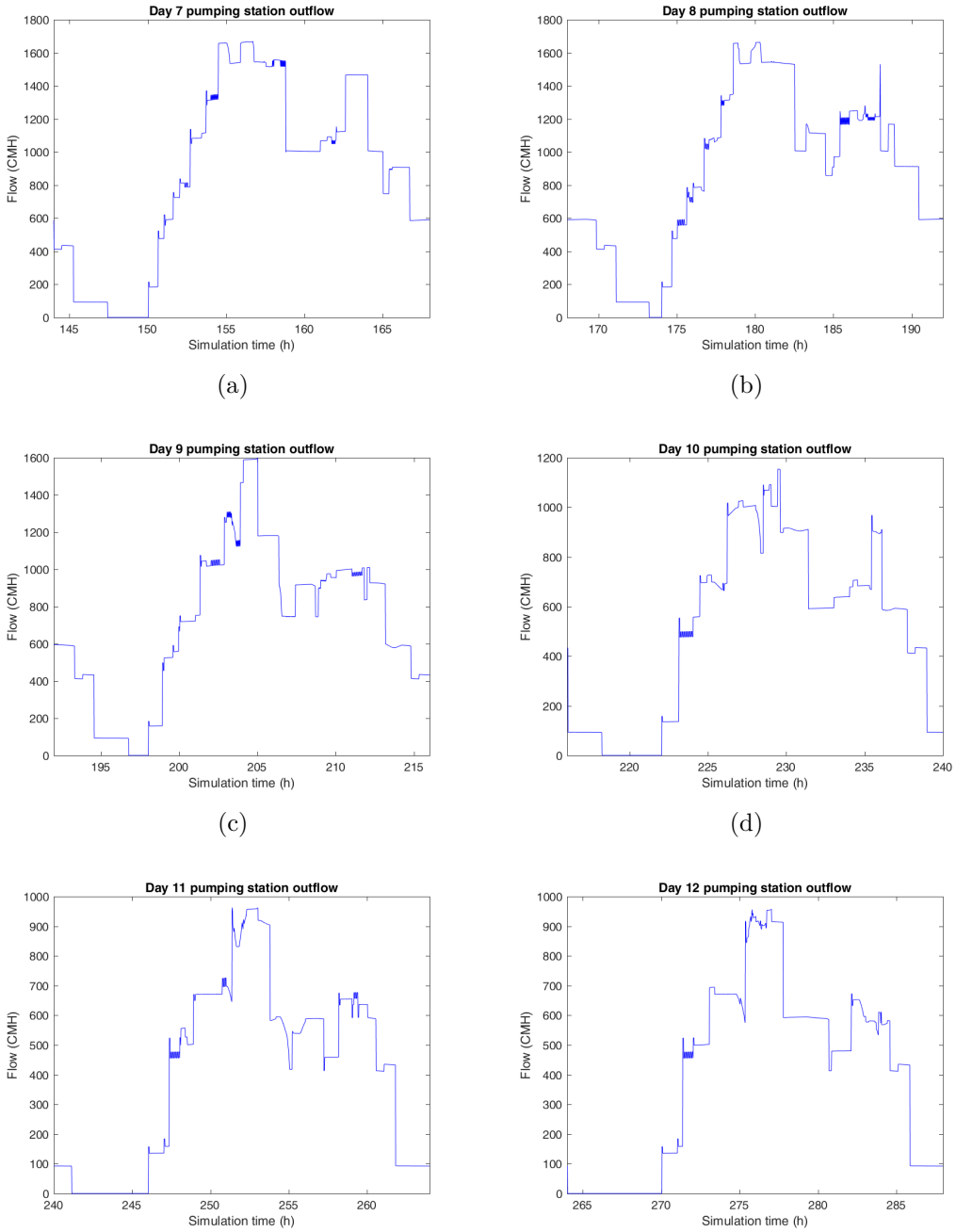

Figure 51: Pumps scheduling control under variable speed operation based on boolean logic simulation results. Vlites pumping station outflow for days 7 to 12.

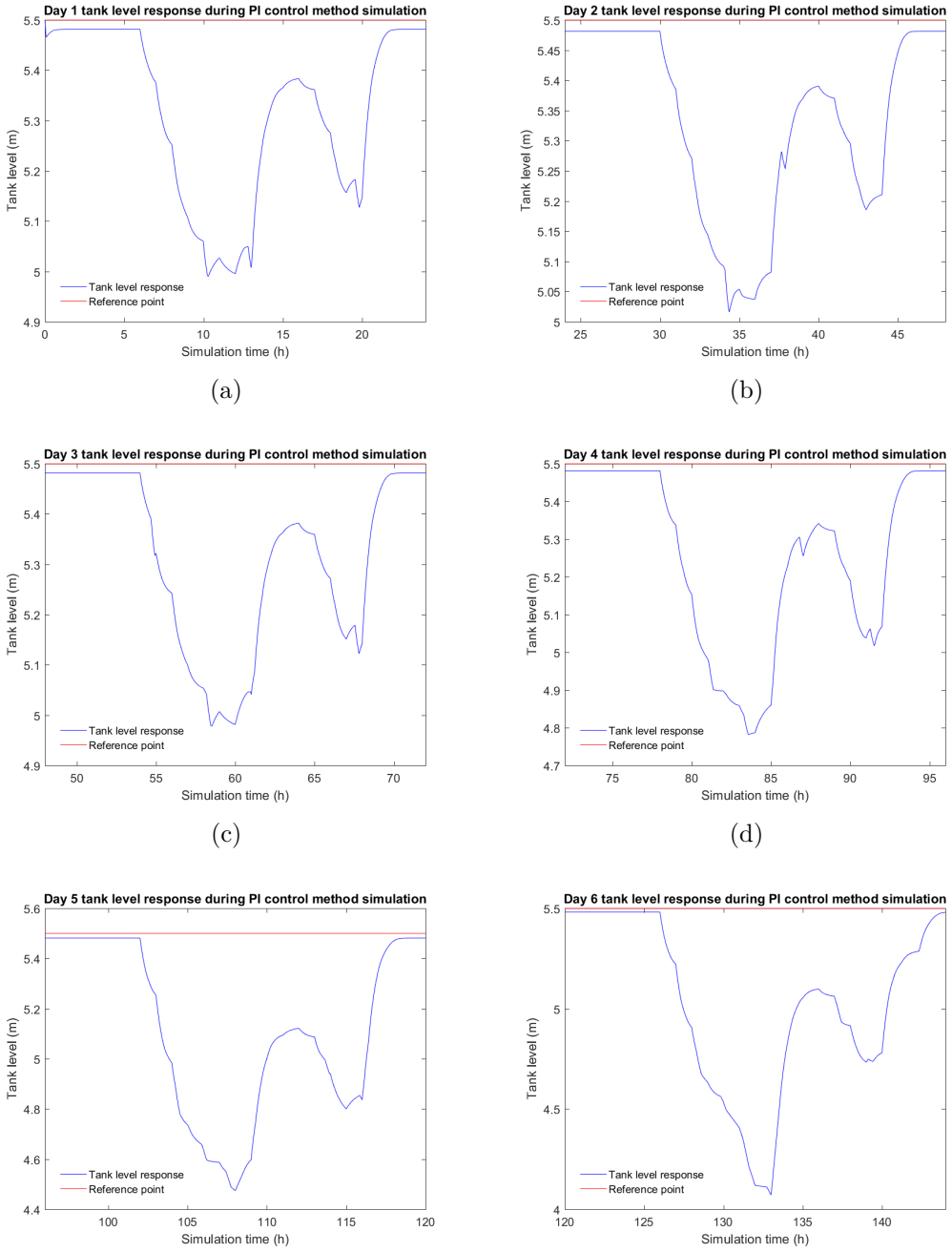

Figure 52: PI pumps control method based on tank level control simulation results. Korakies tank level response for days 1 to 6.

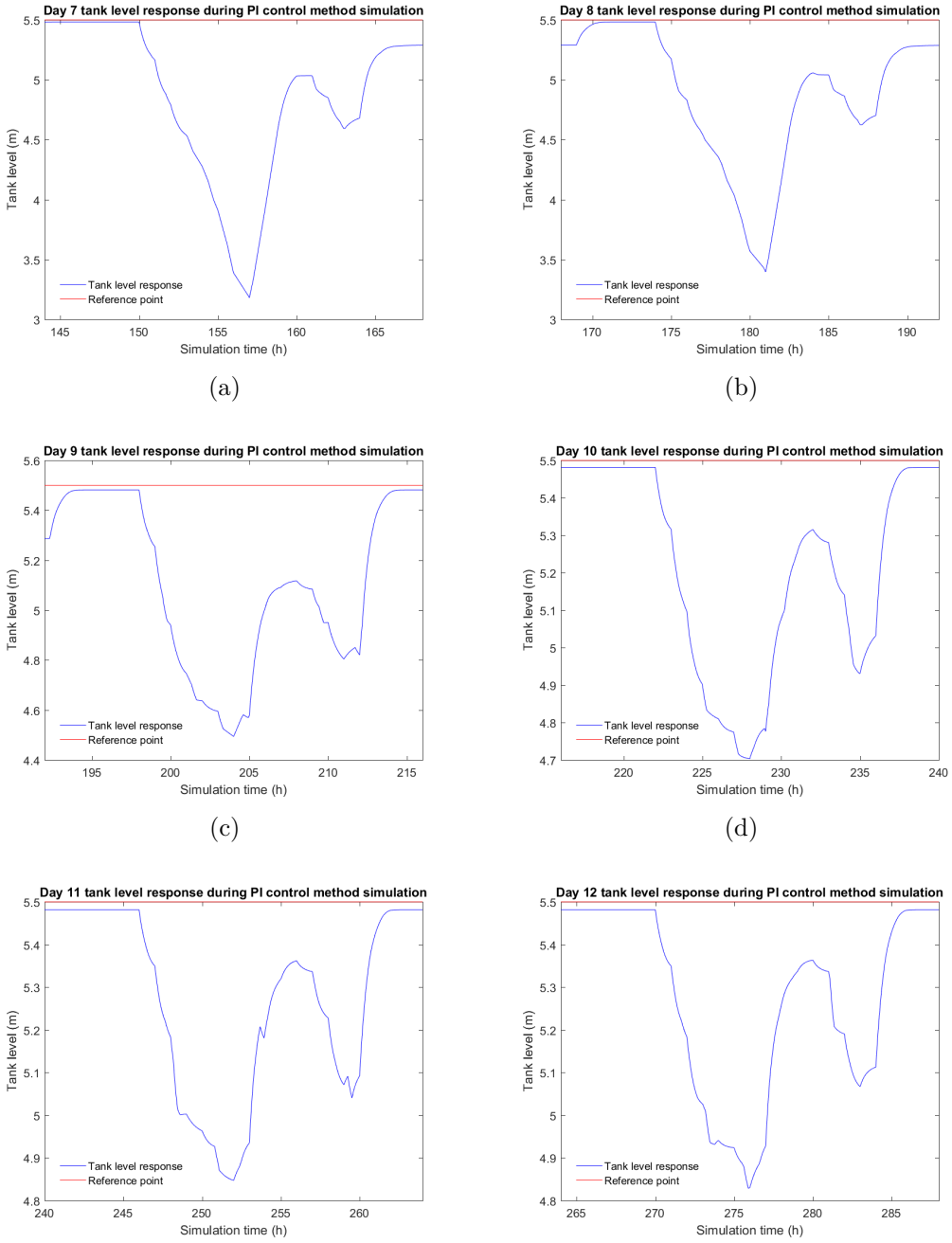

Figure 53: PI pumps control method based on tank level control simulation results. Korakies tank level response for days 7 to 12.

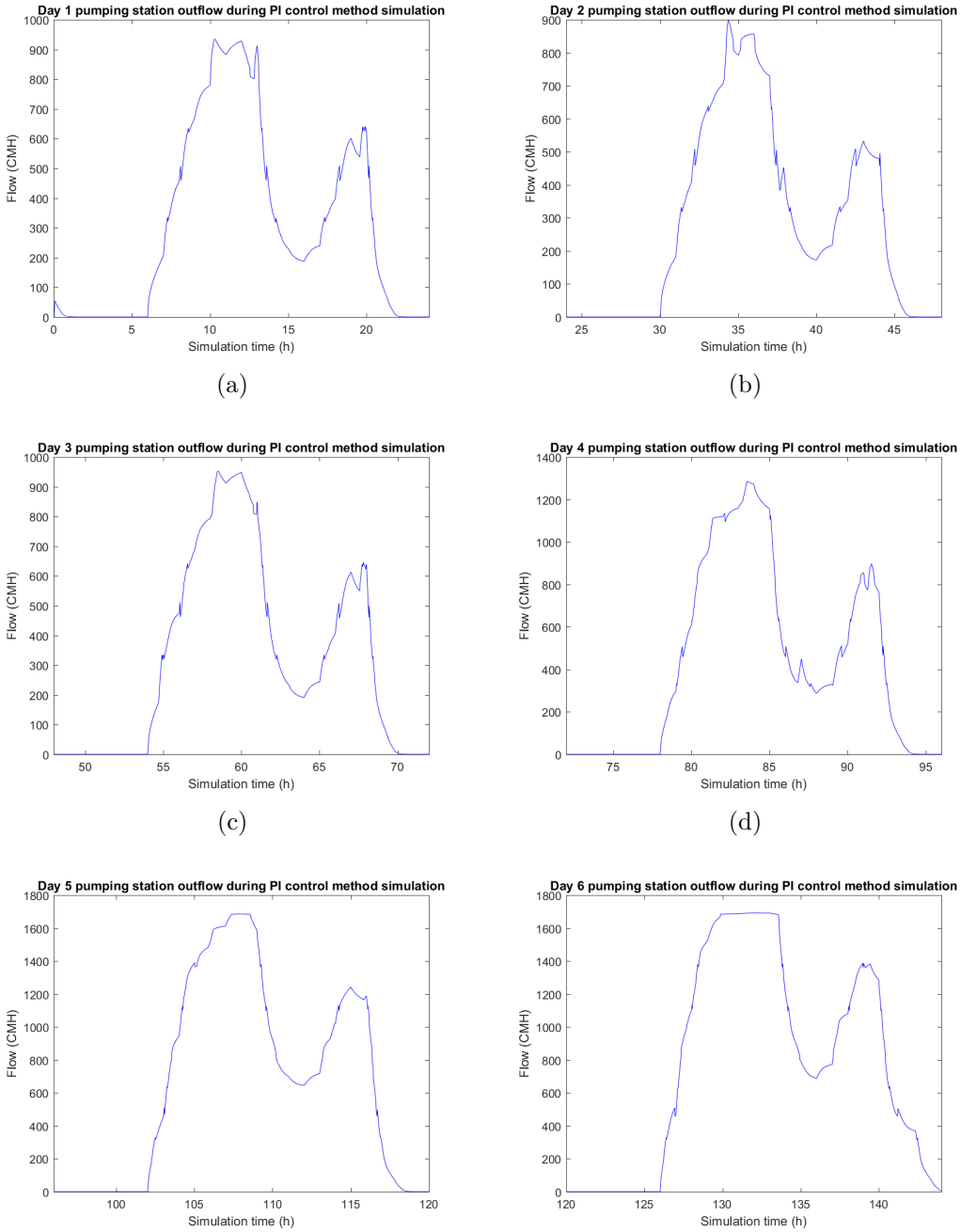

Figure 54: PI pumps control method based on tank level control simulation results. Vlites pumping station outflow for days 1 to 6.

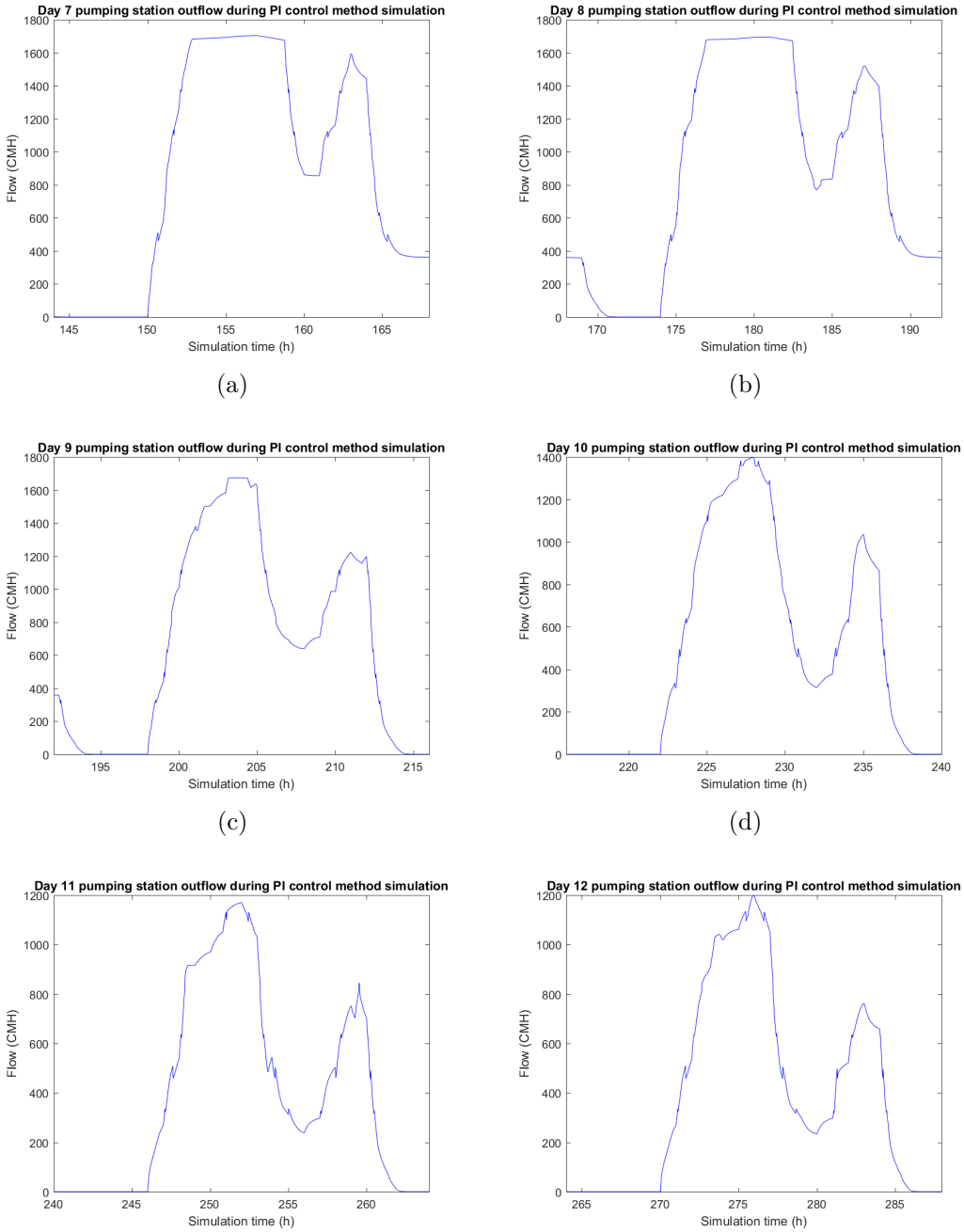

Figure 55: PI pumps control method based on tank level control simulation results. Vlites pumping station outflow for days 7 to 12.

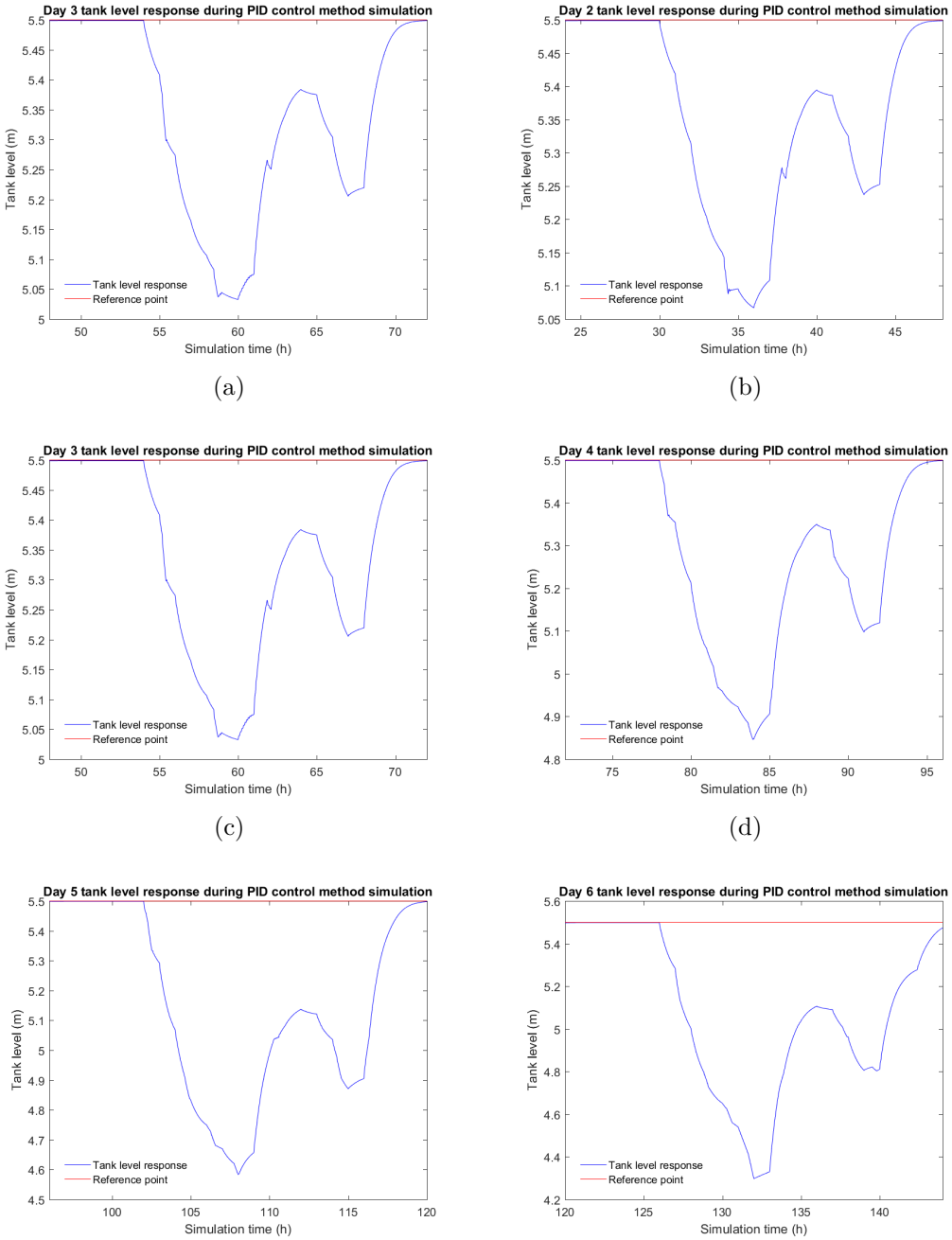

Figure 56: PID pumps control method based on tank level control simulation results. Korakies tank level response for days 1 to 6.

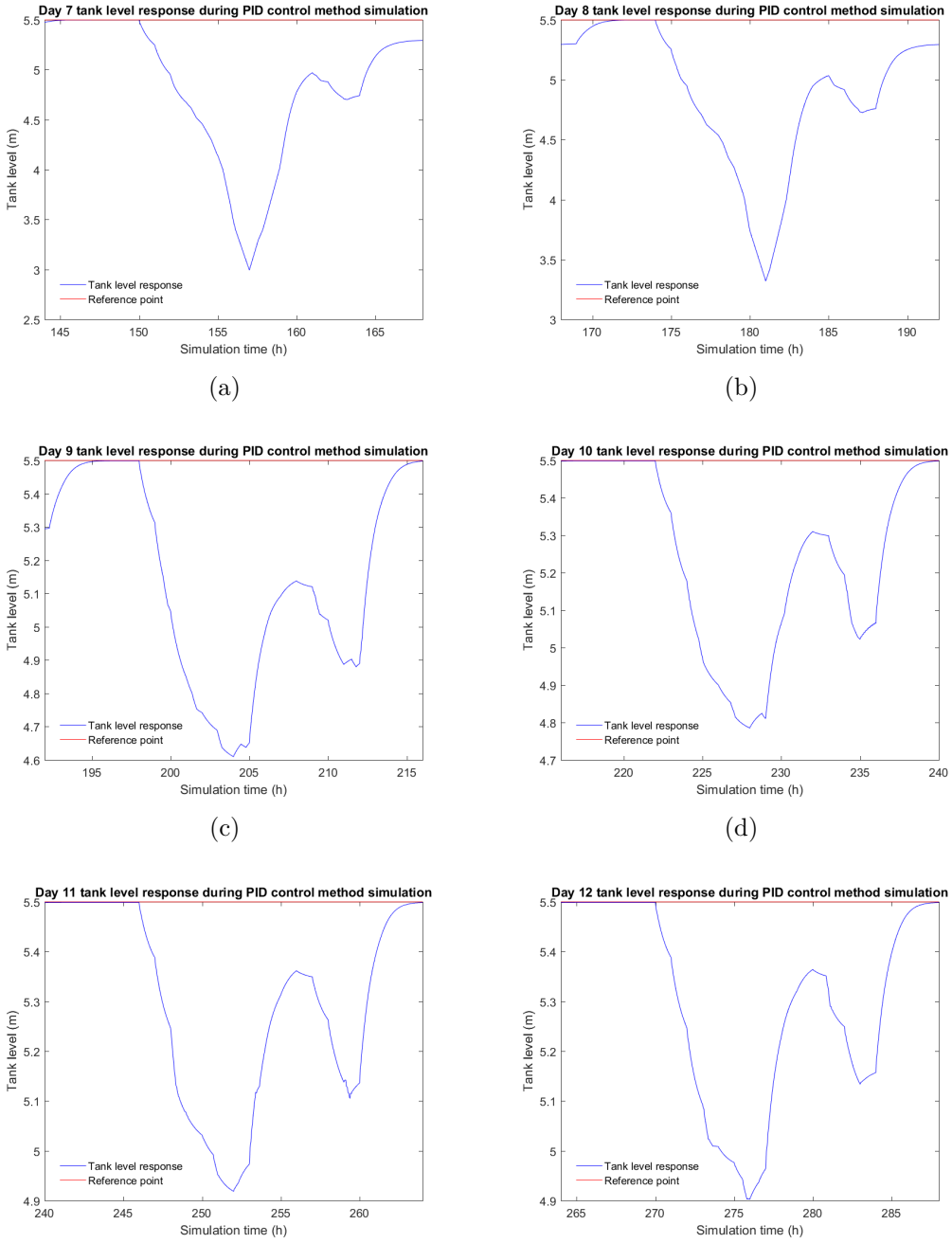

Figure 57: PID pumps control method based on tank level control simulation results. Korakies tank level response for days 7 to 12.

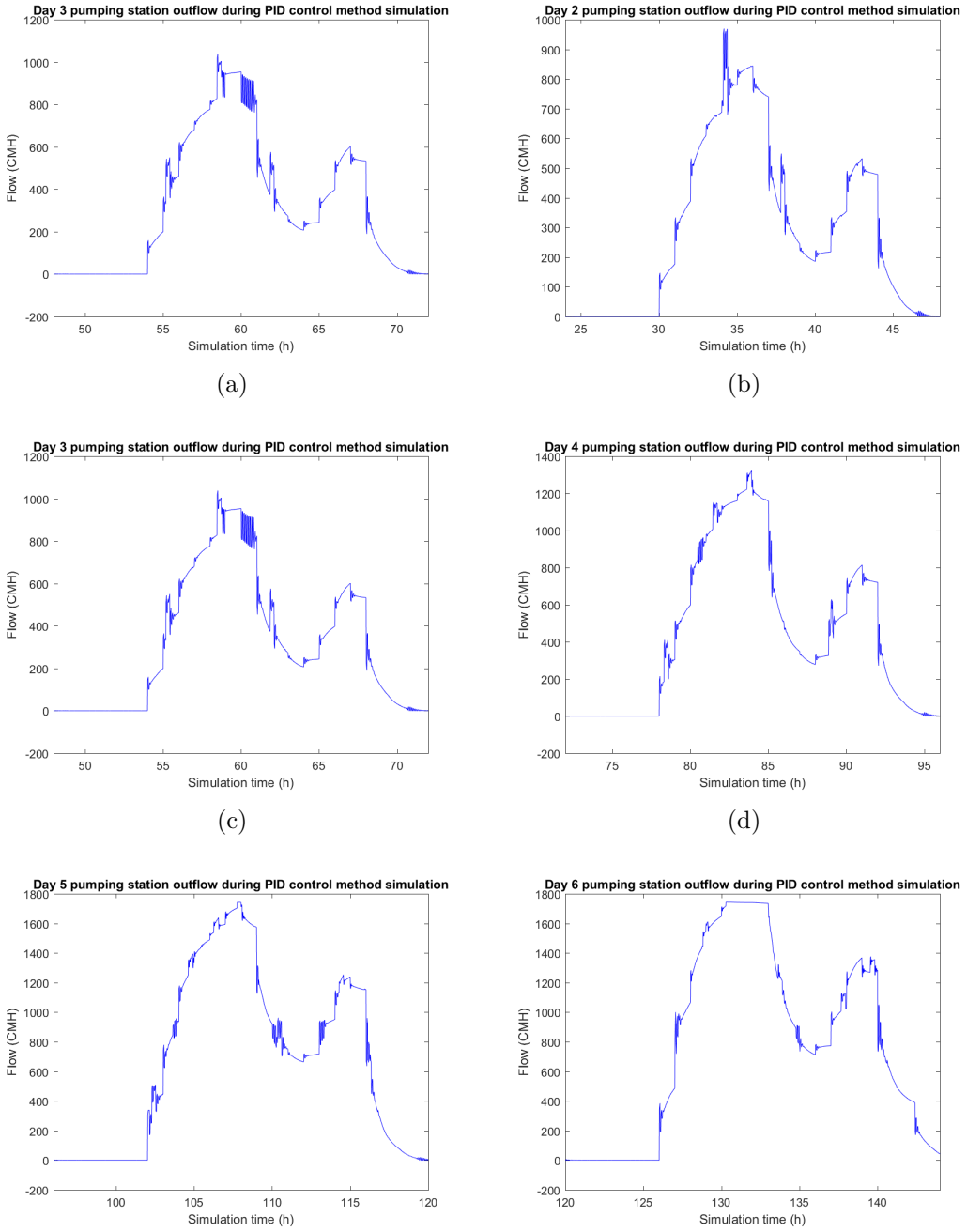

Figure 58: PID pumps control method based on tank level control simulation results. Vlites pumping station outflow for days 1 to 6.

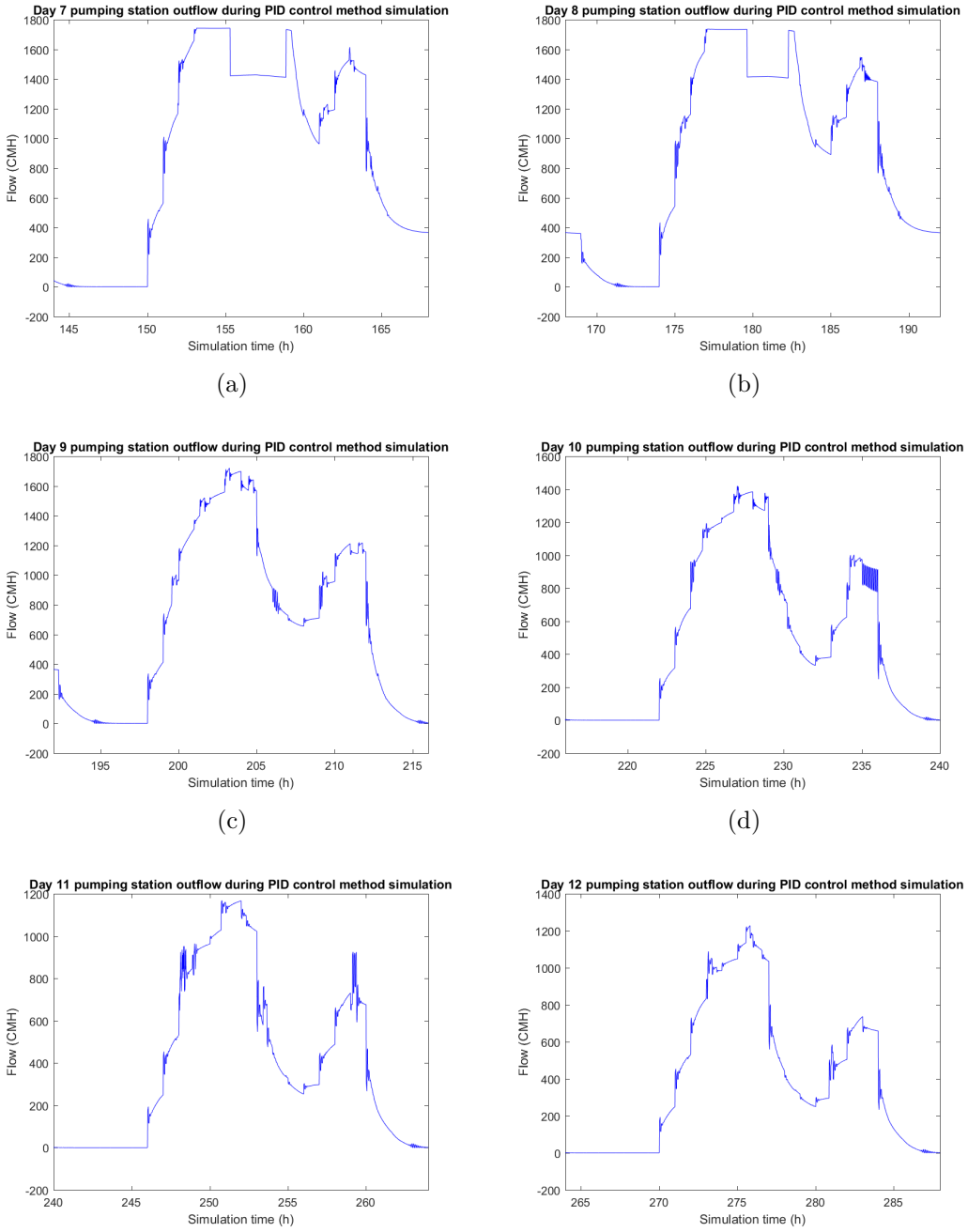

Figure 59: PID pumps control method based on tank level control simulation results. Vlites pumping station outflow for days 7 to 12.